FACULTY OF SCIENCES

Raman analysis on 18th and 19th-century Chinese porcelain

Cedric Wijnants

Supervisor: Prof. Dr. Peter Vandenabeele
Co-supervisor: Anastasia Rousaki

Academic year 2022-2023

GHENT UNIVERSITY

Acknowledgements

I would like to thank a couple of people who helped me throughout my thesis. Firstly, I would like to thank the people from the Raman Spectroscopy Research Group at Ghent University. I would like to thank professor Vandenabeele for the opportunity to do my thesis in this group. Professor Vandenabeele and Anastasia guided me throughout this thesis and were always helpful if I had any questions. Also thank you for helping me with securing my internship spot at KIK-IRPA. Also a big thank you to Sylvia and Eva. You were always helpful and provided positive feedback to write the best possible thesis.

I would also like to thank my family, friends and my girlfriend for the moral support in the process of writing my thesis. Thank you to my grandmother and grandfather for always taking care of me and believing in me when no one else would.

Raman analysis on 18th and 19th-century Chinese porcelain.

PART 1: SCIENTIFIC PAPER

Raman analysis on 18th and 19th-century Chinese porcelain.

C. Wijnants[a], P. Vandenabeele[a,b], A.Rousaki[a], D. Braekmans[c,d]

[a] Raman Spectroscopy Research Group, Department of Chemistry, Ghent University, Ghent, Belgium
[b] Archaeometry Research Group, Department of Archaeology, Ghent University, Ghent, Belgium
[c] Cranfield Forensic Institute, Cranfield University, Defence Academy of The United Kingdom, Shrivenham, UK
[d] Department of Archaeological Sciences, Faculty of Archaeology, Leiden University, Leiden, The Netherlands
correspondence: Cedric Wijnants, Raman Spectroscopy Research Group, Department of Chemistry, Ghent University, Ghent, Belgium.
Email: Cedric.wijnants@ugent.be

Abstract

Two sample sets of 18th and 19th-century Chinese porcelain have been subjected to Raman analysis. The sample sets included *cloisonné, famille rose*, and *famille jaune* style porcelain. The artifacts were assigned to the Qianlong (1736-1795) and Jiaqing (1795-1820) periods. A benchtop and a portable Raman instrument were used to analyze the different pigments on the porcelains. Seven pigments were identified, including hematite, ultramarine, lead tin yellow II, lead arsenate, anatase, PB15, and barium sulfate. PB15 is a synthetic organic pigment originating from the 20th century, clearly not belonging on these porcelains. The origin of this pigment is not known as it was detected on two different samples. The portable instrument was proven useful for the *in situ* analysis of these types of artifacts.

keywords: Raman analysis; porcelain; cloisonné; *famille rose*; *famille jaune*; pigment analysis; archaeometry

Introduction

Raman spectroscopy is an exceptionally well-suited analytical technique for porcelain analysis.[1-4] Raman spectroscopy has several important advantages in regard to these analyses. Raman spectroscopy is a non-invasive technique, meaning that it has the ability to perform measurements without damaging the sample (if the right parameters are chosen). As no or little sample preparation is needed, measurements are very straightforward. One of the biggest advantages is the miniaturization of Raman spectrometers, enabling one to measure *in situ*. As porcelain is fragile and museums or collection holders are understandably reluctant and cautious to move their collection to perform measurements on them. Using a portable Raman instrument avoids risky transport of collections.

Two sample sets consisting of three different styles of porcelain were analyzed using two different Raman spectrometers. All the samples were late 18th century or early 19th-century Chinese porcelain. This is an important era in the manufacturing of porcelain. Here, a switch was made between natural pigments and the first synthetic pigments.[1] Although Raman

analysis has been performed on similar types of artifacts, the information is rather scarce concerning the pigments.[5-7] The three different styles of porcelain were *famille rose, famille jaune,* and *cloisonné*-style porcelain. *Famille rose* and *famille jaune* porcelains were named after the color of their glaze. Famille rose is not only pink porcelainware but also some lighter shades of colored glazes are considered to be *famille rose* porcelain. *famille jaune* only considers the yellow porcelainwares. *C*loisonné-style porcelain refers to the manufacturing technology. This style is made by decorating enamelware with polychrome patterns. Enamel is a vitrified coating that is applied to a metallic body.[8] This is different than for the other two styles, where the body is manufactured out of ceramic material.
The samples were previously investigated by SEM-EDX and LA-ICP-MS.[8, 9] This enabled to compare the data from these two analytical techniques with the new Raman insights.

Experimental

Sample sets

In this article, 18th and 19th-century Chinese porcelains were subjected to Raman analysis. Two different sample sets were investigated by two different Raman spectrometers.

The first sample set consisted of *famille rose* porcelain and was dated to be from the Qianlong and Jiaqing periods. These artifacts are from the private collection of Colin Sheaf, Deputy Chairman of Bonhams and Global Head of Asian Art. Dr. R.Giannini performed LA-ICP-MS on these samples as a part of her PhD. The samples were provenanced to be from the Jingdezhen kilns.[9] The two artifacts that were examined are given in Figure 1. This sample set will be referred to as ‘sample set 1’.

A second sample set was provided by Dr. Dennis Braekmans. These samples were previously investigated by ESEM-EDX and more recently by LA-ICP-MS.[8] The sample set consist of two subsets. The first subset consisted of 18th century cloisonné-style Chinese porcelain. The SEM-EDX results of these artifacts were already published.[8] The other subset contained *famille rose* and *famille jaune* styles of porcelain. For the previous research, all the samples from both subsets were embedded into a polymer. To obtain these embedded samples, small fragments of damaged areas were scalped off, surface cleaned, and mounted on stubs. The advantage of embedded samples is that it facilitates measuring underneath the glaze. This sample set will be referred to as ‘sample set 2’ Detailed pictures of the artifacts are given in Figure 2.

Raman spectrometers

Two different Raman spectrometers were used for the analyses. The first instrument was a benchtop instrument and the second was a portable one.

Senterra Raman benchtop instrument

The Raman spectra were obtained via the Senterra dispersive Raman instrument from Bruker optics. The Senterra is equipped with a confocal microscope type BX51. It holds four objectives: a 5x, 20x, 50x, and 100x magnification. The instrument has a 532 nm green Nd:YAG laser and a 785 nm red diode laser. The power at the source for the 785 nm laser is

100 mW and 20 mW for the 532 nm laser. In this research, the spectral resolution was fixed at 3-5 cm^{-1} (high resolution), setting the spectral region for the 532 nm green laser between 40-2730 cm^{-1} and for the 785 nm laser between 80-2630 cm^{-1}. The laser power ranged from 1% to 100% and the aperture was varied between 25 µm and 50 µm depending on the amount of fluorescence. The detector is a CCD detector that is thermoelectrically cooled at a working temperature of -65°C. Neon spectra are automatically recorded by the instrument to correct for changes in the spectrograph and laser excitation. The operating system is the OPUS© software which has tools to gain quick insights into the obtained spectra. The obtained spectra were furtherly treated via the program GRAMS/AI™ Spectroscopy Software.

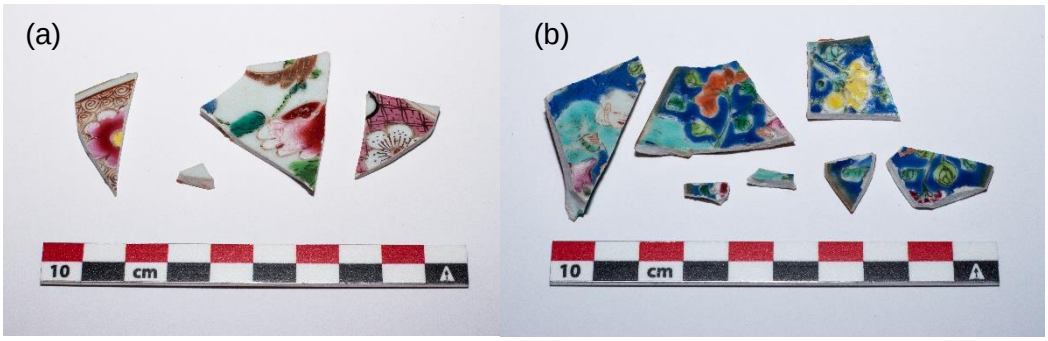

Figure 1: Sample set 1 consisting of Qianlong and Jiaqing famille rose Chinese porcelain. (a) sample B.fr.1750.2: Qianlong period porcelain dish (b) Sample B.fr.1800.1: Jiaqing period spoon tray.

i-Raman Portable instrument

The portable Raman instrument is the i-Raman® EX from B&WTEK. The instrument is equipped with a 1064 nm laser with CleanLaze® technology. The spectral resolution is set at 9.5 cm^{-1} and the spectral range is between 100 cm^{-1} and 2500 cm^{-1}. The detector is an InGaAs detector thermoelectrically cooled at -20°C. The power at the source is 499 mW and the power can be varied from 1-100% in steps of 10%. The Raman instrument was calibrated using five different chemical substances, namely, sulfur, caprolactam, polystyrene, a solution of 50% water and hexane, and cyclohexane. Two different setups can be used. The first one is via a cuvette holder for mostly liquid and gas phase samples. The other setup is more classical with a probe head holder that is perpendicular to the samples. The obtained spectra were furtherly treated via the program GRAMS/AI™ Spectroscopy Software.

Analytical procedure

Both the sample sets were analyzed by the benchtop Raman instrument. In addition to this, sample set 1 was also analyzed using the portable Raman instrument.

Analytical procedure-Benchtop Raman instrument

The analytical procedure for sample set 1 and 2 differ due to the nature of the artifacts. Sample set 1 are porcelain shards and sample set 2 are embedded samples.
For every sample on the mounted block, first the area was scanned for the different colors present using the microscope. For example, for sample EPC8, red, blue, and yellow spots were present. Then, one of the observed colors was chosen and one or more spots of this color were analyzed. The focusing was done manually using the microscope and the video wizard software on OPUS. If possible, the highest magnification (100x) was used to focus on the individual granules of the pigments. Certain glazes were colored glazes, meaning that a certain surface has

a specific color without showing any individual granules. For the colored glazes, defocusing the laser or tilting the sample was needed in order to get a usable Raman spectrum.
For the porcelain shards (sample set 1), the colors were visible with the naked eye. So in this case, a color was chosen and then the video wizard software was used to focus. As the samples were larger and not flat, a lower magnification was used (20x). Due to the lower magnification, larger colored areas were measured and not individual granules.

Figure 2: Sample set 2 consisting of *cloisonnè*, *famille rose*, and *famille jaune* style porcelain. (a) CPESU1: cloisonné-style ewer from the Qianlong period (b) CPEAS1: cloisonné-style censer in the Fangding form from of the Qianlong period (c) CPE253: *famille rose* style mirror frame from the Qianlong period (d) CPE312: *famille jaune* style vase from the Qianlong period (e) EPC8: *famille rose* style appetizer plates from the Qianlong-jiaqing periods (f) EPC9: *famille rose* style divided plate from the Qianlong-Jiaqing period (g)EPC11: *famille rose* style jewelry box from the Qianlong period. (h) CPE313: *famille jaune* style ewer from the Qianlong period.

Analytical procedure-Portable Raman instrument

Only sample set 1 was analyzed using the portable Raman instrument. The porcelain shards were placed on a platform and the laser was put in a stand vertical to the porcelain shards. For focusing, continuous measurements were performed. When the continuous measurements were performed, the laser was moved up and down until an acceptable S/N-ratio was achieved.

Results and discussion

Benchtop Raman instrument

Hematite (Fig 3(a)) was detected on the red area of sample B.fr.1750.2 from sample set 1 and on seven samples from sample set 2 (CPEAS1, CPE253, CPE312, CPES20, EPC8, EPC9 and EPC11). Hematite has already been used in Chinese porcelains since the 15th century.[10] Different researchers already reported findings of hematite in Chinese porcelains of this specific era.[6, 9-10] These results are consistent with the findings of Dana Norris et al.[8] who had subjected these samples to ESEM-EDX. Elevated amounts of Fe_2O_3 were found in sample CPEAS1. Hematite has seven distinguishable bands at 227, 246, 293, 412, 499, 613, and 1310 cm^{-1}.[6] The bands at 227 and 293 are assigned to be from the bending vibrations of the iron atoms. The band at 244 is ascribed to be from the stretching vibrations of these. The bands at 412, 499, and 613 cm^{-1} are assigned to be from the oxygen vibrations.[11-14] The intense band around 1310 cm^{-1} corresponds to the two-magnon scattering of hematite. This bands is enhanced when using the green laser due to resonance enhancement.[15] It is usually used as a measure for the detection of hematite when using a green laser.[6, 16-18]

Ultramarine blue (Fig 3(b)) was detected on sample CPE253 (sample set 2). Ultramarine blue comes from the rare gemstone *lapis lazuli* and was the most expensive pigment during the Renaissance, even more valuable than gold. Ultramarine was mostly used in paintings or in murals, but not many porcelains have been found containing this pigment. P. Vandenabeele et al.[1] have published on finding ultramarine in rare 19th century porcelain cards. Although this is rather rare, it is known that ultramarine blue was used in art pieces at that time.
The most intense band in the spectrum of ultramarine blue is visible at 549 cm^{-1}, four relatively intense bands can also be found at 260 cm^{-1}, 585 cm^{-1}, 1096 cm^{-1}, and 1644 cm^{-1}. Broader bands can be found at 804 cm^{-1}, 1360 cm^{-1}, 1904 cm^{-1}, and 2194 cm^{-1}. Ultramarine blue has the following chemical formula: $Na_{8-10}Al_6Si_6O_24S_{2-4}$. S_{2-4} can partially be replaced by SO_4^- if exposed to air for a longer period of time.[19] The most intense band at 549 cm^{-1} is caused by the symmetric stretch of the S_3^- anions. The first vibrational overtone of the S_3^- anions is visible in the spectrum at 1096 cm-1. The second and third overtones are visible at respectively 1644 and 2194 cm^{-1}. The bending vibration of the S_3^- anions is visible in the lower spectral region at 257 cm^{-1}.[20] The band at 585 cm^{-1} in the spectrum corresponds to the symmetrical stretch of the S_2^- anions. The bands showing at 804 cm^{-1} and 1360 cm^{-1} are combination bands ($\nu_1+\nu_2(S_3^-)$) and ($2\nu_1+\nu_2(S_3^-)$) of the S_3^- anions. Combination bands are a consequence of electrical anharmonicity.[21]
Due to the use of the green laser, a resonance effect occurs. This is because the frequency of the laser matches the maximum allowed electronic transition. This allows for the enhancement of the fundamental vibrations and overtones. Ultramarine has three different chromophores. the S_2 group is the yellow chromophore, the S_3 group is a green chromophore, and a disordered S_3 group causes the deep blue color. The specific ratios will thus alter the color from deep blue to

a more greenish color. Ultramarine can have a synthetic and a natural origin. This means that the artifact probably contains the natural variant as the synthetic variant was not yet synthetized in this era. Although, this cannot be concluded from the recorded spectrum of the sample. Nonetheless, different studies have focused on finding differences in the Raman spectra between the natural and synthetic variants. Pulsed Raman spectroscopy combined with laser-induced breakdown spectroscopy (LIBS) hast yielded the best results.[20]

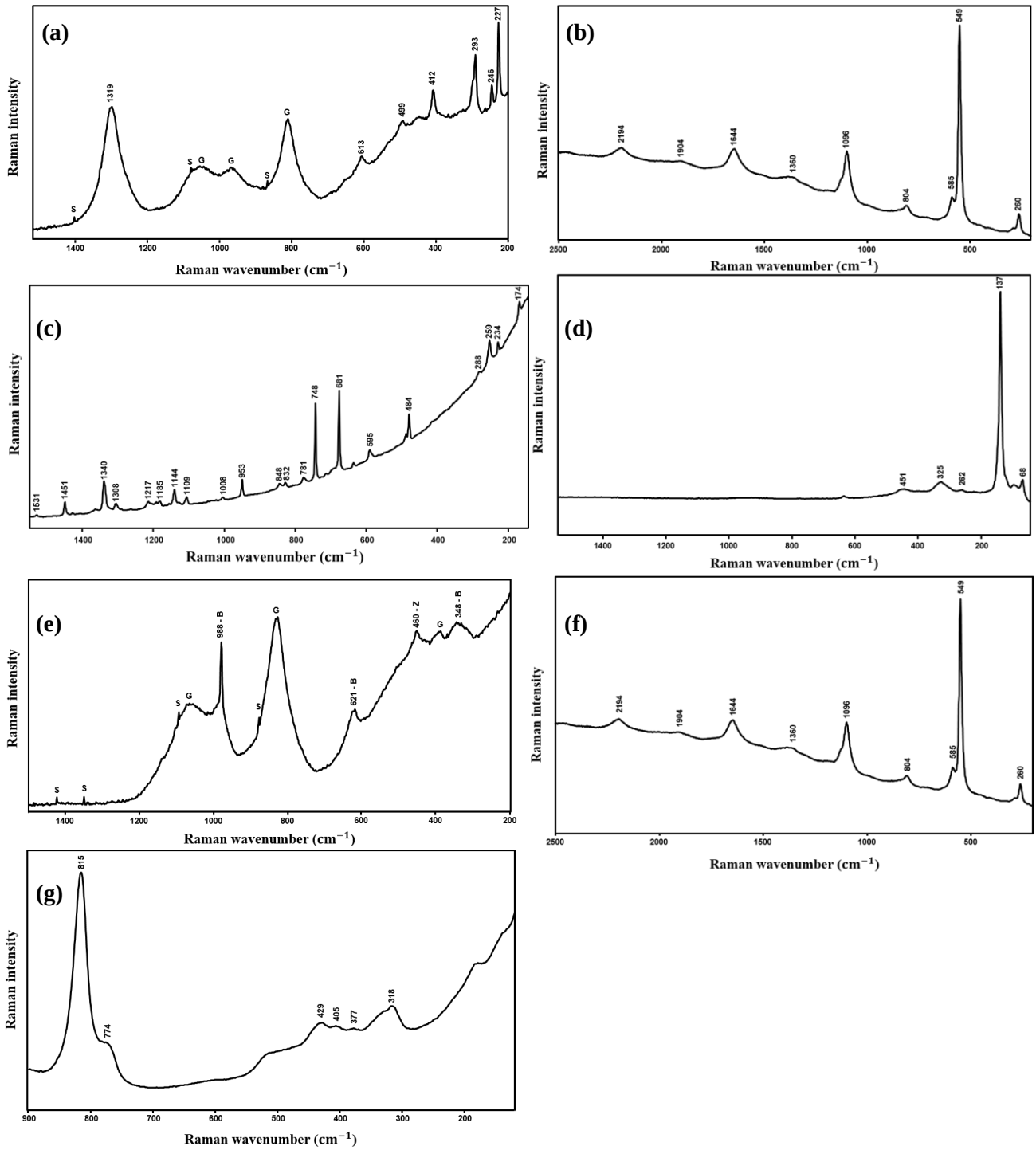

Figure 3: Overview of the Raman spectra recorded on the samples. G=glaze S=spike U=ultramarine blue B=barium sulfate Z=zinc sulfide

Phthalocyanine blue (PB15) (Fig 3(c)) was found on two different samples from sample set 2 (EPC8 and CPESU1). This is an interesting result because PB15 is an organic synthetic pigment. The first time PB15 was synthesized dates back to 1927.[22] This is after the period that these samples are supposedly from.
PB15 has seven known polymorphs, whereas each polymorph has a slightly different lattice structure. Only five polymorphs are used in art and are commercially available as a pigment. The pigment found in these samples corresponds to the β-form also denoted as PB15:1.[23, 24] PB15 is a copper complex. The most important bands visible below 1000 cm^{-1} correspond to the macrocycle vibration. Between 1100 cm^{-1} and 1600 cm^{-1}, the bands correspond to the vibration of the pyrrole group, with the most intense band (1531 cm^{-1}) coming from the pyrrole stretching vibration. In this range, one will also find the isoindole vibrations. Some weaker bands at higher wavenumbers correspond to the carbon-hydrogen and metal-hydrogen vibrations.[23]
It is very unlikely that PB15 was applied before the firing process of the porcelain. PB15 shows high thermal decomposition at 400 degrees Celsius meaning that it would degrade during the firing process of the porcelain.[25] There are two more likely scenarios regarding the presence of PB15 on these samples. The first theory is that maybe in the course of time, somebody overpainted one of the porcelains. Although, larger blue areas should then be visible. Only one spot was found on sample EPC8 and a couple of tiny spots were found on sample CPESU1. Further research will have to be conducted to point out the possible source of this contamination.

Lead tin yellow II (Fig 3(d) (($PbSn_{1-x}Si_xO_3$, where x=0.25).[10] was positively identified on four different samples. One sample from sample set 1 (B.fr.1800.1) and three samples from sample set 2 (EPC11, CPE313, and CPE312). Lead tin yellow II was a commonly used pigment in 18^{th} to 19^{th}-century Chinese porcelains.[7, 26, 27] Before the 18^{th} century, lead tin yellow II was more commonly known as giallorino, especially in Italy.[28] The pigment was mostly used in paintings and became popular with the Renaissance painters and the Old Masters.
The most pronounced band is the band at 137 cm^{-1}. This bands corresponds to the lead oxide lattice stretching vibrations.[29] The bending vibration of lead oxide can then be found at 68 cm^{-1}. The band at 451 cm^{-1} is probably coming from the bending vibration of the silicate matrix. The assignment of the bands at 262 cm^{-1} and 325 cm^{-1} have not been discussed in literature. These bands could be from the tin oxide bending vibrations, or from the silicate matrix.
Lead tin yellow has two types: type I and type II. Lead tin yellow type I (Pb_2SnO_4) was more commonly known as yellow of the Old Masters and was already used since the 13^{th} century in oil paintings.[28] Because lead tin yellow II has a silicate matrix, differences in Raman spectrum can be observed. This makes the two different pigments distinguishable by Raman spectroscopy.[29]

Barium white (Fig 3(e)) was found as a whitener on sample CPEAS1 to obtain a brighter blue color. Possibly, the spectrum also exhibited the signature of lithopone. Barium white is pure Barium sulphate whilst lithopone also contains Zinc sulfide (BaSo4.ZnS). It is important to know that lithopone was first used in 1874 while Barium white was already used a century before (18^{th} century).[30, 31] This is important in regard to the dating of this sample.
The most pronounced bands in the recorded spectra are present at 348, 460, 621, and 988 cm^{-1}. Apart from that, some bands coming from the glaze are also present. The most intense band at 988 cm^{-1} is the symmetrical stretch of the sulfate ion.[32] The bands of the symmetrical bending vibration of the sulfate ion are visible at 453 cm^{-1} and 462 cm^{-1}. At 617 cm^{-1} the asymmetrical

stretch of the sulfate ion is visible.[33] The most pronounced band of zinc sulfide is present at 378 cm^{-1}. The second band should be visible at 670 cm^{-1}, but is not visible in the recorded spectrum. This is confirmed in literature reports, stating that the band at 670 cm^{-1} is not always visible or very weakly visible due to the weak scattering abilities of ZnS.[34]
As said before, a difficulty here is that the bands of ZnS might not be visible due to the overlap of other bands and the weak scattering abilities of ZnS.[35] Due to the fact that no band is visible at 670 cm^{-1} and the low intensity of the band at 348 cm^{-1}, no conclusion can be drawn with a great degree of certainty. The band at 348 cm^{-1} might be a feature from the glaze and not from ZnS. It has to be remarked that the signal-to-noise-ratio and the background are not the best quality making interpretation harder. On the other hand, the ESEM-EDX data of Dana Norris et al.[8] showed the presence of Zn in the blue glaze of sample CPEAS1. This is the only analyzed spot on the sample that had traces of Zn on the painted enamels.
To conclude, it can be said with a high degree certainty that barium sulfate was used to obtain a lighter blue glaze. Although, it cannot be concluded that it is lithopone. To be certain that it might be, or might not be lithopone, further research is required.

Anatase (Fig 3(f)) was detected together with ultramarine blue on sample CPE253. As it was found together with ultramarine, this could mean that this was added to obtain a brighter blue color.
The bands of interest regarding anatase are located at 143 cm^{-1}, 288 cm^{-1}, and 385 cm^{-1}.[36] The other bands are bands coming from ultramarine blue. The symmetrical stretch of titanium oxide is observed at 143 cm^{-1} and is the most intense band visible in the spectrum. This band is used in literature as a measure for the identification of anatase. The planar bending vibration of Fe-O is visible at 385 cm^{-1}. The band at 288 cm^{-1} is not of titanium oxide but of iron oxide, more specific hematite (α-Fe_2O_3). The slight red shift is due the combination of Titanium oxide and iron oxide.[37] Anatase does contain a slight amount of iron oxide and this is more of a contamination than a deliberately added substance.
Titanium white has three different polymorphs namely anatase (α-TiO_2), rutile (β-TiO_2), and brookite (γ-TiO_2).[36, 38] Rutile is the more stable form and consist of 90% TiO2 and around 10% iron oxides. These polymorphs can be converted into each other, especially anatase and rutile. Anatase and brookite are metastable, especially brookite is a rare form of TiO_2. The temperature in which anatase is converted to rutile is between 750-950 °C.[37] The transition temperature is dependent on different factors including the grain size and the amount of iron oxide present.
The presence of anatase has been positively concluded on the basis of the intense band at 143 cm^{-1}. In addition to this, anatase is a component of kaolin, the base clay for the manufacturing of Chinese porcelain. So there is also the possibility that the detected anatase is coming from the body and that this was not necessarily added to the ultramarine blue. As anatase is a very strong Raman scatterer, this can overwhelm the spectrum pretty easily, masking other Raman scatterers. But if this was the case, this signature should've been noticed in other spectra as well.

Lead arsenate (Fig 3(g)) was positively identified as a whitener on sample CPESU1. This was detected on a green glaze, as an additive to obtain a brighter green color. Lead arsenates were often used to whiten colors and were also commonly used opacifiers in porcelain.[5, 7, 39] The first use of lead arsenate in Chinese porcelainware date back to an early 18^{th} century water dropper.[7] Lead arsenates are strong Raman scatterers, so this is probably why in the recorded spectrum, only lead arsenate was detected and not a green pigment as would be expected.
The most pronounced band is located at 820 cm^{-1} and corresponds to the symmetric As-O stretching vibration of the AsO_4^- ion. The shoulder of this band, located at 774 cm^{-1} also

corresponds to this symmetric stretching. In the region between 300 and 450 cm^{-1} a couple of bands overlap. These bands correspond to the in plane bending vibrations of the AsO_4^- ion.

Portable Raman instrument

lead tin yellow II was detected on two different areas of sample B.fr.1800.1. The first spot was the same yellow area that was analyzed with the benchtop instrument. The second spot was a green area. The LA-ICP-MS data of R.Giannini et al.[28] showed elevated amounts of SnO_2 on these brighter green areas. This means that lead tin yellow II was most probably added to obtain a brighter green color.
This area was also analyzed by the benchtop instrument but no lead tin yellow II was detected. The concentration of SnO_2 detected by LA-ICP-MS was rather low (1.53wt%), meaning that only a little bit of lead tin yellow II was added. Even though, the amounts added were probably small, the portable instrument could still pick up this signal due to the use of thr near-IR laser. Still, the intensity of the laser had to be increased to 20% to pick up this signal. With the benchtop instrument, a higher intensity of laser was also used, but still no signal could be recorded.

Conclusion

In total, seven pigments were identified: one red pigment, two blue pigments, one yellow pigment, and three white pigments. All these pigments and their characteristic Raman bands have been summarized in Table 1.

Table 1: Overview of the different pigment and their characteristic Raman bands. vw=very weak, w=weak, m=medium, s=strong, vs=very strong, br=broad band, sh=shoulder

Pigment	Chemical formula	Raman wavenumbers (cm^{-1})
Hematite	α-Fe_2O_3	227(s), 246(w), 293(vs), 412(m), 449(vw), 613(w), 1319(s-br)
Phthalocyanine blue	$C_{32}H_{16}CuN_8$	174(w), 234(w), 259(w), 288(vw), 484(m), 595(w), 681(s), 748(vs), 781(w), 832(w), 848(w), 953(m), 1008(vw), 1109(w), 1144(m), 1185(vw), 1217(vw), 1340(m), 1451(w), 1531(s)
Ultramarine blue	$Na_{8-10}Al_6Si_6O_{24}S_{2-4}$	260(m), 549(vs), 585(m), 804(w), 1096(s), 1360(vw-br), 1644(m), 1904(vw-br), 2194(w-br)
Lead tin yellow II	$PbSn_{1-x}Si_xO_3$ (x=0.25)	68(w), 137(vs), 262(vw), 325(w-br), 451(vw-br)
Anatase	α-TiO_2	153(vs), 288(s), 385(vw)
Barium sulfate	$BaSO_4$	460(w), 621(w), 988(s)
Lead arsenate		318(w-br), 377(vw-br), 405(vw-br), 429(w-br), 774(m-sh), 815(vs)

Hematite was found in samples of the three different porcelain styles. This indicates the popularity and importance of hematite in 18th and 19th-century Chinese porcelain. Lead tin yellow II was also found on all the samples that had yellow areas. So, lead tin yellow II was also a popular yellow pigment is this period. As found, lead tin yellow II was also used to brighten green areas. Ultramarine blue on the other hand was only found on one sample. As it was a very expensive pigment, this indicates that this porcelain sample was from a higher-end porcelain not destined for the common household. PB15 was found on two different samples.

As stated before, this is probably a contamination and should be furtherly researched. Three different whiteners were found on three different samples, namely anatase, barium sulfate and lead arsenate. As they were only found once, on three different samples, this concludes about the variety of whiteners used in these periods.
The portable Raman instrument was useful for the analysis of porcelain. Only a preliminary study was carried out on sample set 1 as a proof of concept. Further research will have to be conducted to determine the usefulness on larger sample sets or whole artifacts.

References

1. Vandenabeele, P., P. De Paepe, and L. Moens, *Study of the 19th century porcelain cards with direct Raman analysis.* Journal of Raman Spectroscopy, 2008. **39**(8): p. 1099-1103.
2. Wang, T., et al., *Raman study of Yuan Qinghua porcelain: the highlighting of dendritic CoFe2O4crystals in blue decorations.* Journal of Raman Spectroscopy, 2017. **48**(2): p. 267-270.
3. Carter, E., et al., *Porcelain shards from Portuguese wrecks: Raman spectroscopic analysis of marine archaeological ceramics.* Heritage Science, 2017. **5**.
4. Edwards, H.G.M., *Porcelain Analysis and Its Role in the Forensic Attribution of Ceramic Specimens*. 2022: Springer.
5. Colomban, P., L. Arberet, and B. Kirmizi, *On-site Raman analysis of 17th and 18th century Limoges enamels: Implications on the European cobalt sources and the technological relationship between Limoges and Chinese enamels.* Ceramics International, 2017. **43**(13): p. 10158-10165.
6. Colomban, P., A.-T. Ngo, and N. Fournery, *Non-Invasive Raman Analysis of 18th Century Chinese Export/Armorial Overglazed Porcelain: Identification of the Different Enameling Techniques.* Heritage, 2022. **5**(1): p. 233-259.
7. Colomban, P., Y. Zhang, and B. Zhao, *Non-invasive Raman analyses of Chinese huafalang and related porcelain wares. Searching for evidence for innovative pigment technologies.* Ceramics International, 2017. **43**(15): p. 12079-12088.
8. Norris, D., D. Braekmans, and A. Shortland, *Emulation and Technological Adaptation in Late 18th Century Cloisonné‐Style Chinese Painted Enamels.* Archaeometry, 2022. **64**.
9. Giannini, R., *Optimisation of the LA-ICP-MS technique to provenance and authenticate Chinese porcelain*, in *Cranfield Forensic institute*. 2014-2015, Cranfield University. p. 499.
10. Van Pevenage, J., et al., *A combined spectroscopic study on Chinese porcelain containing ruan-cai colours.* Analytical methods, 2013. **6**: p. 387-394.
11. Jain, S., et al., *Significance of interface barrier at electrode of hematite hydroelectric cell for generating ecopower by water splitting.* International Journal of Energy Research, 2019. **43**.
12. Hajiyev, P., et al., *Contrast and Raman spectroscopy study of single- and few-layered charge density wave material: 2H-$TaSe_2$.* Sci Rep, 2013. **3**: p. 2593.
13. Marshall, C., W. Dufresne, and C. Rufledt, *Polarized Raman spectra of hematite and assignment of external modes.* Journal of Raman Spectroscopy, 2020. **51**.
14. Kırmızı, B., P. Colomban, and B. Quette, *On-site analysis of ChineseCloisonnéenamels from fifteenth to nineteenth centuries.* Journal of Raman Spectroscopy, 2009: p. n/a-n/a.

15. Wang, L., et al., *Micro‐structural characterization of red decorations of red and green color porcelain (Honglvcai) in China.* Journal of Raman Spectroscopy, 2009. **40**: p. 998-1003.
16. Colomban, P., et al., *The Technology Transfer from Europe to China in the 17th–18th Centuries: Non-Invasive On-Site XRF and Raman Analyses of Chinese Qing Dynasty Enameled Masterpieces Made Using European Ingredients/Recipes.* Materials, 2021. **14**(23): p. 7434.
17. Colomban, P., et al., *Raman identification of the different glazing technologies of Blue-and-White Ming porcelains.* Ceramics International, 2022. **48**(2): p. 1673-1681.
18. Colomban, P., et al., *Investigation of the Pigments and Glassy Matrix of Painted Enamelled Qing Dynasty Chinese Porcelains by Noninvasive On-Site Raman Microspectrometry.* Heritage, 2020. **3**(3).
19. Ballirano, P. and A. Maras, *Mineralogical characterization of the blue pigment of Michelangelo's fresco - "The Last Judgment".* AMERICAN MINERALOGIST, 2006. **91**: p. 997-1005.
20. Osticioli, I., et al., *Analysis of natural and artificial ultramarine blue pigments using laser induced breakdown and pulsed Raman spectroscopy, statistical analysis and light microscopy.* Spectrochimica Acta Part A: Molecular and Biomolecular Spectroscopy, 2009. **73**(3): p. 525-531.
21. Long, D., *The Raman Effect: A Unified Treatment of the Theory of Raman Scattering by Molecules*. 2002. p. 49-84.
22. Erk, P. and H. Hengelsberg, *Phthalocyanine Dyes and Pigments.* The Porphyrin Handbook: Phthalocyanines: Spectroscopic and Electrochemical Characterization, 2003. **16**: p. 117-170.
23. Defeyt, C., et al., *Micro-Raman spectroscopy and chemometrical analysis for the distinction of copper phthalocyanine polymorphs in paint layers.* Spectrochimica acta. Part A, Molecular and biomolecular spectroscopy, 2013. **115C**: p. 636-640.
24. Defeyt, C., et al., *Distinction by Micro-Raman Spectroscopy and Chemometrical Analysis of Copper Phthalocyanine Blue Polymorphs in Oil-Based and Acrylic Paint Samples*, in *Issues in Contemporary Oil Paint*, K.J. van den Berg, et al., Editors. 2014, Springer International Publishing: Cham. p. 105-116.
25. Agnieszka, P., et al., *The thermal properties and the flammability of pigmented elastomeric materials. Part I. Phthalocyanine pigments.* Journal of Thermal Analysis and Calorimetry, 2014. **117**: p. 789-798.
26. Miao, J., B. Yang, and D. Mu, *Identification and differentiation of opaque Chinese overglaze yellow enamels by Raman spectroscopy and supporting techniques.* Archaeometry, 2009. **52**: p. 146-155.
27. Colomban, P., et al., *Distinguishing Genuine Imperial Qing Dynasty Porcelain from Ancient Replicas by On-Site Non-Invasive XRF and Raman Spectroscopy.* Materials (Basel), 2022. **15**(16).
28. Ciaramitaro, V., et al., *Portable Spectroscopic Techniques for the Non-invasive Identification of two historical yellow pigments: Applications and Practical Challenges.* Journal of Physics: Conference Series, 2022. **2204**(1): p. 012056.
29. Šefců, R., Š. Chlumská, and A. Otmarová Hostašová, *An investigation of the lead tin yellows type I and II and their use in Bohemian panel paintings from the Gothic period.* Heritage Science, 2015. **3**.
30. Cazzanelli, E., et al., *Micro-Raman Analysis of the Pigments on a Crucifix in Calabria.* Applied Sciences, 2022. **12**: p. 6715.

31. Bellei, S., et al., *Multianalytical Study of Historical Luminescent Lithopone for the Detection of Impurities and Trace Metal Ions.* Analytical Chemistry, 2015. **87**(12): p. 6049-6056.
32. Srilakshmi, C., et al., *Fourier transform Raman spectral measurements of powdered quaternary mixtures of organic compounds: Exceptional pure component spectral reconstruction using band-target entropy minimization (BTEM).* Talanta, 2007. **72**(2): p. 847-853.
33. Franguelli, F., et al., *Thermal decomposition and spectral characterization of di[carbonatotetraamminecobalt(III)] sulfate trihydrate and the nature of its thermal decomposition products.* Journal of Thermal Analysis and Calorimetry, 2020. **145**.
34. Košařová, V., et al., *The efficiency of micro-Raman spectroscopy in the analysis of complicated mixtures in modern paints: Munch's and Kupka's paintings under study.* Spectrochimica Acta Part A: Molecular and Biomolecular Spectroscopy, 2016. **156**: p. 36-46.
35. Franquelo, M.L., et al., *Comparison between micro-Raman and micro-FTIR spectroscopy techniques for the characterization of pigments from Southern Spain Cultural Heritage.* Journal of Molecular Structure, 2009. **924-926**: p. 404-412.
36. Buzgar, N., et al., *The Raman study of the white pigment used in Cucuteni pottery.* Analele ştiinţifice ale Universităţii "Al. I. Cuza" din Iaşi. Seria Geologie., 2013. **59**: p. 41-50.
37. Zhu, S.-C., S.-H. Xie, and Z.-P. Liu, *Nature of Rutile Nuclei in Anatase-to-Rutile Phase Transition.* Journal of the American Chemical Society, 2015. **137**(35): p. 11532-11539.
38. Balasubramaniam, R., A.V.R. Kumar, and P. Dillmann, *Characterization of Rust on Ancient Indian Iron.* Current Science, 2003. **85**.
39. Colomban, P., T.-A. Lu, and V. Milande, *Non-invasive on-site Raman study of blue-decorated early soft-paste porcelain: The use of arsenic-rich (European) cobalt ores – Comparison with huafalang Chinese porcelains.* Ceramics International, 2018. **44**(8): p. 9018-9026.

Raman analysis on 18th and 19th-century Chinese porcelain.

PART 2: RESEARCH PLAN

Table of contents

1) Introduction

This master's dissertation will be conducted on the analysis of 18th and 19th-century Chinese porcelain using Raman spectroscopy. The background of this research is the Ph.D. performed by R. Giannini that focused on using laser ablation-inductively coupled plasma-mass spectrometry (LA-ICP-MS) on Chinese porcelain. She also optimized handheld-XRF for a comparative study between the results of LA-ICP-MS and XRF.[1] A subset of the samples used by R. Giannini will be analyzed by Raman spectroscopy. The main focus will be on analyzing the pigments. The goal is to build a database for pigments used in 18th and 19th century Chinese porcelain. This database has the purpose of helping in the detection of possible forgeries. The research will also focus on the identification of the glazes using micro-Raman spectroscopy. Lastly, a comparative study will be performed of the data obtained by Raman spectroscopy, LA-ICP-MS and XRF.

a) Raman spectroscopy

Raman spectroscopy is a non-invasive technique based on the Raman effect i.e. the inelastic scattering of light. It is a molecular technique, meaning that information about chemical structure, phases, crystallinity, molecular interactions and polymorphism can be obtained.[2]

When an incident beam hits a sample, the molecules are excited towards a virtual state. An energy transfer will take place from the photons to the molecule, resulting in vibrational transitions.[3] This technique is complementary to Infrared (IR) spectroscopy where the major difference between these two techniques is that the Raman effect is due to a change in polarizability of the chemical bonds while IR spectroscopy will detect a change in the dipole moment. In most cases, IR lasers will be less energetic than the lasers used in Raman spectroscopy. Infrared lasers are typically in the range of 800 nm to 1064 nm while Raman lasers can range from the UV region to the near-IR region. In IR spectroscopy, the molecules will absorb the energy resulting in the excitation of the molecule. This process is depicted in figure 1a.

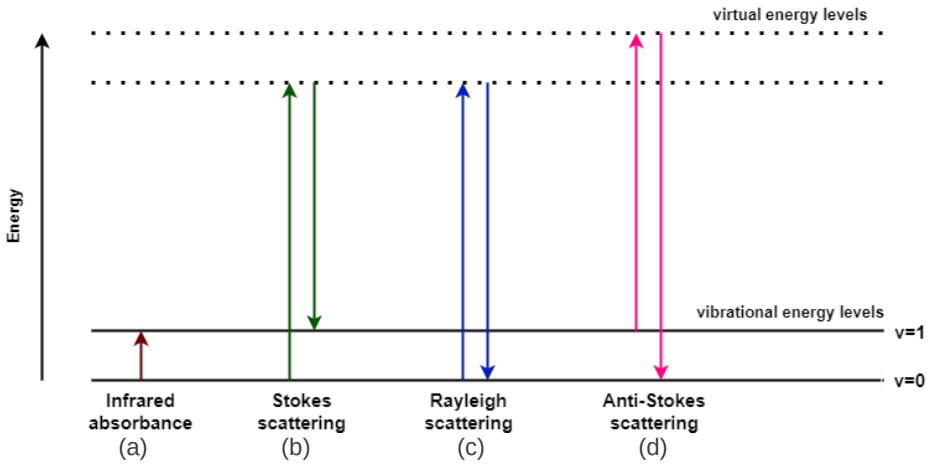

Figure 4: Overview of infrared absorbance and the transitions regarding the Raman effect.

After irradiation of the sample, the molecules can undergo different types of scattering. In figure 1, a schematic overview of the most important transitions regarding the Raman effect are given. In the first case, the molecule is excited from the ground state to the virtual state (figure 1b). The molecule will not fall back to the ground state but to a first vibrational level. In this case, the wavelength of the outgoing photon is less energetic and has thus a longer wavelength, this is known as Stokes scattering. In the second case, the molecule is excited to the virtual state and falls back to the ground state (figure 1c). Here, the energy of the

incoming photon is the same as the energy of the outgoing photon, this is the elastic scattering of light also known as Rayleigh scattering. Lastly, the molecule can already be in a first vibrational level and will be excited to a higher energetic virtual energy level (figure 1d). After excitation, the photon will fall back to the ground state. In this case, a photon will be emitted with a shorter wavelength, this is anti-Stokes scattering.

b) Porcelain

Up to this day, there is still no clear definition of porcelain. Nevertheless, a good definition would be: "Porcelain is a type of earthenware that is vitrified and glazed. Porcelains are fired in kilns in a reducing atmosphere at temperatures of typically around 1100°C up to 1400°C. They have a high translucency and could be classified according to their body composition, geological origin or external characteristics."[4-6]
Porcelain was originally discovered in China. Although a specific date cannot yet be attributed to the finding of porcelain, archaeological findings suggest that the first porcelains were made back in the Han dynasty (202BCE – 220CE).[7-8] During the early dynasties, porcelain was only manufactured commissioned by and for the emperors. It was not until the Song dynasty (960CE – 1279CE) that the privatization of the porcelain industry occurred.[9] With a thriving silk road, porcelain was a luxury trade item that was sought after by the riches from all over the world. Very soon, Jingdezhen became the porcelain capital of the world. This was partly due to the presence of *Kaolin* mines, which is the clay mineral used for the manufactory of porcelain in China. Porcelain only made its way to Europe in the 14th century after Marco Polo discovered and named it back in the 13th century.[10] In the centuries after this, Europe became obsessed with porcelain and the *maladie de la porcelaine* was spreading rapidly across the continent.
Porcelains are made by firing the raw materials at high temperatures in kilns. The main raw product is a clay-type material. Clay consists mostly of silica, alumina, magnesia and water where different types of clay and different elemental ratios are dependent on the provenance. In China, they had a clay called kaolinite ($Al_2(OH)_4Si_2O_5$), addressed as Kaolin earlier, which was the best suited for porcelain manufacturing. Due to the fact that these are fired at high temperatures, the chemical composition changes throughout this process. This is why chemical composition studies of the bodies and to a lesser degree the glazes are very difficult to perform. Therefore when analyzing the bodies of porcelains, raw materials or additives are studied that are the only possessor of a certain elemental oxide.[11] This means that a targeted elemental oxide can only be found in one certain material used for the manufactory of porcelain. Afterward, several other firing steps can be performed to add glazing and paint to the material.
A glaze is a glassy substance that covers the body of the porcelain. A glaze consists of three main ingredients: a glass former, a flux, and a stabilizer.[12] The glass former is usually a silica-based substance like clay. Because silica has a high melting point (1710°C),[13] fluxes were added to fire the glazes. A flux, typically lime or soda will lower the melting point. This made it easier to melt at temperatures that were more easily achieved.[12, 14] The flux will also make the glaze malleable enough to adhere to the porcelain. They will promote the liquefaction of the solid, meaning that they will promote the solid into the liquid phase more easily. In the liquid phase mass transfer will occur more easily, hereby, Al^{2+} can be substituted by for example K^+ or Na^+ and Si^{4+} (tetrahedral position) can be substituted by for example S^{6+} or P^{5+}. This process will thus lower the melting point of (alumino)sillicates.[15]
Lastly, stabilizers were added to strengthen the glaze, this would make sure that the glaze stuck to the body. Other oxides could be added to give color to the glazing. The main difference between glass and glaze is their crystallinity. While glass is usually completely amorphous, the network of glazes contains some crystalline phases.
There are two types of glazes, namely under- and overglazes. For overglaze porcelains, the paint is applied after the glazing is performed. For underglaze porcelains on the other hand, the paint is applied before the

glazing is performed. This has several consequences regarding the pigments that are used and the technique that's used to identify them. When an underglaze is applied, the glaze is fired at around 1300°C dissolving most of the paints and thus protecting them underneath the glaze. Due to the high temperatures, some pigments cannot be used as they degrade at these temperatures.[16] Overglaze porcelains are fired at around 850°C allowing more pigments to be used, like most red and gold pigments which cannot be used in underglaze porcelain.[17]

Porcelains can be subdivided based on their body composition. The body types became more elaborate throughout history, and new body types were added frequently. Table 1 gives an overview of the different body compositions of porcelain. Depending on the elemental oxides, colors were added to indicate a low (red) or a high (green) amount of that specific oxide. To be considered high or low varies from elemental oxide to elemental oxide. The three original body types were hard paste porcelain, soft paste porcelain and hybrid porcelain. The major difference between hard paste and soft paste porcelain is that hard paste porcelain contains a much higher amount of silicates and are fired at higher temperatures (1400°C vs 1200°C). Soft paste porcelains on the other hand contain much more phosphates. So, bone China and phosphatic bodies are soft paste porcelain (table 1). Historically hard paste porcelains are described as 'true porcelains' since the early Chinese porcelains were hard paste porcelain. Hybrid porcelains are porcelains that exhibit mixed traits from both hard- and soft paste porcelains.

Table 2: Overview of the different body types of porcelains, data collected by Howell G.M. Edwards.[11]

Body types\content	SiO_2(%)	Al_2O_3(%)	CaO(%)	P_2O_5(%)	MgO(%)	PbO(%)
hard paste	73[a]	19[b]	1	<1	<1	<1
magnesian	73	4	4	<1	10	2
glassy	73	4	9	<1	<1	7
bone china	42	13	23	17	<1	2
phosphatic	42	13	23	17	<1	<1
hybrid	73	4	1	<1	10	7

[a]Color scale is indicative of the concentrations, going from dark red = very low concentration to dark green = very high concentration.

[b]All values are numerical averages.

The recipe for porcelain stayed a secret to the Europeans for many centuries and it was only after the Jesuit missionaries in the 17th century that the recipe got leaked to Europe.[18] In the following period, Europe began to master the art of making porcelain and thus lowering the demand for Chinese porcelain. This resulted in China importing raw materials, especially European synthetic pigments to upper the quality of their porcelain. Colomban *et al*.[18] reported the use of European smalt (Cobalt silicates, K, Al) and Naples yellow ($Pb_2Sb_2O_7$) pigments in 18th century Chinese porcelains. Because there was an exchange of raw materials between Europe, China and other parts of the world, forgeries became more difficult to detect. As such, a proper database is needed for the characterization of porcelain.

In this research, pigments will be analyzed in the first place together with the glazes. Because all the artifacts have been provenanced, an overview can be given of the pigments that were used. Micro-Raman spectroscopy will be used for this. This will enable further research to simplify the detection of possible forgeries when analyzing the pigments and glazes using Raman spectroscopy.

2) Objectives

In this chapter, The objectives of this research will be explained as well as previous studies on the artifacts. The samples and their background will also be discussed in deep.

a) Previous research: Optimization of the LA-ICP-MS technique to provenance and authenticate Chinese porcelain.

This dissertation is the continuation of the Ph.D. of R. Giannini in 2015.[1] R. Giannini optimized laser ablation-inductively coupled plasma-mass spectrometry (LA-ICP-MS) for the analysis of Chinese porcelain. LA-ICP-MS was used to investigate the body compositions, glazes and pigments of 13th to 20th century Chinese porcelain. Provenance studies and dating of the samples were also conducted, classifying the artifacts by provenance and date. ICP-MS is one of the techniques that can be used for both dating and provenance studies. All the artifacts were authenticated and dated, this will be the starting point of this research. This research will use a subset of the samples that were analyzed by R. Giannini.

However, ICP-MS is not often used for the analysis of porcelain. The reason for this is the destructive character of this technique. Therefore, the researcher optimized the settings of the LA-ICP-MS to inflict minimal damage on these artifacts. Nonetheless, a minimal crater size is required to have enough material for analysis. The research was conducted to find the optimized parameters and it was found that a spot size of 80 µm was enough to collect accurate data. This crater size will not be visible to the naked eye.

b) Samples

The samples used for this research are a subset of the samples that R. Giannini researched. All the samples were dated, provenanced and classified accordingly. They were all provenanced to be from the Jingdezhen kilns and were manufactured between the 18th and 19th centuries.

The artifacts are from the Qing dynasty (1616CE – 1911CE) and it was during this dynasty the recipe of porcelain got leaked to Europe, in which followed an exchange of raw materials between China and Europe. This stresses the importance of researching these types of samples and the need for a proper database.

The names of the artifacts contain a suffix and a prefix. The suffix exists of two parts B. followed by BW or fr, BW stands for blue-and-white, fr stands for *famille rose*. The prefix contains the year and the number of the sample, so for example 1750.1. An overview of the samples is given in table 2.

- B.BW

These artifacts are from the private collection of Colin Sheaf, deputy chairman of Bonhams. Art Experts of Bonhams estimated the dates for these artifacts. All these are assigned to be from the kilns of Jingdezhen. All samples belong to the class of blue-and-white porcelains.

Interestingly, artifact B.BW.1780.1a shows a different body composition in comparison to the other porcelain shards. The research found that the body composition was more likely to be made out of raw material from the Zhejiang or Fujian provinces. R. Giannini provided three possible scenarios for this difference in body composition.[1]

a) they were originally potted in kilns located in either Zhejiang or Fujian provinces and, successively, decorated, glazed and fired at Jingdezhen.
b) they were both shaped and fired at Jingdezhen by employing raw materials imported from outside areas.
c) they were produced in kilns outside Jingdezhen, which had easy access to both types of raw materials.

- B.fr

These artifacts are also from the same private collection and have been dated by Chinese art experts. These artifacts belong to another porcelain family, the *famille rose* porcelains. They were all provenanced to be from the Jingdezhen kilns and are also from the Qing dynasty. Pictures of the samples are provided in figures 3a-I and a timeline of the different emperors of the Qing dynasty is provided in figure 2.

Table 3: Overview of the porcelain artifacts used in this research.

Artifact	Figure	Reign period	# of shards	Dimensions[a] (cm)	Provenance	Type of artifact
B.BW.1850.1	3a	Daoguang	1	1.5x2.0	Jingdezhen, Jiangxi	vase
B.BW.1720.2	3b	Kangxi	1	1.0x1.5	Jingdezhen, Jiangxi	Saucer dish
B.BW.1750.1	3c	Qianlong	1	1.7x0.8	Jingdezhen, Jiangxi	Octagonal dish
B.BW.1780.1a	3d	Qianlong	4	0.2x0.2 - 1.6x2.3	Jingdezhen, Jiangxi*	Coffee cup
B.FR.1850.4	3e	Daoguang	4	0.8x0.5 - 3.5x4.0	Jingdezhen, Jiangxi	Breakfast cup
B.FR.1830.1	3f	Daoguang	6	0.6x0.5 - 4.0x3.5	Jingdezhen, Jiangxi	Egg cup
B.FR.1800.1	3g	Jiaqing	7	1.5x0.4 - 2.0x3.4	Jingdezhen, Jiangxi	Spoon tray
B.FR.1750.2	3h	Qianlong	4	1.0x0.5 - 3.1x3.2	Jingdezhen, Jiangxi	dish
B.FR.1730.6	3i	Yongzheng	4	0.2x2.0 - 6.0x4.2	Jingdezhen, Jiangxi	Wine cup

[a]Dimensions of artifacts with more shards are expressed in a range from the smallest to the largest artifact.

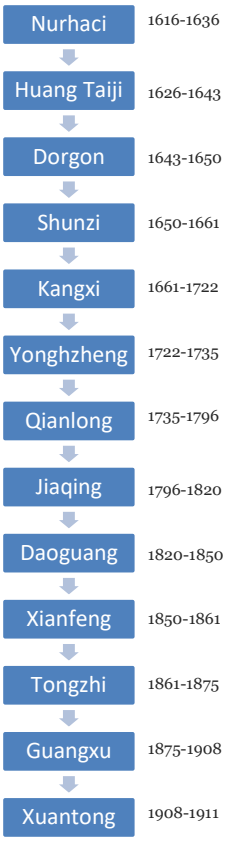

Figure 5: Timeline of the emperors in the Qing dynasty.

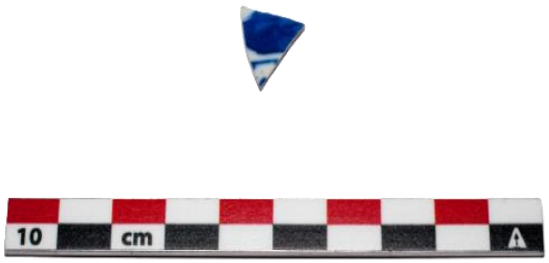

Figure 3a

Figure 3f

Figure 3b

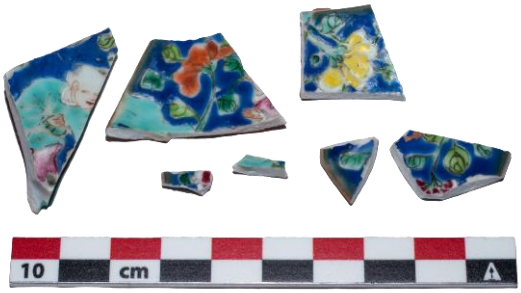

Figure 3f

Figure 3c

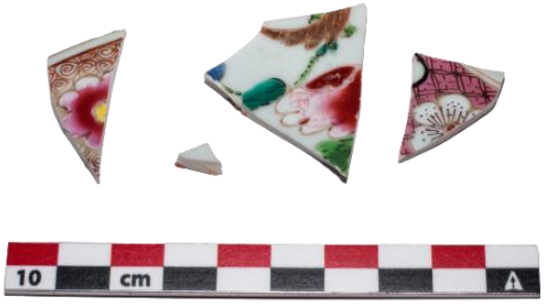

Figure 3h

Figure 3d

Figure 3i

Figure 3e

c) Objectives

In the 19th century, the west began to understand the basics of porcelain manufacturing, whereas China already performed the art for many centuries. As such, the hard paste porcelains coming from China were still superior to the ones made in Europe. Many forgeries were and still are on the market.

The research will be based on comparing the results of Raman spectroscopy with other analytical techniques. If proven effective for the study of porcelains, Raman data will be used to build a database. In the next paragraphs, an overview will be given of the objectives of this research.

Firstly, the settings of the Raman instrument will be optimized for the analysis of such precious artifacts. No damage can be inflicted on these, so the laser settings will be of utmost importance. This includes laser wavelength, laser power, focal position, exposure time, etc. In the next chapter, information about the lasers used for Raman spectroscopy and their characteristics will be given in detail.

In the next part, the compatibility of Raman spectroscopy with the samples will be tested. Although previous research has suggested compatibility, different glazes and pigments will behave differently depending on the type of laser, instrument, software, etc. For this dissertation, a dispersive confocal micro-Raman instrument will be used. In chapter 3 more information will be given about the different components of Raman instruments.

The first goal is to make a database of the pigments used in 18th and 19th century Chinese porcelain. It is important to be able to detect forgeries, an original piece is quickly worth over 50.000 euros whereas a forgery has at most decorative value. If Raman spectroscopy can be proven effective in the analysis of these pigments, the database can be a quick tool to achieve this. More samples will have to be analyzed before a proper database can be built. This research will hopefully be the start of such a database.

The second goal of this dissertation is to compare the results of the pigments obtained with LA-ICP-MS and Raman spectroscopy. As ICP-MS gives elemental information and Raman spectroscopy gives molecular information, both give complementary information. Raman spectroscopy can distinguish between different crystalline phases, polymorphism and oxidation states of the same compound where ICP-MS cannot. This is why Raman spectroscopy is useful because it gives more elaborate information about the used pigments in porcelain.

When the full database will be successfully constructed and after the comparative studies are performed, the research can shift toward the analysis of the body and glazes. R. Giannini also analyzed the body and glazes, meaning that the data for a comparative study are available. Here, probably another wavelength laser has to be used in comparison to the pigments. This brings some extra precautions with it as no damage can be inflicted on the samples.

Research question:

Is Raman spectroscopy suited for the analysis of pigments used in 18th and 19th century Chinese porcelain and can the settings be optimized so that spectra with high resolution can be recorded?

3) Porcelain analysis

In this chapter, a deeper look will be taken into previous research on porcelain in general. Further, the different techniques used in the past/present will be discussed.

a) Previous research

After 1300 years of keeping the recipe of porcelain a secret, the Jesuit mission in China during the 17th century took part of the recipe with them to Europe.[11, 19] Europe was more developed in the colors they had used for other types of ceramics, paintings, etc. The use of synthetic pigments like Naples yellow was already a part of European culture whereas China was sticking to its own techniques of painting glazes. After the fall of the Ming dynasty in 1644, Chinese artists fled to Japan.[20] Japan was more open to European techniques and Jesuits were already trading techniques with the Japanese in that era. The Kangxi emperor of China was impressed by European enamelware and set up a glass workshop at the imperial palace in 1695.[21] This marked the beginning of an exchange of techniques, materials and a new trade route between Europe and China.[22] After 1300 years of only small improvements, new raw materials and techniques were exchanged along the silk road, resulting in the fast improvement of porcelain and the founding of new porcelain families. Although these new improvements resulted in more vivid and better quality China, there were also some consequences. First off, this made it more difficult to assign certain pieces to the right manufactory, country and era and secondly, more and better forgeries hit the market.

Colomban *et al*.[18-19, 23] did extensive research on the raw materials and pigments found in 18th, 19th and 20th century Chinese porcelains. One of the biggest improvements in Chinese porcelain was due to the import of European synthetic pigments. Colomban *et al*. reported on the findings of Naples yellow, "Cassius purple" and European smalt in 18th century Chinese porcelains. This underlines the need for a proper database of the pigments that were used in 18th and 19th century porcelain. To achieve this, all information available is taken into consideration. By this, it is meant that the focus will not only be on one technique or only one field of science. In this case, the artifacts were firstly studied by Chinese art experts and were then analyzed by LA-ICP-MS and XRF. This research will provide new data that can be compared with the previous analytical techniques and the conclusions obtained by the Chinese art experts. By doing this, more elaborate information will be gained on these samples and a more entire perspective can be acquired.

Porcelain, also addressed as China is a type of earthenware that is vitrified and glazed as defined earlier in chapter 1.b. China has the denotation that it is better quality than porcelain although they are chemically the same. China refers to the country of origin while porcelain is derived from the Latin word "*porcella"* (seashell), the word china is more used in the United States while porcelain is more used in Europe.[24] Nonetheless, some researchers distinguish Porcelain and China as two different types of ceramics. Carty et al.[25] distinguished these based on the process used to manufacture them. Sometimes, china is also referred to as chinaware which is false because chinaware is tableware made out of china.[26] In this thesis, the word porcelain is used.

Porcelain consists of a body, a glaze and optionally some pigments. The body of classical triaxial porcelain contains a clay-type material, feldspar and quartz. In Chinese porcelain, Kaolinite was the primarily used clay. Feldspar is used as a fluxing agent in porcelains. It is an aluminum tectosilicate mineral meaning that it consists of Aluminosilicates bound to a metal, mostly Na, Ca or K (or rarer: Ba, Sr, Fe or Rb).[27] The different aluminum tectosilicates are bound to each other, forming repeating units, for example, $KAlSi_3O_8$ – $NaAlSi_3O_8$ –

$CaAl_2Si_2O_8$. Feldspars are divided according to their specific ratios of K/Na/Ca.[28] Sometimes, feldspar is substituted by Nepheline syenite ($K_2O.3Na_20.4Al_20_3.9SiO2$).[25] Lastly, quartz (Silicate) is used as a filler in the body, their role is to strengthen the body. Quartz can also be substituted by alumina if higher strength is required.[25]

The first analyses on porcelain were performed back in the 18th century.[29] The primary goal of the early European scientists of porcelains was knowing the recipe and the raw materials used for the craft. After the improvements of the analytical techniques, the research shifted toward the processes going on during the firing of porcelain. Soon after, the analyses shifted towards the scientific authentication of porcelain. In the following paragraphs, more information will be given about the techniques used for porcelain analysis.

b) Techniques used in the past/today

Several analytical techniques have been tested for the analysis of porcelain. The first modern analytical method used that gave information about the elemental composition of porcelains was scanning electron microscopy (SEM) in 1971.[30] Today still, scanning electron microscopy with electron dispersive X-ray analysis (SEM/EDX) stays the reference for porcelain analysis, especially for body composition. It is a technique used for analyzing the elemental compositions of the artifacts. Techniques like particle-induced X-ray fluorescence (PIXE), Mössbauer spectroscopy and neutron activation analysis (NAA) have been tested but the number of publications containing these techniques is rather low, as seen in figure 4. In this figure, the amount of publications per year starting from the first analytical study of porcelain up to 2021 is shown. Under the timeline, the names of the techniques indicate the year of the first published study containing that specific technique.[31-37] All data was found via webofscience.com by finding publications containing 'porcelain' and 'technique' as topics.

The amount of articles containing ICP-MS is rather low. Despite the accuracy that ICP-MS can achieve, its main drawback is its destructive character. For this research, LA-ICP-MS is of utmost importance for the authentication and provenance determination of the samples. XRD is used for crystalline structure analysis and phase analysis.[38] To identify the mineral composition of the sample, XRD is the main technique used.[39]

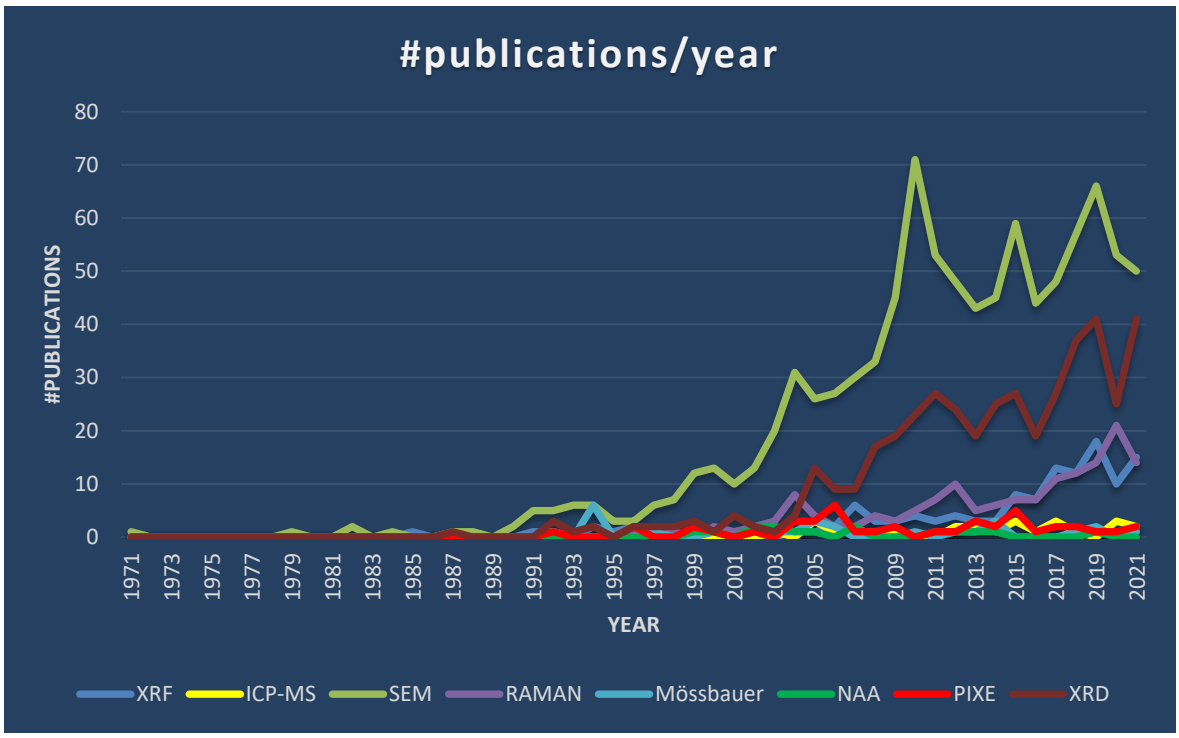

Figure 4: The number of publications per year containing porcelain analyses, data obtained via webofscience.com.

In the next paragraphs, the focus will lie on XRF, ICP-MS and Raman spectroscopy as these are the techniques that were used throughout the whole investigation of the samples.

i) X-Ray fluorescence (XRF)

X-ray fluorescence (XRF) is a widely used technique for the analysis of porcelain, especially portable XRF. XRF will give elemental information about the samples but cannot distinguish between different oxidation states of an element or crystalline properties.

The technique is semi-quantitative because only the counts can be compared and no absolute concentration is measured. For quantification, references are needed which are not always readily available for this kind of study. XRF is an important technique in the analysis of porcelain. It can confirm if certain elements/elemental oxides are present in the artifact. Another upside about XRF is that one can also compare certain analyzed areas on the same artifact. XRF is nearly always used together with XRD or Raman spectroscopy as they provide molecular information. The combination of XRF and XRD is mostly used when studying the body compositions while XRF and Raman are mostly combined for the study of pigments.

A lot of researchers have used portable XRFs for porcelain analysis. As some artifacts are quite big, portable XRF is an easy and straightforward technique that can be used to analyze these. The importance of using XRF mappings on porcelains have also been proven effective.[18-19, 40] XRF mappings show the distribution of several elements. This might be useful when analyzing overglazed porcelains that contain several different pigments.

ii) Inductively coupled plasma-mass spectrometry (ICP-MS)

As ICP-MS is a destructive technique, it is not always straightforward to use it in the analysis of porcelain. R. Giannini has demonstrated that LA-ICP-MS can be a solution if the inflicted damage is minimal and not visible to the naked eye. It can be used for provenance studies and dating and it is a very useful technique for the authentication of artifacts. It is of utmost importance with this kind of artifacts to strive for minimal or no inflicted damage during the analysis. This is why LA-ICP-MS can be helpful in the following years to authenticate artifacts. Once authenticated, the artifacts can be analyzed by other techniques like Raman spectroscopy or XRD and databases can be created using non-invasive techniques.

T. Zhu et al.[41] used LA-ICP-MS to investigate blue-and-white porcelains from the Yuan dynasty (1271CE – 1368 CE), focusing on the provenance determination of these artifacts. As a part of this research, T. Zhu et al. investigated the Co/FeO-ratio because all the artifacts contained Cobalt-based blue pigments. It was long thought that the amount and purity of cobalt determined the brightness of blue pigments. It was found that the less bright artifacts contained a higher Co/FeO-ratio than the brighter blue artifacts. This suggests that the amount of Cobalt has less influence than firstly thought and also demonstrates that the firing process, atmosphere and duration of the process play an important role in the color palette of porcelains. This underlines the importance of LA-ICP-MS in porcelain research.

c) Raman spectroscopy

In Raman spectroscopy, multiple geometries can be used for collecting the scattered laser light. The two major geometries in Raman spectroscopy are backscattering Raman spectroscopy and transmission Raman spectroscopy.

The most commonly used geometry for porcelain analysis is Raman backscattering spectroscopy (figure 5(a)). Here, the detector and the incident beam are on the same side of the sample. Due to the backscattering, there will be a strong signal coming from the surface layers,[42] which is needed in the analysis of the pigments. Photons have no mass and tend to backscatter more than heavier particles. So the likelihood of photons scattering backward and thus moving away from the sample is much higher than that they would scatter forward.

In the transmission Raman spectroscopy (figure 5(b)), the detector is positioned on the other side of the sample. Transmission Raman spectroscopy is a relatively new method and is used in different fields such as pharmaceuticals and geographical studies.[43-44] This geometry will lower the fluorescence and Raman signals from the top layer because the detector is on the other side of the sample.[42] Although there is less contribution from the surface layers, transmission Raman spectroscopy cannot differentiate between the

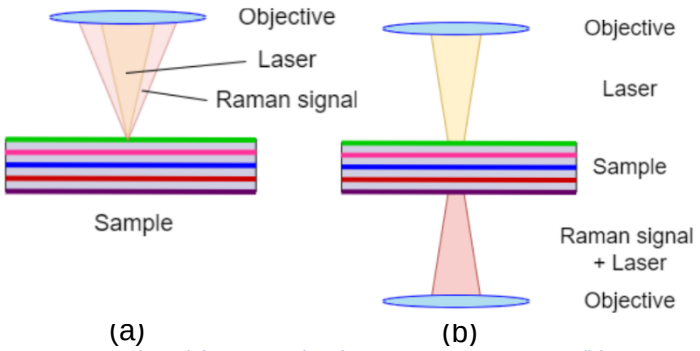

Figure 5: The different Raman geometries. (a) Raman backscatter spectroscopy (b) Raman transmission spectroscopy Figures based on data provided by Qin et al.[42]

signals of the different individual layers of the samples. The sample thickness also plays an important role

when using this geometry. If the sample is too thick, the scattered Raman signal may not be able to reach the detector on the other side of the sample.

In this research, Raman backscattering geometry will be used to perform the analysis of the porcelain shards. Low-powered lasers are equipped so that the upper layer can be investigated, in this case, the pigments. For overglaze porcelains this is quite straightforward, the beam can be focused on the exact spot that is analyzed. For underglaze porcelains on the other hand, the microscope has to be a little out of focus to be able to measure beneath the glaze.

i) Microscope

When using a micro-Raman spectrometer, a microscope is used to focus the laser beam on the sample to find the exact spot that needs to be analyzed. In this setup, the Raman spectrometer is equipped with a microscope with confocal pinholes between the incoming/outgoing beam and the sample. This way, an improved spatial resolution and a 3-dimensional map can be obtained.[45] The confocal pinhole consists of a small aperture that will only allow light to pass coming from the focal plane as seen in figure 6. By doing this, the light coming from other planes within the sample will not pass the pinhole thus improving the depth resolution drastically.[45] The pinhole is also called the detector pinhole because it is in front of the detector.[46] Figure 6 is a schematic overview of a confocal Raman spectrometer. It is a simplified schematic depicting the most important parts of the confocal instrument. The microscope is also equipped with a digital camera used to take microphotographs of the different analyzed spots on the sample.

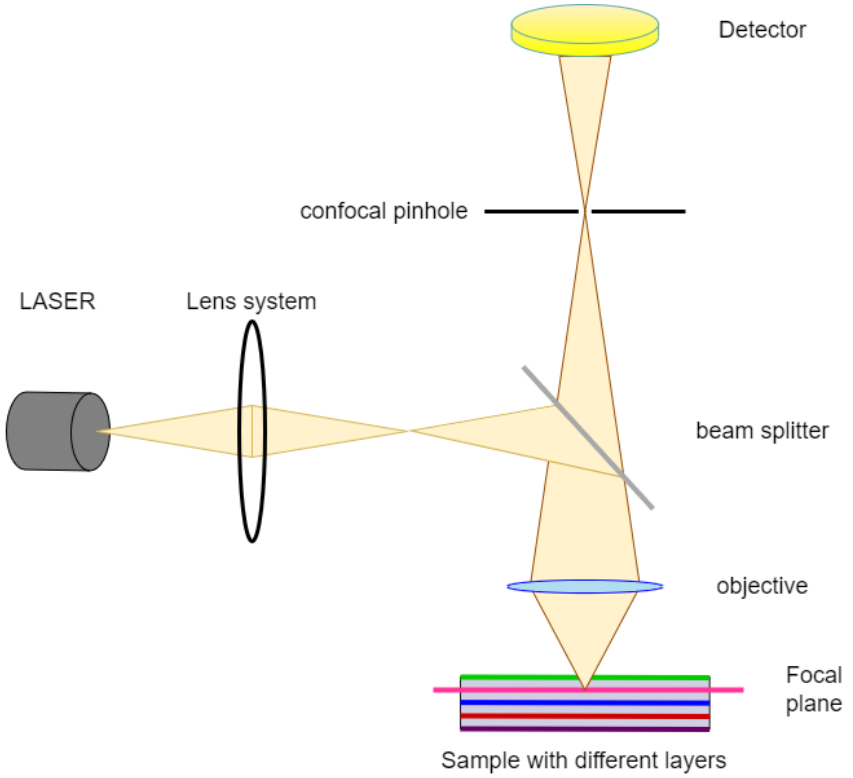

Figure 6: Confocal microscope in a Raman instrument. Figure based on research by Frohlich et al.[46]

ii) Lasers

The incident beam used for Raman spectroscopy is a laser. A laser is a highly monochromatic and intense beam of electromagnetic radiation. The importance of lasers in Raman spectroscopy lies in the fact that lasers with different wavelengths will affect the outcome of experiments differently. Lasers with different wavelengths are available, ranging from the UV region to the near-IR region.

For the analysis of porcelain, the 532 nm and 785 nm lasers are preferred. Especially the 785 nm laser as this laser tends to give the least fluorescence. If the fluorescence is too high, this can become higher than the Raman signal and thus masking the signal. The higher the wavelength, the lower the energy of the incoming beam, the lower the scattering. Higher wavelength lasers have higher power and give rise to weaker Raman signals and thus so, the exposure time should be prolonged.[47] This can induce laser damage which is tried to be avoided. Lower wavelength lasers (<500 nm) give too much fluorescence making them not suitable for porcelain analysis.

As the pigments are not known for this research, both the 532 nm and 785 lasers will be used. Some pigments exhibit a resonance effect when the excitation wavelength is close to the absorption wavelength of this molecule, enhancing the Raman signal.[48] The resonance effect is not predictable and thus the most information on the pigments is gained by using both lasers.

iii) Dispersive Raman instruments

For wavelengths below 800 nm, dispersive instruments are used. This has to do with the sensitivity of the detector. The most commonly used detectors are charged coupled devices (CCDs). The efficiency of these detectors drops fast after 800 nm making them not sensitive to infrared lasers.[3] For higher wavelength lasers, a Fourier-Transform Raman instrument is used. Here, semiconductors are used to detect Incoming photons. Because in this research the 532 nm and the 785 nm lasers are used, a dispersive Raman instrument is used.

The collected backscattered photons pass through the confocal pinhole and are then headed to the spectrograph. In the spectrograph, a diffraction grating will separate the Raman signal in its according wavelengths. The separation of light is based on constructive and destructive interference due to the presence of lines in the grating.[49]

Dispersive Raman instruments can achieve very high sensitivity, making it possible to measure at trace and ultra-trace levels. They need lower laser power and acquisition times than FT-Raman instruments[50] lowering the chances of damaging the porcelains. Another advantage of dispersive Raman instruments is that they have a lower signal-to-noise ratio than FT-Raman instruments.

Nowadays, dispersive instruments with a CCD and a semiconductor detector are available on the market, making them suitable for all wavelength lasers.[51] Also more in general, the miniaturization of Raman instruments plays a prominent role in the evolution towards the use of dispersive instruments. As the transportation of porcelains has some risks, the on-site analysis of porcelains is gaining interest. Colomban et al.[18-19, 23, 40, 52] have proven the feasibility of using on-site Raman spectroscopy using a dispersive Raman instrument for the analysis of porcelain, especially the glazes and pigments.

iv) Filters

When a molecule gets excited, the biggest part of the scattered light will be Rayleigh scattering (elastic scattering of light). As the Raman effect is relatively weak, it is crucial to block out the elastic scattering to ensure the detector does not get overwhelmed. This can be done by using filters before the scattered signal reaches the detector.[53] Two types of filters are used for this purpose, namely a notch or an edge filter.

A dielectric edge filter can either be a long pass filter or a short pass filter.[54] These filters will block the light under/over a certain threshold. A long pass edge filter on an instrument with a 532 nm laser will for example absorb all the light beneath 534 nm. This implies that only a Stokes or anti-Stokes spectrum can be recorded using these filters.

Holographic notch filters are band block filters, these only block the Rayleigh scattering. They are based on destructive interference. When irradiated, the filter will bock out the photons with the same wavelength as the incoming beam. The only disadvantage of this filter is that they degrade, due to the fact that part of the laser light is absorbed and released as heat.[53] For the analysis of porcelain, it is also necessary to use a neutral density filter. This filter reduces the intensity of the incoming laser beam to avoid any damage.

v) Miniaturization

The miniaturization of Raman instruments is an ongoing process. The first portable Raman instrument for art analysis was MArtA, made by the Raman group at Ghent University in 1997.[55] Since then, further miniaturization has taken place and even handheld Raman spectrometers have been developed. These instruments are used for on-site analysis. This is especially useful for the analysis of artifacts that cannot be transported or that are too expensive to transport like example rock paintings, frescos, large paintings or porcelains. Portable and handheld instruments are specially designed for identification rather than quantification. Most miniaturized instruments are dispersive instruments.

d) Advantages regarding Raman spectroscopy

the biggest advantage of using Raman spectroscopy is the fact that it is a non-invasive technique. With such precious artifacts, the need for these techniques is really important, especially when talking about whole artifacts. Raman spectroscopy will provide information on the vibrations of the molecules and thus Raman spectroscopy can differentiate between different molecules and phases present as mentioned earlier. Especially for pigment analysis, it is together with XRD the only technique that will be able to achieve this. Raman spectroscopy can be used for analyzing gasses, liquids and solids. Depending on the acquisition time, the number of scans, required resolution and chosen spectral range the time of analysis can differ between a couple of seconds to a couple of hours. Still, Raman is a relatively quick technique, especially for handheld instruments the scans can be recorded within several minutes.

Because different lasers can be used, problems occurring with one laser can be resolved by using another one. This simple solution is why it is a very versatile technique. Of course, other wavelengths can bring other challenges with them like longer measuring times, higher laser powers, etc. Lateral and depth resolution can be enhanced by switching between different geometries, increasing the number of scans or by adapting the aperture when working with a confocal microscope. Different filters can also be used to improve spectra such as polarization filters, neutral density filters, etc.

Another upside is that little or no sample pretreatment is needed. Little pieces of samples can be scalped of, to be embedded in a polymer film. However, this is not required meaning that most samples can directly be analyzed. Although, by embedding samples, there is no Raman signal coming from other layers of the whole artifact, improving the spectra. Raman spectroscopy can detect the pigments in porcelain as well as the degradation products if present. This is also an advantage as the original pigment can be traced back via the degradation product.[56]

An advantage of Raman- over IR-spectroscopy is that there will be no interference from water. In IR-spectra the presence of water or an alcohol group gives rise to a very broad band whereas this is not valid for Raman spectra. Also, glass vials can be used whereas for IR-spectroscopy this would cause interference.

e) Challenges regarding Raman spectroscopy

When performing Raman experiments, several problems might occur. The problems themselves and their solution(s) will be discussed.

i) Rayleigh scattering

As aforementioned, the Raman effect is relatively weak while Rayleigh scattering is much more intense. It is thus vital that the elastic scattering is filtered out, these filters have been addressed in chapter 4.c.iv.

ii) Absorption

When a molecule absorbs the incoming radiation, the molecules are excited. The Raman effect is based on the excitation of vibrational states of the molecule. Nonetheless, When the energy of the laser corresponds to one of the absorption bands, the molecule can absorb the incoming light. This is clearly in competition with the Raman effect. This can be avoided by using a different wavelength laser.

iii) Fluorescence

Fluorescence is the most occurring problem when doing Raman experiments. When the energy of the laser corresponds to the energy difference between electronic states, the molecule can get electronically excited. The molecule then first releases its energy via radiationless transitions until the molecule reaches a lower excited electronic state. After this, the molecule will emit a photon, this means that the photon released will have a longer wavelength than the incoming photon.[57-58] For some molecules the fluorescence background interferes so that it will be higher than the Raman effect. The only way to solve this problem is to not get the molecules in an electronically excited state. This can only be done by choosing another wavelength laser. The higher the wavelength of the laser, the lower the chances of fluorescence as the incoming energy is lower. If the molecules cannot reach an electronically excited state, they cannot fluoresce. Florescence can thus be a problem when using a 532 nm laser.

iv) Laser damage

The intensity of the Raman signal is proportional to the fourth power of the laser frequency.[59] This implies that if the laser frequency is increased, the intensity of the Raman signal enhances drastically. The problem with this is that this can also lead to permanent damage to the sample. So if not careful, Raman spectroscopy can lose its non-destructive character.

When a high-power laser is used, a plasma is generated. A plasma in its turn will generate a recoil pressure which will drive a compression wave onto the sample,[60] which is the first process that can damage the sample. A second process that might occur is heating of the sample. A lot of energy reaches the sample, if the heat generated cannot escape quickly enough to the environment, the sample will start to heat up. The heating of the sample can also interfere with the measurements as the emission of blackbody radiation (by the heated samples) can overrule the spectrum.[61] Neutral density filters are used to lower the power of the lasers and so avoiding possible damage to the porcelains.

v) Boson peak

There is a peak for glassy materials at lower wavenumbers, usually around 100-200 cm^{-1} which is called the boson peak.[40] When the molecules get excited, a certain amount of molecules will reach a virtual state. The amount of molecules that are in this state is described by the density of states. The quantum mechanical equivalent of a normal vibrational mode is addressed by the term phonon. It is defined as a unit of vibrational energy that arises from oscillating atoms within a crystal.[62] When a certain value is exceeded, the Debye value, low energy scattering occurs and is seen as a narrow peak in a Raman spectrum. Most software

eliminates this peak by using a baseline subtraction. The best baseline subtraction for this problem is a 4-segment baseline correction.[18]

vi) Spikes

Spikes are narrow peaks appearing in a Raman spectrum. Spikes are coming from cosmic rays hitting a CCD detector.[63] These are by consequence only a problem if you are working with a dispersive Raman instrument. Spikes cannot be avoided and will thus always be present. Nonetheless, data algorithms are developed to remove these when performing the data treatment.

f) Conclusion

XRF and ICP-MS retrieve elemental information which is different from Raman spectroscopy as is a molecular technique. As such, Raman spectroscopy will give supplementary information on the Chinese porcelains. This is why by combining these different techniques, an overview can be acquired regarding the pigments used in 18th and 19th century Chinese porcelains. . By combining the different techniques, the whole picture will be gained. The ICP-MS provenance data and dating will provide a baseline for this research. A dispersive Raman instrument will be used in backscatter geometry using a confocal microscope. By analyzing the pigments used, a database can be built and used in further research/authentication of porcelain.

4) Research methodology

The research plan of this dissertation will be divided into 6 work packages (WP). The work packages will be a guideline for the whole thesis, especially for the experimental work. Every work package will consist of the goal of the respective package and a brief description of the work to be performed.

a) WP 1: Writing the research plan

The first part of this master's dissertation consists of writing the research plan. This includes conducting a literature study, writing the objectives, going over the work packages and situating this research regarding to other related research.

b) WP2: Optimizing the settings of the Raman instrument

The settings of the Raman instrument will be optimized to get spectra that are as free from interferences as possible. The Raman instrument used is the Senterra Raman spectrometer from Bruker equipped with a 532 nm and a 785 nm laser.[64] It is important to optimize the measuring conditions including the number of scans, acquisition time, spectral region and laser settings. The laser and laser power will be important factors to consider because no damage can be inflicted on the samples, they will thus have to be chosen carefully.

c) WP3: Focusing the confocal microscope and taking microscopic pictures of the analyzed spots

Before every measurement, the microscope will have to be focused on the right spot. For the underglaze porcelains, the microscope will have to be a bit defocused to measure under the glaze. The Hirox is going to be used to take microphotographs. The Hirox microscope has a higher magnification and a better quality than the confocal microscope of the Raman instrument. These pictures can visualize certain stratigraphic information like inclusions, imperfections, laser ablation craters, etc which can influence the measurement.

d) WP4: Performing the analyses

A roadmap will have to be set up to work as efficiently as possible. Two options are considered here. Firstly, an object-to-object approach can be performed, this means that all the different pigments within the same artifact are analyzed and so forth. A second approach is the color-to-color approach. Here, a comparison is made between the same color on different artifacts. So first yellow can be analyzed, then green, blue, and so on. The object-to-object approach will give a much broader view while the color-to-color approach is a much more comparative approach. For this research, the object-to-object approach is going to be used.

e) WP5: Data analysis

The data analysis will be split up into several different parts. First of it is important to learn how to interpret Raman spectra, this will be the start of the data analysis. Followed by comparing the acquired data with literature spectra coming from the same types of research. When all data is treated, the focus will be on the following main goals.

i) Building a database

This research will serve as the start of a database for pigments in 18th and 19th century Chinese porcelain. The data will be summarized and the goal is to use this data in the future to authenticate these artifacts more straightforwardly by using Raman spectroscopy.

ii) Comparative study of LA-ICP-MS and Raman spectroscopy (pigments)

The second goal of this research is the comparative study of the pigments between LA-ICP-MS and Raman spectroscopy. A qualitative comparison will be made with the data obtained by R. Giannini.

iii) Comparative study of XRF and Raman spectroscopy (pigments)

R. Giannini used handheld-XRF for a comparative study with LA-ICP-MS. For this research, the Raman group at the Ghent university performed micro-XRF on some samples if clarity was needed. Here, a comparison can be made between Raman spectroscopy, handheld-XRF and micro-XRF to test the feasibility of XRF for these studies.

iv) Comparative study of LA-ICP-MS and Raman spectroscopy (body and glazes)

In the last step, the body and glazes will be analyzed. R. Giannini did extensive work on these and enough data is provided to do a comparative study between LA-ICP-MS and Raman spectroscopy.

f) WP6: Writing the thesis

In the last step, the thesis is going to be written and all data will be interpreted and visualized.

5) References

1. Giannini, R. Optimisation of the LA-ICP-MS technique to provenance and authenticate Chinese porcelain. Cranfield University, 2014-2015.
2. scientific, H. What is Raman spectroscopy? https://www.horiba.com/usa/scientific/technologies/raman-imaging-and-spectroscopy/raman-spectroscopy/#top.
3. Vandenabeele, P., *Practical Raman Spectroscopy: An introduction*. Wiley: 2013.
4. Merriam-Webster Definition of porcelain. https://www.merriam-webster.com/dictionary/porcelain.
5. Britannica, T. E. o. E. p. E. B., 10 Jan. 2020, https://www.britannica.com/art/porcelain. .
6. Press, C. U. Porcelain. https://dictionary.cambridge.org/dictionary/english/porcelain.
7. Liu, C., Prosperity of ceramics—History and features of ancient Jingdezhen city. *Jianghan Archaeology* **2008,** *106* (1), 104-109.
8. Zhang, X.; Xie, H.; Zhou, C.; Zeng, B., Jingdezhen: The millennium porcelain capital. *Cities* **2020,** *98*, 102569.
9. Xiao, X.; Li, S.; Li, X., The landscape evolution of Jingdezhen ceramic industrial settlements and its driving factors. *Journal of Ceramics* **2013,** *34* (2), 255-260.
10. Tharp, L., Treasures of Chinese porcelain. Denyer, I., Ed. BBC, 2011.
11. Edwards, H. G. M., *Porcelain Analysis and Its Role in the Forensic Attribution of Ceramic Specimens*. Springer: 2022.
12. Rhodes, D., *Clay and Glazes for the Potter* Literary Licensing, Llc: 1973.
13. Nippon Sheet Glass Co., L. The chemistry of glass. https://www.pilkington.com/en/us/architects-page/glass-information/the-chemistry-of-glass.
14. Zaid, S.; Halim, M.; Abdullah, M. A. A.; muhamad nor, M., The Effect of Flux to Physical and Chemical Properties of Ceramic Body Using Ball Clay from Kampung Dengir, Besut, Terengganu. *Materials Science Forum* **2017,** *888*, 157-161.
15. Kiss, E.; Panic, S., Accelerated physical and chemical transformations in ceramics processing. *Journal of the Serbian Chemical Society* **2019,** *84* (10), 1055-1071.
16. Bersani, D.; Lottici, P. P., Raman spectroscopy of minerals and mineral pigments in archaeometry. *Journal of Raman Spectroscopy* **2016,** *47* (5), 499-530.
17. House, T. D. P. What is the difference between overglaze und underglaze? https://www.dphtrading.com/customer-service/guides/tips-and-ideas/what-is-the-difference-between-overglaze-und-underglaze#:~:text=What%20is%20the%20important%20difference,Thus%20underglaze.
18. Colomban, P.; Kırmızı, B.; Zhao, B.; Clais, J.-B.; Yang, Y.; Droguet, V., Investigation of the Pigments and Glassy Matrix of Painted Enamelled Qing Dynasty Chinese Porcelains by Noninvasive On-Site Raman Microspectrometry. *Heritage* **2020,** *3* (3).
19. Colomban, P.; Gironda, M.; Vangu, D.; Kırmızı, B.; Zhao, B.; Cochet, V., The Technology Transfer from Europe to China in the 17th–18th Centuries: Non-Invasive On-Site XRF and Raman Analyses of Chinese Qing Dynasty Enameled Masterpieces Made Using European Ingredients/Recipes. *Materials* **2021,** *14* (23), 7434.
20. Tougher, S.; Abusch, R. a.; Bardel, R.; Bullough, V. L.; Gaul, N.; Hales, S.; Lightfoot, J. L.; Llewellyn-Jones, L.; Mullett, M.; Sidéris, G.; Stevenson, W.; Tsai, S.-s. H.; Witt, R., *Eunuchs in Antiquity and Beyond*. Classical Press of Wales: 2002.
21. Ma, H.; Henderson, J.; Cui, J.; Chen, K., Glassmaking of the Qing Dynasty: A Review, New Data, and New Insights. *Advances in Archaeomaterials* **2020,** *1* (1), 27-35.
22. Montanari, R.; Murakami, N.; Colomban, P.; Alberghina, M. F.; Pelosi, C.; Schiavone, S., European ceramic technology in the Far East: enamels and pigments in Japanese art from the 16th to the 20th century and their reverse influence on China. *Heritage Science* **2020,** *8* (1), 48.
23. Colomban, P.; Ngo, A.-T.; Fournery, N., Article Non-invasive Raman Analysis of 18 th Century Chinese export/armorial Overglazed Porcelain: Identification of the Different Enameling Techniques. *Heritage* **2022**.

24. Noritake What is China. https://noritakechina.com/what-is-china.
25. Carty, W.; Senapati, U., Porcelain—Raw Materials, Processing, Phase Evolution, and Mechanical Behavior. *Journal of the American Ceramic Society* **2005,** *81*, 3-20.
26. Merriam-Webster Chinaware. https://www.merriam-webster.com/dictionary/chinaware
27. Dietrich, R. V. Feldspar. https://www.britannica.com/science/feldspar.
28. King, H. M. Feldspar. https://geology.com/minerals/feldspar.shtml.
29. Joseph Needham, T. T.-H., Science and Civilisation in China: Volume 5, Chemistry and Chemical Technology. Cambridge University Press: 2004; pp 37-42.
30. Daniels, W. H.; Martin, G. A., FRACTURE ANALYSIS OF A TRIAXIAL PORCELAIN USING SEM. *AMERICAN CERAMIC SOCIETY BULLETIN* **1971,** *50* (4), 444-&.
31. Lin, E. K.; Wang, C. W.; Teng, P. K.; Huang, Y. M.; Chen, C. Y., ELEMENTAL ANALYSIS WITH EXTERNAL-BEAM PIXE. *NUCLEAR INSTRUMENTS & METHODS IN PHYSICS RESEARCH SECTION B-BEAM INTERACTIONS WITH MATERIALS AND ATOMS* **1992,** *68* (1-4), 281-284.
32. Gao, Z. Y.; Chen, S. H.; Zhu, W. L., MOSSBAUER-SPECTRA STUDY OF SKY-GREEN GLAZE OF THE IMITATION ANCIENT RU PORCELAIN. *CHINESE SCIENCE BULLETIN* **1992,** *37* (19), 1598-1602.
33. Wu, J.; Li, J. Z.; Guo, J. K.; Xu, K.; Chen, B. L., Study on trace element of Yue ware unearthed at different kiln sites. *SCIENCE IN CHINA SERIES E-TECHNOLOGICAL SCIENCES* **1999,** *42* (4), 376-382.
34. Yap, C. T.; Tang, S. M., Quantitative XRF Analysis of Trace Barium in Porcelains by Source Excitation. *Applied Spectroscopy* **1985,** *39* (6), 1040-1042.
35. Buerhop, C.; Condrate, R. A.; Moertel, H.; Hapanowicz, R. P., RAMAN MICROPROBE STUDY OF INCLUSIONS IN GLAZES ON PORCELAIN DISHES. *APPLIED SPECTROSCOPY* **1992,** *46* (10), 1545-1547.
36. Bagby, M.; Marshall, S. J.; Marshall, G. W., XRD PEAK SHAPE-ANALYSIS OF 2 ALLOYS DURING PORCELAIN APPLICATION. *JOURNAL OF DENTAL RESEARCH* **1987,** *66*, 205-205.
37. Li, B., Application of ICP-MS trace element analysis in study of ancient Chinese ceramics. *Chinese Science Bulletin* **2003,** *48* (12), 1219.
38. Sherwood, P. M. A., Carbons and Graphites: Surface Properties of. In *Encyclopedia of Materials: Science and Technology*, Buschow, K. H. J.; Cahn, R. W.; Flemings, M. C.; Ilschner, B.; Kramer, E. J.; Mahajan, S.; Veyssière, P., Eds. Elsevier: Oxford, 2001; pp 985-995.
39. Meor Yusoff Meor, S. In *Application of XRF and XRD in the study of ceramics and pottery*, Proceedings of National Conference on Science and Technology in Conservation of National Heritage: Integration of Science, Technology and Heritage, Malaysia, Malaysian Inst for Nuclear Technology Research MINT: Malaysia, 2004; p 274.
40. Simsek, G.; Casadio, F.; Colomban, P.; Bellot-Gurlet, L.; Faber, K. T.; Zelleke, G.; Milande, V.; Moinet, E., On-Site Identification of Early BÖTTGER Red Stoneware Made at Meissen Using Portable XRF: 1, Body Analysis. *Journal of the American Ceramic Society* **2014,** *97* (9), 2745-2754.
41. Zhu, T.; Ding, X.; Kusimba, C.; Feng, Z., Using laser ablation inductively coupled plasma mass spectroscopy (LA-ICP-MS) to determine the provenance of the cobalt pigment of Qinghua porcelain from Jingdezhen in Yuan Dynasty of China (1271–1368AD). *Ceramics International* **2015,** *41*.
42. Qin, J.; Kim, m. s.; Chao, K.; Schmidt, W.; Dhakal, S.; Cho, B.-K.; Peng, Y.; Huang, M., Subsurface inspection of food safety and quality using line-scan spatially offset Raman spectroscopy technique. *Food Control* **2017,** *75*, 246–254.
43. Pelletier, M. J.; Larkin, P.; Santangelo, M., Transmission Fourier Transform Raman Spectroscopy of Pharmaceutical Tablet Cores. *Applied Spectroscopy* **2012,** *66* (4), 451-457.
44. Hwang, J.; Kang, S.; Lee, K.; Chung, H., Enhanced Raman spectroscopic discrimination of the geographical origins of rice samples via transmission spectral collection through packed grains. *Talanta* **2012,** *101*, 488-494.

45. Giridhar, G.; Manepalli, R. R. K. N.; Apparao, G., Chapter 7 - Confocal Raman Spectroscopy. In *Spectroscopic Methods for Nanomaterials Characterization*, Thomas, S.; Thomas, R.; Zachariah, A. K.; Mishra, R. K., Eds. Elsevier: 2017; pp 141-161.
46. Frohlich, V.; Pawley, J., Tutorial on Practical Confocal Microscopy and Use of the Confocal Test Specimen. 2010; pp 627-649.
47. instruments, E., How to choose your lasers for Raman spectroscopy. https://www.edinst.com/, 2022.
48. Fujisawa, T.; Unno, M., Vibrational optical activity spectroscopy. Elsevier: 2020; pp 41-82.
49. Borio, V.; Jr, R.; Nicolau, R.; De Oliveira, H.; Lima, C.; Silveira, L., Quantitative Evaluation of Acetaminophen in Oral Solutions by Dispersive Raman Spectroscopy for Quality Control. *Journal of Spectroscopy* **2012,** *27*.
50. kaiserEHtech, Advantages of Dispersive Over Fourier Transform (FT) Raman Spectroscopy. In *Raman Products Technical Note*, Number 1105 ed.; kaiserEHtech, Ed. 2014.
51. Patil, C. A.; Pence, I. J.; Lieber, C. A.; Mahadevan-Jansen, A., 1064 nm dispersive Raman spectroscopy of tissues with strong near-infrared autofluorescence. *Opt. Lett.* **2014,** *39* (2), 303-306.
52. Colomban, P.; Milande, V., On-site Raman analysis of the earliest known Meissen porcelain and stoneware. *Journal of Raman Spectroscopy* **2006,** *37* (5), 606-613.
53. Owen, H., Holographic notch filter. *Proceedings of SPIE - The International Society for Optical Engineering* **1991**.
54. Shukla, R. P.; Kumar, S.; Sinha, A. K.; Mallick, M.; Thakur, S.; Sahoo, N. K., A comparative performance evaluation of micro-Raman spectrograph using holographic notch filter and dielectric filter. *Pramana* **2006,** *67* (2), 277-289.
55. Vandenabeele, P.; Castro, K.; Hargreaves, M.; Moens, L.; Madariaga, J. M.; Edwards, H. G., Comparative study of mobile Raman instrumentation for art analysis. *Analytica chimica acta* **2007,** *588* (1), 108-16.
56. Deneckere, A. Development, optimisation and application of Raman

spectroscopic and X-ray fluorescence spectroscopic

methodology in the field of cultural heritage. hent University, 2011.
57. Ramsteiner, M.; Wild, C.; Wagner, J., Interference effects in the Raman scattering intensity from thin films. *Applied optics* **1989,** *28* (18), 4017-23.
58. Schaller, C.; Wong, D.; Neils, T. Electronically Excited Molecules can Relax by a Number of Processes. https://chem.libretexts.org/@go/page/13647.
59. Fan, F.; Feng, Z.; Li, C., UV Raman Spectroscopic Studies on Active Sites and Synthesis Mechanisms of Transition Metal-Containing Microporous and Mesoporous Materials. *Accounts of Chemical Research* **2010,** *43* (3), 378-387.
60. Rastogi, V.; Chaurasia, S.; Munda, D. S., Laser induced damage studies in borosilicate glass using nanosecond and sub nanosecond pulses. *Journal of Non-Crystalline Solids* **2017,** *463*, 138-147.
61. Renishaw, Advantages of dispersive Raman over FT-Raman. *Renishaw apply innovation* **2004,** *SPD/TN/014* (4.0).
62. Perkowitz, S. Phonon. https://www.britannica.com/science/phonon.
63. Tian, Y.; Burch, K., Automatic Spike Removal Algorithm for Raman Spectra. *Applied Spectroscopy* **2016,** *70*.
64. Bruker, Senterra user manual. bruker, Ed. bruker.com, 2022.

Raman analysis on 18th and 19th-century Chinese porcelain.

PART 3: RESEARCH PROJECT

Table of contents

1) Experimental

In this thesis, 18th and 19th-century Chinese porcelains were subjected to Raman analyses. Two different sample sets were investigated by means of two different Raman spectrometers. On the one hand, a benchtop Raman instrument was used, on the other hand, a portable Raman instrument was used to analyze the samples. The first sample set has been discussed in Part 1 of this master thesis, while the other sample set will be discussed in section 1.a.ii.

a) Sample sets

i) Collin Sheaf's private collection (sample set 1)

The first samples are a set of porcelain shards belonging to Collin Sheaf, Deputy Chairman of Bonhams and Global Head of Asian Art. These samples have been extensively discussed in Part 1, section 2.b. This sample set will be referred to as 'sample set 1'.

ii) Qianlong and Jiaqing porcelain (sample set 2)

The second sample set was provided by Dr. Dennis Braekmans of Leiden University.[1] This sample set contains two subsets. One contains 18th century cloisonné-style Chinese porcelain. This subset was previously investigated by means of ESEM-EDX and LA-ICP-MS. *C*loisonné-style refers to the manufacturing technology. This style is made by decorating enamelware with polychrome patterns. Enamel is a vitrified coating that is applied to a metallic body.[1] The other subset contains *famille rose* and *famille jaune* styles porcelain. For the previous research, all the samples from both subsets were embedded into a polymer. To obtain these embedded samples, small fragments of damaged areas were scalped off, surface cleaned, and mounted on stubs. The advantage of embedded samples is that it facilitates measuring underneath the glaze. This sample set will be referred to as 'sample set 2'. Detailed pictures of the embedded samples and artifacts are given in Appendix 1.

b) Raman instruments

As mentioned before, within the scope of this thesis, both a benchtop Raman instrument as well as a portable one were used. It was expected that the benchtop instrument would yield the best results in terms of spectral quality. In addition, the amount of pigments that could be identified was expected to be higher with the benchtop instrument. An important reason to use the portable Raman instrument is, that it allows to measure in situ. It was thus used to test if this would work accordingly for porcelain artifacts.

i) Senterra Raman benchtop instrument

The Raman spectra were obtained via the Senterra dispersive Raman instrument from Bruker optics. The Senterra is equipped with a confocal microscope type BX51. It holds four objectives: a 5x, 20x, 50x, and 100x magnification. The instrument has a 532 nm green Nd:YAG laser and a 785 nm red diode laser. The power at the source for the 785 nm laser is 100 mW and 20 mW for the 532 nm laser. For this research, the spectral resolution was fixed at 3-5 cm^{-1} (high resolution), setting the spectral region for the 532 nm laser between 40-2730 cm^{-1} and for the 785 nm laser between 80-2630 cm^{-1}. The laser power ranged from 1% to 100%. The aperture was varied between 25 µm and 50 µm depending on the amount of fluorescence. The detector is a CCD detector which is thermoelectrically cooled at a working temperature of -65°C. Neon spectra are automatically recorded by the instrument to correct for changes in the spectrograph and laser excitation. The operating system is the OPUS© software, which has tools to gain quick insights into the obtained spectra. The obtained spectra were furtherly treated via the program GRAMS/AI™ Spectroscopy Software.

ii) Portable Raman instrument

The portable instrument is the i-Raman® EX from B&WTEK. The instrument is equipped with a 1064 nm laser with CleanLaze® technology. The spectral resolution is set at 9.5 cm^{-1} and the spectral range is between 100 cm^{-1} and 2500 cm^{-1}. The detector is an InGaAs array detector which is thermoelectrically cooled at -20°C . The power at the source is 499 mW and it can be varied from 1-100% in steps of 10%. The Raman instrument was post-calibrated using five different chemical substances: sulfur, caprolactam, polystyrene, a solution of 50% water and hexane, and cyclohexane. Two different setups can be used. The first one is via a cuvette holder for mostly liquid and gas phase samples. The other setup is more classical with a probe head holder that is perpendicular to the samples. The obtained spectra were furtherly treated via the program GRAMS/AI™ Spectroscopy Software.

c) Experimental procedure for sample set 2

For every sample on the mounted block, first the area was scanned for the different colors present using the microscope. For example, for sample EPC8, red, blue, and yellow spots were present. Then, one of the observed colors was chosen and one or more spots of this color were analyzed. As different filters are in between the tip of the laser and the microscope, the image was not always clear regarding the color. These different filters greyed the image, making the interpretation of the colors more difficult. Ideally, for a more accurate analysis of the colors present on the samples, the HIROX-microscope could be used. Unfortunately however, during this research, the HIROX microscope was located in Portugal and therefore not available during the duration of this thesis. As stated before, different experimental parameters were investigated. After identifying the pigment via literature reports, the raw pigment itself was also analyzed using the Senterra Raman instrument to create reference spectra for comparison. If possible, the reference spectra were recorded with the same settings as the settings that were used to measure the porcelain samples. Not all pigments were available, so some reference spectra were included from the RRUFF database.

Before the pigments were analyzed, the resin and glaze were also measured. These spectra could then be used as an overlay to the measured spectra of the pigments. This way, a differentiation could be made between bands coming from the glaze/resin and the bands coming from the pigments/additives.

d) Laser power

Lastly, to be more precise about the laser power that reaches the samples, this was measured using an Ophir PD300-1W coupled to a Nova power meter. This was only done for the Senterra benchtop instrument. As the laser power reduces over time due to its extensive use, it is necessary to know the exact laser power. The PD300W can measure intensities between 50 pW and 1 W and has a 0.2 s response time. The Nova power meter enables one to read the results instantaneously on the display.

A filter between the laser source and optic system of the Senterra instrument reduces the laser power to respectively 0.1%, 1%, 10%, 25%, 50%, or no filter meaning 100% laser intensity. The laser intensity can thus be chosen with these filters. The results of the laser power measurements are given in Appendix 3 Table 1.

2) Results and discussion

Both the sample sets were analyzed by the benchtop Raman instrument. In addition to this, sample set 1 was also analyzed using the portable Raman instrument. The results of these measurements will be given in the following paragraphs. First, sample set 2 will be discussed. This sample set was analyzed the longest and yielded the most results. This is why this sample set will be discussed first.

a) Sample set 2

In this first part of the results, sample set 2 was investigated. These samples were previously investigated by Dana Norris et al.[1] using SEM-EDX. The first focus of the current study was to optimize an experimental procedure to analyze the pigments on these samples, using the benchtop instrument. The experimental parameters were: the laser, laser power, integration time, amount of accumulations, and aperture. The resolution, magnification, and integration range were kept constant (see also Part 1 section 4.b). The second aim was to identify all the pigments possible on the samples.

It is important to note that there is a difference between the colors applied to the porcelains. On the one hand, there are pigments where visible granules are present on the sample. On the other hand, there are colored glazes, meaning that a certain surface has a specific color without showing any individual granules. For the colored glazes, defocusing the laser or tilting the sample might be needed to get a usable Raman spectrum. Otherwise, the glaze or resin will be measured instead of the pigments.

i) Experimental design

The different experimental parameters to optimize, as discussed in Part 1 (research plan) section 4.b, were investigated. For every pigment investigated, this optimization process was repeated. To clarify the thought process behind this, hematite was chosen as an example. These results are presented in Figure 1. All the shown spectra of hematite were recorded with the red laser. Using the other laser might cause an enhancement of certain bands and an increase of fluorescence in another area, masking other signals. For these reasons, the laser was kept constant for the optimization process.

A part of the obtained spectra are shown in Figure 1 and their parameters are shown in Table 1. These results indicate that when the measuring time was increased, the baseline of the spectra smoothened. Longer measuring times allow for gathering more information, influencing the signal-to-noise ratio (S/N-ratio) positively. Nonetheless, longer measurements can also have damaging effects on the samples. Therefore, if longer measuring times are used, the laser power should be lowered. Spectrum (e) has the smoothest baseline as the laser power was set at 100%. Still, this should be done cautiously, as a slight downshift (±3 cm^{-1}) of the band at 293 cm^{-1} is visible. This indicates a certain degree of degradation of the pigment. In this case, it is most probable that a certain degree of photobleaching occurred. This implies that a balance has to be made between laser power and measuring time. The best results were obtained using parameters (a), (b) and (c) (Table1). Parameters (a) are preferred as the laser power is lower than for parameters (c) and the measurement time is lower than for parameters (b).

In the case of hematite, there was no high degree of fluorescence meaning that the aperture could always be left at 50 µm. For other samples, if the fluorescence background was too high, the aperture was lowered to 25 µm. Another solution was to switch the laser between the red and the green laser or vice versa. If the aperture was lowered, less Raman scattering reached the detector, so not only the fluorescence was lowered but also the Raman scattering signals. This means that with a lower aperture, a longer measuring time should be considered.

Table 1: The different experimental parameters of the spectra shown in Figure 1.

Parameters	Measuring time (s)	Accumulations	Laser power (%)	Aperture (µm)
(a)	50	40	10	50
(b)	60	60	10	50
(c)	50	40	25	50
(d)	60	30	10	50
(e)	30	30	100	50

As discussed earlier, another laser can cause a resonance effect, meaning that the intensity of the bands will increase. In the case of ultramarine blue for example, the green laser caused a resonance effect increasing the bands and increasing combination bands that were not visible with the red laser.

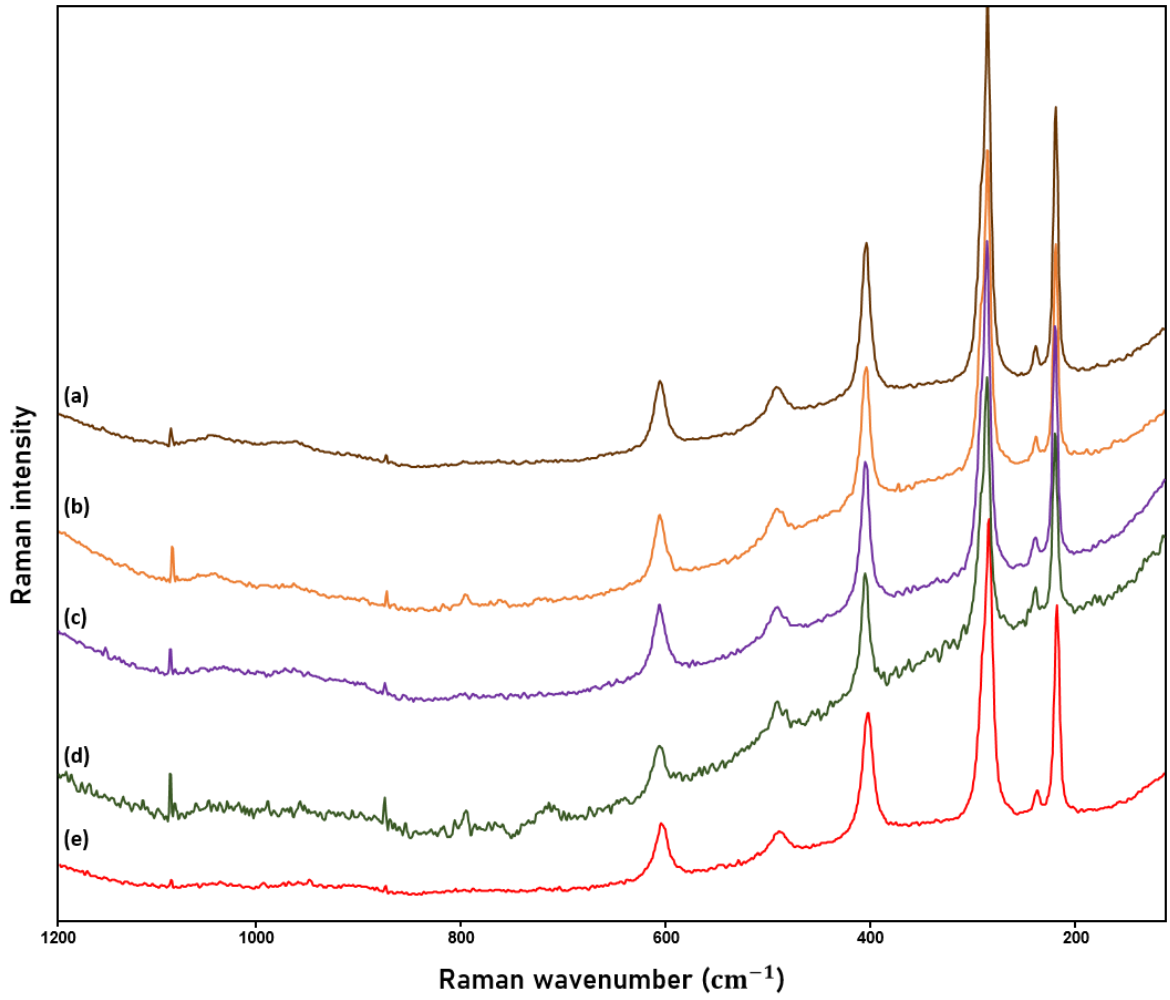

Figure 1: Spectra of hematite recorded on sample EPC8 with the different experimental parameters given in Table 1.

ii) Identification of the pigments

An overview of the different pigments that were identified is given in the next paragraphs. As sample set 2 consisted of embedded samples, measuring underneath the glaze was facilitated. Also, these samples are more flat making them more practical to focus on. All the reference spectra were bundled in Appendix 2. Sometimes, to clarify certain bands, the reference spectra were stacked underneath the measured spectra of the samples. For the more straightforward Raman spectra, they were not added.

(1) Red-Hematite

The red pigment observed in samples CPEAS1, CPE253, CPE312, CPES20, EPC8, EPC9 and EPC11 was identified as hematite (α-Fe_2O_3). This is shown in Figure 2 (a-g). These results are consistent with the findings of Dana Norris et al.[1] who subjected these samples to ESEM-EDX and who found elevated amounts of Fe_2O_3 in sample CPEAS1. Hematite was already used in Chinese porcelains since the 15th century.[2] Different researchers already reported findings of hematite in Chinese and also European porcelains of this specific era.[3-7]

As hematite is a strong Raman scatterer, the reference spectrum (Appendix 2 Figure 1) had to be measured with other experimental parameters. Because the detector was overloaded using a measuring time of 60 seconds, the measuring time was lowered as well as the laser power.

Hematite has six distinguishable bands at 227, 246, 293, 412, 499, and 613 cm^{-1}.[8] The bands at 227 and 293 are assigned to be from the bending vibrations of the iron atoms. The band at 244 is ascribed to be from the stretching vibrations of these. The bands at 412, 499, and 613 cm^{-1} are assigned to be from the oxygen vibrations.[9-12]

The spectra collected from samples CPEAS1 and CPE312 have an intense band around 1310 cm^{-1} (Figure 2 (a,b)). This band corresponds to the two-magnon scattering of hematite and is characteristic in a spectrum of this pigment. However, this band is not always visible with the red laser because of a high fluorescence background in this spectral region. This band is enhanced when using the green laser due to resonance enhancement.[13] This band is usually used as a measure for the detection of hematite in porcelains when using a green laser.[7-8, 14-15]

In some of the spectra, spikes are visible. Cosmic spikes have already been discussed in Part 1 section 3.a.vi. In this case, it is peculiar that the spikes seem to appear at the same wavenumber. Presumably, these are artifacts coming from the laser itself and are thus not cosmic spikes.

Table 2: Experimental parameters of the spectra shown in Figure 2.

Sample	Measuring time (s)	Accumulations	Laser	Laser power (%)	Aperture (µm)
(a) CPEAS1	60	60	green	10	25
(b) CPE312	60	30	green	10	50
(c) EPC9	60	60	red	10	50
(d) EPC8	60	60	red	10	50
(e) CPE253	30	30	red	10	50
(f) CPE313	60	60	green	1	50
(g) EPC11	50	40	red	25	50

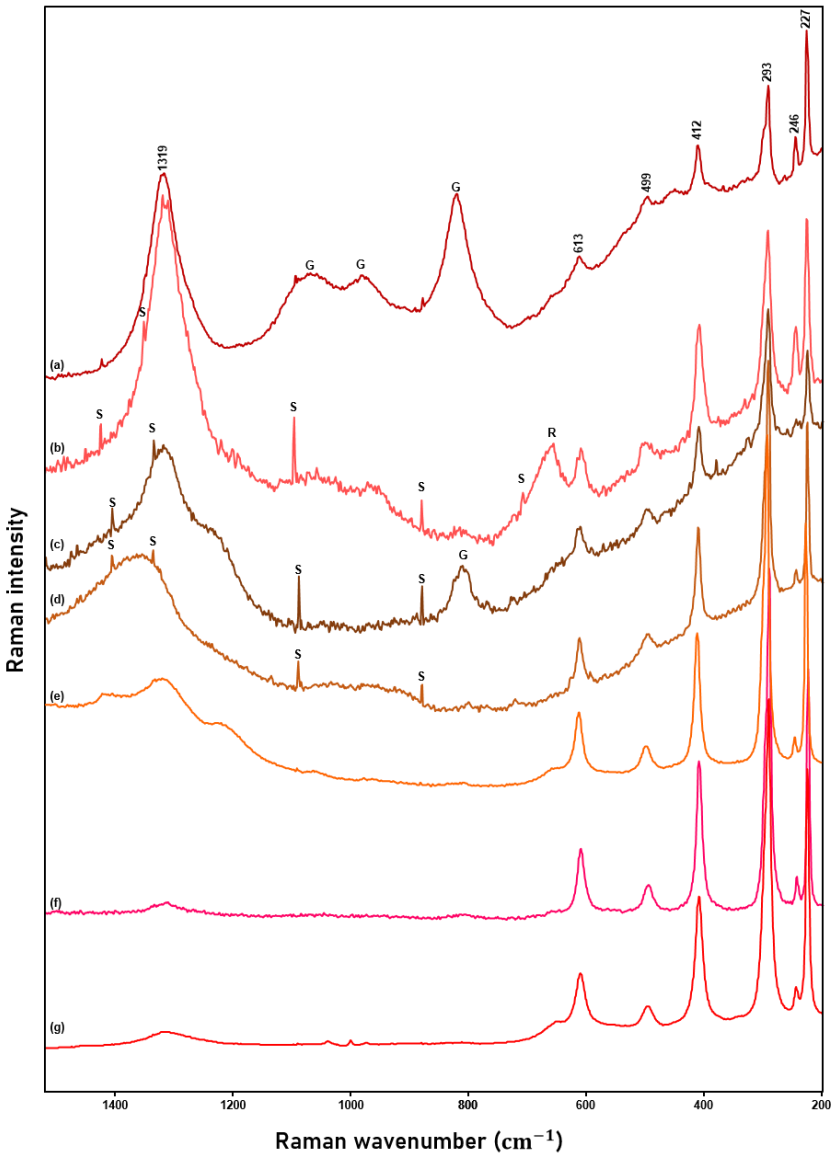

Figure 2: Spectra of hematite recorded on the different samples. S=spike, G=glaze, R=resin

(2) Blue-Phthalocyanine blue

The blue pigment on samples EPC8 and CPESU1 was identified as phthalocyanine blue (PB15). PB15 is an organic synthetic pigment. The first time PB15 was synthesized dates back to 1927.[16] Remarkably, this is after the period that these samples are supposedly from. These results indicate an interesting anachronism between the pigment and the dating of the sample.

PB15 has seven known polymorphs, whereas each polymorph has a slightly different lattice structure. Only five polymorphs are used in art and are commercially available as a pigment. The pigment found in these samples corresponds to the β-form also denoted as PB15:1.[17-18] PB15 is a copper complex, the structure is given in Appendix 3 Figure 1.

In Figure 3, the two spectra recorded on the samples and the reference spectrum of PB15 are shown. The most important bands that are visible below 1000 cm^{-1} correspond to the macrocycle vibration. Between 1100 cm^{-1} and 1600 cm^{-1}, the bands correspond to the vibration of the pyrrole group. The most intense band (1531 cm^{-1}) is coming from the pyrrole stretching vibration. In this range, one also finds the isoindole vibrations. Some weaker bands at higher wavenumbers correspond to the carbon-hydrogen and metal-hydrogen vibrations.[17]

For the reference spectrum, the same parameters were used as for sample EPC8. It can be established that the spectrum recorded on sample CPESU1 is much noisier. The bands are less demarcated and the signal-to-noise ratio is less than for the spectrum recorded on sample EPC8. This is because the measuring time and number of accumulations were much lower. Nonetheless, the spectral quality is good enough to identify the most important bands of PB15.

It is very unlikely that PB15 was applied before the firing process of the porcelain. PB15 shows high thermal decomposition at 400 degrees Celsius meaning that it would degrade during the firing process of the porcelain.[19] There are two more likely scenarios regarding the presence of PB15 in these samples. The first theory is that over time, one or both porcelains were overpainted. However, in this case, larger blue areas should then be visible on the samples. Only one spot was found on sample EPC8 and a couple of tiny spots were found on sample CPESU1. It was not known from which area of the porcelain the samples were scalped off. For this reason, Figure 4 was added indicating which areas might have been overpainted. As PB15 gives rise to a deep blue color, for sample CPESU1, the blue strap around the neck of the vase could have been overpainted. For sample EPC8, the edges had a blue motive on them, which may have been overpainted for this specific sample. Another plausible explanation is that some kind of cross-contamination occurred with no intention to contaminate the sample. It is conceivable that the artifacts came into close contact with an object containing PB15. Nowadays PB15 is mostly used in printing inks and as colorants for plastics. Further, it is known to contaminate very easily. Further research will have to point out the possible source of PB15 in these samples.

Table 3: Experimental parameters of the spectra shown in Figure 3.

Sample	Measuring time (s)	Accumulations	Laser	Laser power (%)	Aperture (µm)
(a) EPC8	60	60	red	10	50
(b) CPESU1	15	5	red	25	50
(c) reference	60	60	red	10	50

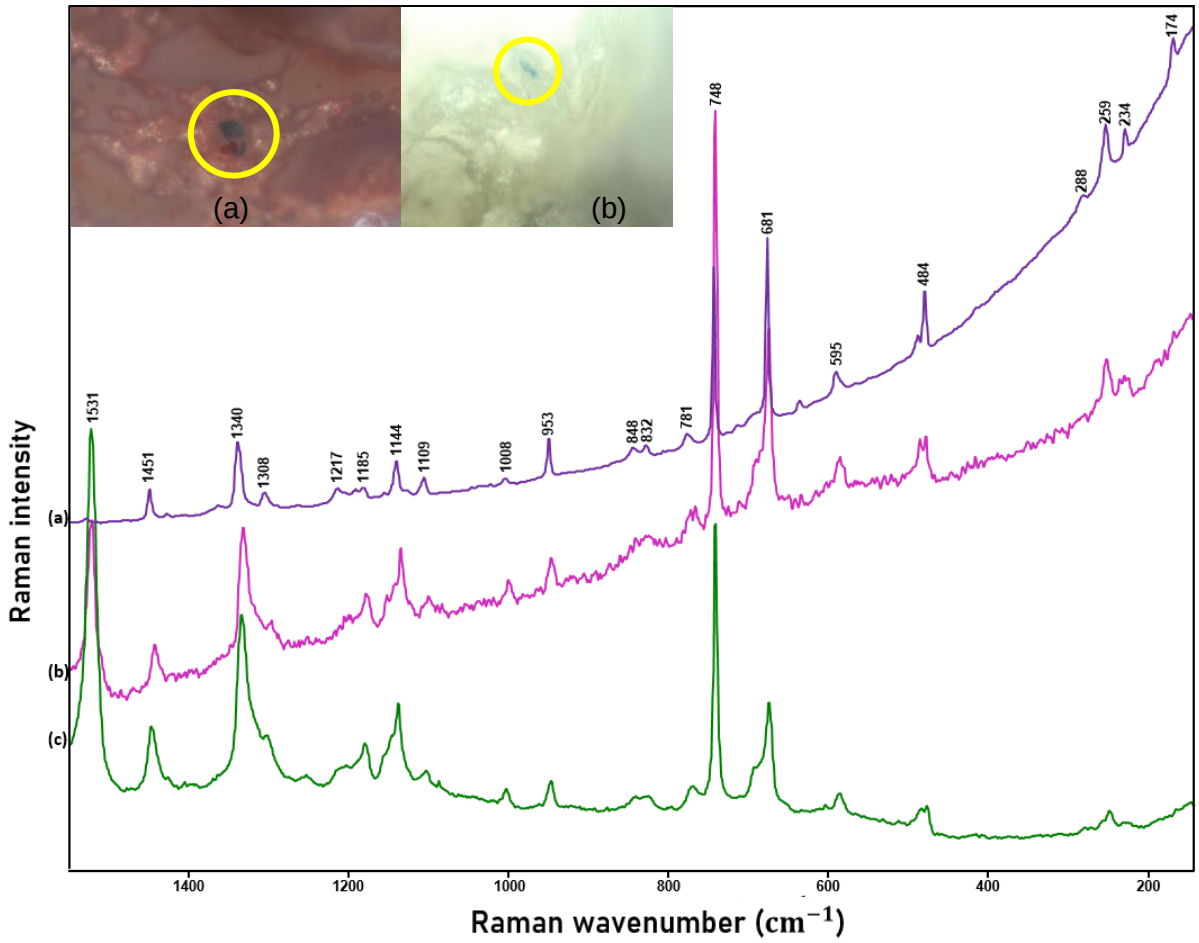

Figure 3: Spectra and images from the blue spots identified as PB15:1.

Figure 4: Images of samples EPC8 and CPESU1. The possible overpainted layers are indicated by the red arrows.

(3) Blue-Ultramarine blue

In sample CPE253, ultramarine blue was positively identified. Ultramarine blue comes from the rare gemstone *lapis lazuli* and was the most expensive pigment during the Renaissance.[20] It was even more valuable than gold. Ultramarine was mostly used in paintings or murals, but not many porcelains have been found containing this pigment. P. Vandenabeele et al.[21] published on finding ultramarine in rare 19th century porcelain cards. Although this is rather exceptional, it is known that ultramarine blue was used in art pieces at that time.

The spectrum of ultramarine blue is shown In Figure 5. The most intense band in the spectrum of ultramarine blue is visible at 549 cm^{-1}, four relatively intense bands can also be found at 260 cm^{-1}, 585 cm^{-1}, 1096 cm^{-1}, and 1644 cm^{-1}. Broader bands can be found at 804 cm^{-1}, 1360 cm^{-1}, 1904 cm^{-1} and 2194 cm-1. Ultramarine blue has the following chemical formula: $Na_{8\text{-}10}Al_6Si_6O_24S_{2–4}$. Here, $S_{2\text{-}4}$ can partially be replaced by SO_4^- if exposed to air for a longer period of time.[22] The most intense band at 549 cm^{-1} is caused by the symmetric stretch of the S_3^- anions. The first vibrational overtone of the S_3^- anions is visible in the spectrum at 1096 cm^{-1}. The second and third overtones are visible in the spectrum at respectively 1644 and 2194 cm^{-1}. The bending vibration of the S_3^- anions is visible in the lower spectral region at 257 cm^{-1}.[23] The band at 585 cm^{-1} in the spectrum corresponds to the symmetrical stretch of the S_2^- anions. The bands at 804 cm^{-1} and 1360 cm^{-1} are combination bands ($\nu_1+\nu_2(S_3^-)$) and ($2\nu_1+\nu_2(S_3^-)$) of the S_3^- anions. Combination bands are a consequence of electrical anharmonicity.[24]

Due to the use of the green laser, a resonance effect occurs. This is because the frequency of the laser matches the maximum allowed electronic transition. This allows for the enhancement of the fundamental vibrations and overtones.

Ultramarine has three different chromophores. The S_2 group is a yellow chromophore, the S_3 group is a green chromophore, and a disordered S_3 group causes a deep blue color. The specific ratios will thus alter the color from deep blue to a more greenish color.[25-26] Ultramarine can have a synthetic and a natural origin. Synthetic ultramarine blue was first synthetized in 1826, which is after the Jiaqing period.[20] This means that the artifact probably contains natural ultramarine. Although, this cannot be concluded from the Raman spectrum recorded on the sample. Nonetheless, different studies have focused on finding differences in the Raman spectra between the natural and synthetic variants. Pulsed Raman spectroscopy combined with laser-induced breakdown spectroscopy (LIBS) has yielded the best results.[23] The reference spectra of synthetic and natural ultramarine blue are given in Appendix 1 Figure 3. In those spectra, it can be seen that these spectra are quite identical. The reference spectrum of natural ultramarine blue was also added in Figure 5 together with the recorded spectrum on the sample.

Table 4: The experimental parameters of the spectra displayed in Figure 5.

Sample	Measuring time (s)	Accumulations	Laser	Laser power (%)	Aperture (µm)
(a) CPE253	30	30	green	10	50
(b) Reference	10	10	green	10	50

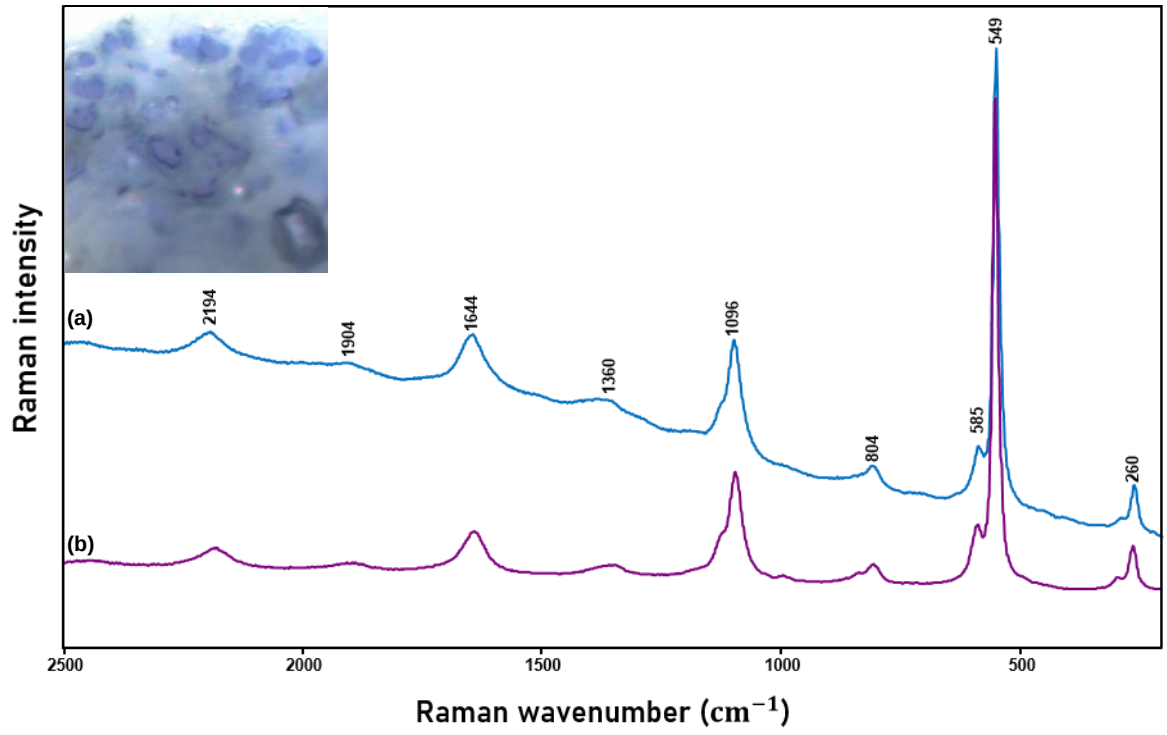

Figure 5: (a) Spectrum of ultramarine blue recorded on sample CPE253. (b) Reference spectrum of natural ultramarine blue.

(4) Blue-Unidentified

Samples CPE321, CPEAS1, CPE329, CPECB1, CPE253, and CPEJP1 contained other blue pigment(s) that could not be identified. Figure 6 shows selected spectra from these blue spots. As no Raman bands were present, this pigment/pigments could not be identified. The ESEM-EDX results from Dana Norris et al.[1] showed elevated amounts of CoO on the samples that had blue glazes. With no certainty, this points towards cobalt blue or smalt. Cobalt minerals are weak Raman scatterers, so a cobalt pigment, probably smalt could be the unidentified blue pigment. Of course, this is not certain. Cobalt blue was not yet available during the Jiaqing period, so smalt would be the most probable.

In Figure 6, three different spectra of the unidentified blue pigment(s) are shown. As seen in spectrum (a) and (b), the fluorescence is quite high in the lower Raman wavenumber region due to the use of the green laser. As can be remarked, the spikes are overwhelming the spectrum. Once again, the spikes appear at the same Raman wavenumbers which is extremely peculiar. Again, the most plausible explanation is that these are artifacts coming from the laser itself. In spectrum (b), there is a Raman signature of the silicate glassy matrix visible. The rest of the spectrum is nearly identical to spectrum (a). Spectrum (c) shows a high fluorescence background in the higher Raman wavenumber region due to the use of the red laser. Here, the fluorescence background overwhelms the higher spectral region.

For the three shown spectra, the experimental parameters are given in Table 4. It can be deduced that the green laser gives rise to a lot of fluorescence in the low Raman wavenumber region whilst the red laser does this for the high Raman wavenumber region. When a smaller aperture was chosen, the signals from the glaze were not visible anymore.

Table 5: Experimental parameters of the unidentified blue pigment(s) shown in Figure 6.

Sample	Measuring time (s)	Accumulations	Laser	Laser power (%)	Aperture (µm)
(a) CPE253	60	60	green	10	25
(b) CPECB1	60	60	green	10	50
(c) CPEAS1	60	60	red	10	50

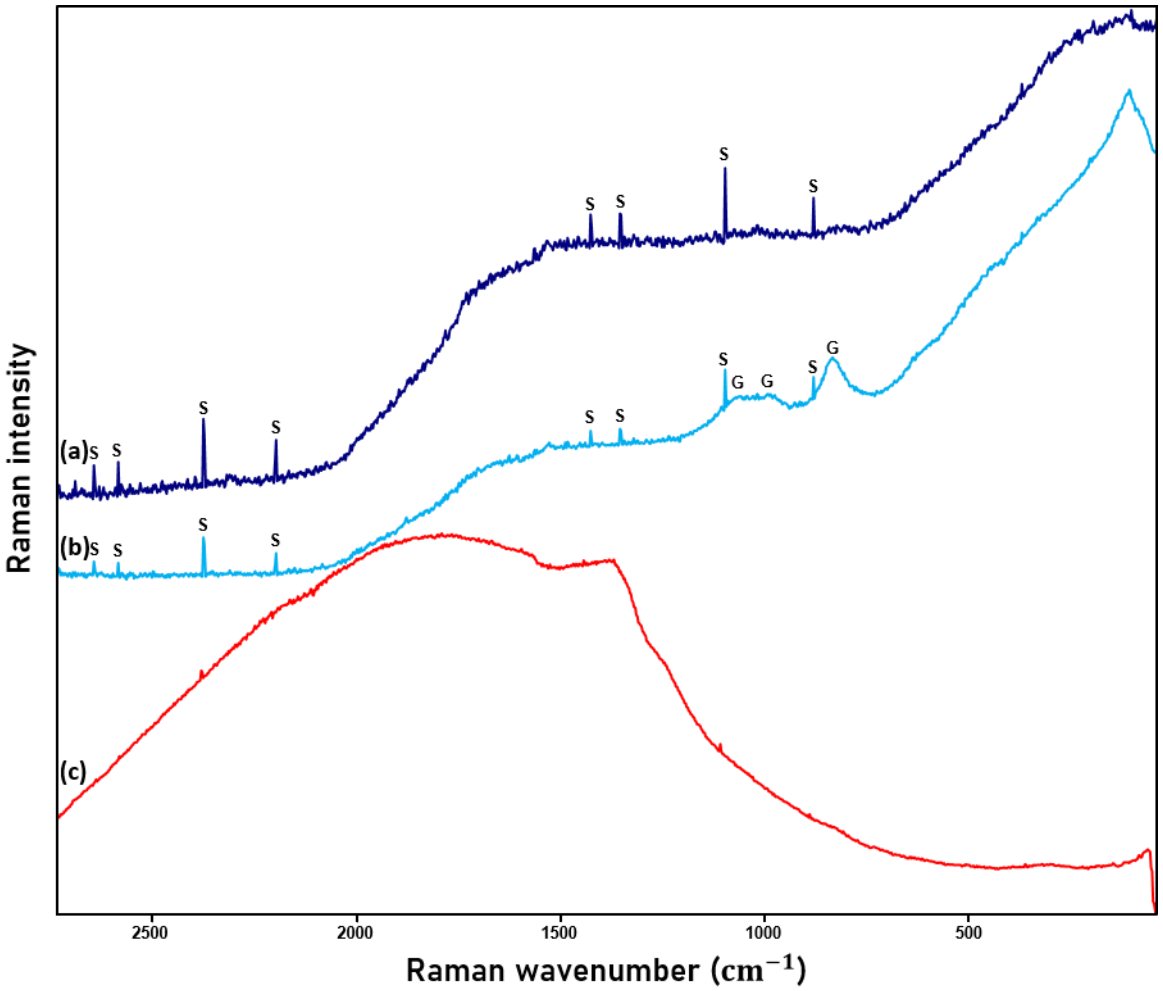

Figure 6: Raman spectra of the unidentified blue pigment(s). S=spike, G=glaze.

(5) Yellow-Lead tin yellow II

In samples EPC11, CPE313, and CPE312, the yellow pigment was positively identified as lead tin yellow II ($PbSn_{1-x}Si_xO_3$, where x=0.25).[2] Lead tin yellow II was a commonly used pigment in 18th to 19th-century Chinese porcelain.[6, 27-28] Before the 18th century, lead tin yellow II was more commonly known as giallorino, especially in Italy.[29] The pigment was mostly used in paintings and became popular with Renaissance painters and the Old Masters.

The spectra of lead tin yellow II are given in Figure 7. The most pronounced band in the spectrum of lead tin yellow II is the one at 137 cm^{-1}. This band corresponds to the lead oxide lattice stretching vibrations.[30] The bending vibration of lead oxide can be found at 68 cm^{-1}. The band at 451 cm^{-1} is probably coming from the bending vibration of the silicate matrix. In the reference spectrum (Appendix 2 Figure 3), there is a very weak band visible around 1035 cm^{-1}. This is probably the stretching vibration of silica. An important band missing in these spectra is the stretching vibration band of cassiterite (Sn-O) at ±635 cm^{-1}. In spectra of lead tin yellow II, this band is most of the time very weak, but normally a small feature should be visible. In spectrum (a), this is weakly visible. In spectrum (b), (c), and the reference spectrum, this band is absent. The assignment of the bands at 262 cm-1 and 325 cm-1 has not been discussed in literature. These bands seem to come from the tin oxide bending vibrations, or from the silicate matrix.

Lead tin yellow has two types: type I and type II. Lead tin yellow type I (Pb_2SnO_4) was more commonly known as yellow of the Old Masters and was already used since the 13th century in oil paintings.[29] Because lead tin yellow II has a silicate matrix, differences in Raman spectrum can be observed. This makes the two different pigments distinguishable by Raman spectroscopy.[30]

Table 6: Experimental parameters of the lead tin yellow II spectra shown in Figure 7.

Sample	Measuring time (s)	Accumulations	Laser	Laser power (%)	Aperture (µm)
(a) EPC11	30	30	green	10	25
(b) CPE313	30	30	green	10	25
(c) CPE312	60	30	green	10	50

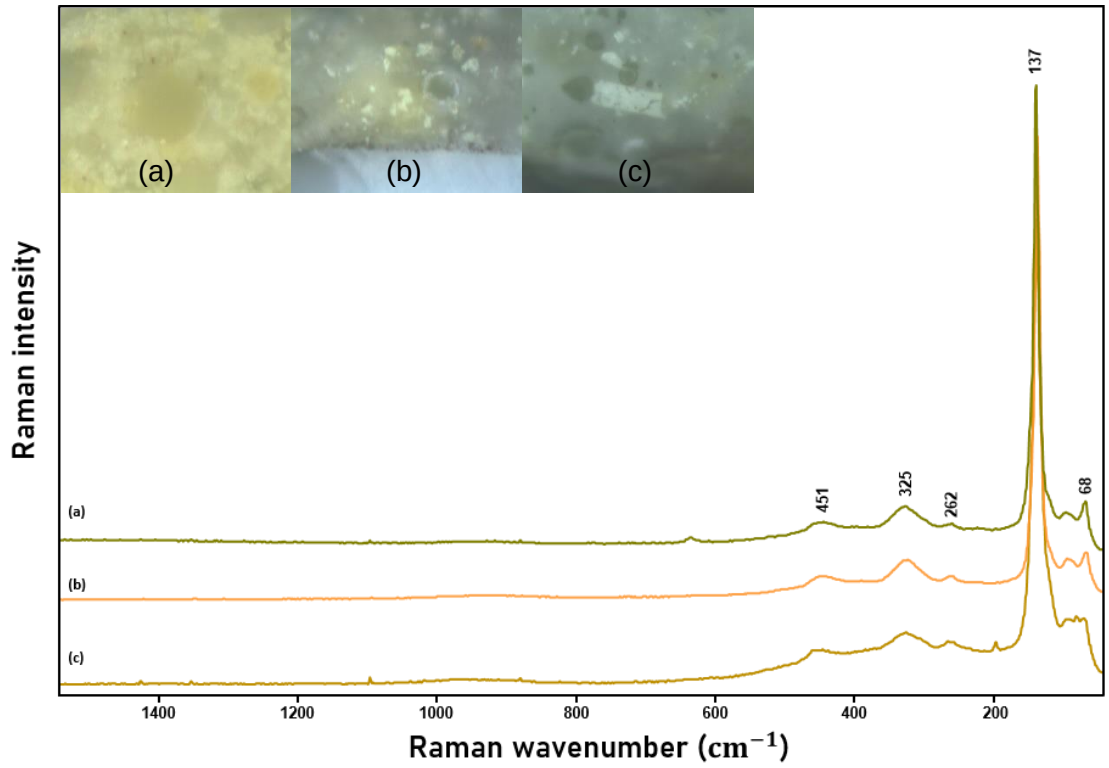

Figure 7: Spectra of lead tin yellow II recorded on samples EPC11 (a), CPE313 (b), and CPE312 (c). Images of the sample spots are shown in the top left corner.

(6) White-Lithopone/Barium sulfate

Sample CPEAS1 contains a light and a dark blue glaze. The light blue glaze exhibited the signature of barium white (BaSO4) and possibly of lithopone. Barium white is pure $BaSO_4$ whilst lithopone also contains Zinc sulfide (BaSo4.ZnS). It is important to know that lithopone was first used in 1874 while Barium white (barium sulfate) was already used a century before (18th century).[31-32] This is important concerning the dating of this sample.

The most pronounced bands in the recorded spectrum of the sample (Figure 8(a)) are present at 348, 460, 621, and 988 cm^{-1}. Apart from that, some bands from the glaze are also present. In spectrum (b) the glaze is displayed to make it easier to distinguish bands coming from the glaze and those coming from the pigment. The spectrum of the glaze was recorded on a darker blue area. The most intense band at 988 cm^{-1} is the symmetrical stretch of the sulfate ion.[33] The bands of the symmetrical bending vibration of the sulfate ion are visible at 453 and 462 cm^{-1}. At 617 cm^{-1} the asymmetrical stretch of the sulfate ion is visible.[34] The most pronounced band of zinc sulfide is present at 378 cm^{-1}. A second band of zinc sulfide should be visible at 670 cm^{-1}, but is not visible in the recorded spectrum. This is confirmed in literature reports, stating that the band at 670 cm^{-1} is not always visible or very weakly visible due to the weak scattering abilities of ZnS.[25]

A closer look at the reference spectrum (Appendix 2 Figure 5) and the spectrum recorded on the sample show that the bands of the recorded spectrum are slightly shifted. The main band (988 cm^{-1}) is at the same wavenumber but the asymmetrical stretch of the sulfate ion (617 cm^{-1}) has a blue shift of 4 cm^{-1}. The symmetrical bending vibration of the sulfate ion is a singlet instead of a doublet and is broader than the band found in the reference spectrum. Here, a slight red shift of 2 cm^{-1} is visible. The same red shift is visible for the supposed band of zinc sulfide at 348 cm^{-1}.

As stated before, a difficulty here is that the bands of ZnS might not be visible due to the overlap of other bands and the weak scattering abilities of ZnS.[26] Due to the fact that the second band of zinc sulfide (670 cm^{-1}) was not visible and the low intensity of the band at 348 cm^{-1}, no conclusion can be drawn with a great degree of certainty. The bands at 348 cm^{-1} and 460 cm^{-1} are also very weakly visible in the spectrum of the glaze. So maybe the band at 348 cm^{-1} might be from the glaze and not from ZnS. It has to be remarked that the signal-to-noise ratio and the background are not the best quality making interpretation harder. On the other hand, the ESEM-EDX data of Dana Norris et al.[1] showed the presence of Zn in the blue glaze of sample CPEAS1. This is the only analyzed spot on the sample that had traces of Zn on the painted enamels.

To conclude, it can be said with a high degree of certainty that Barium sulfate was used to obtain a lighter blue glaze. Although, it cannot be concluded that it is lithopone. To be more certain that it could be lithopone, further research is required. There are no studies available of 18th to 19th-century Chinese porcelains containing either of these whiteners. This is a very interesting result as it seems that these whiteners were more commonly used in paintings.

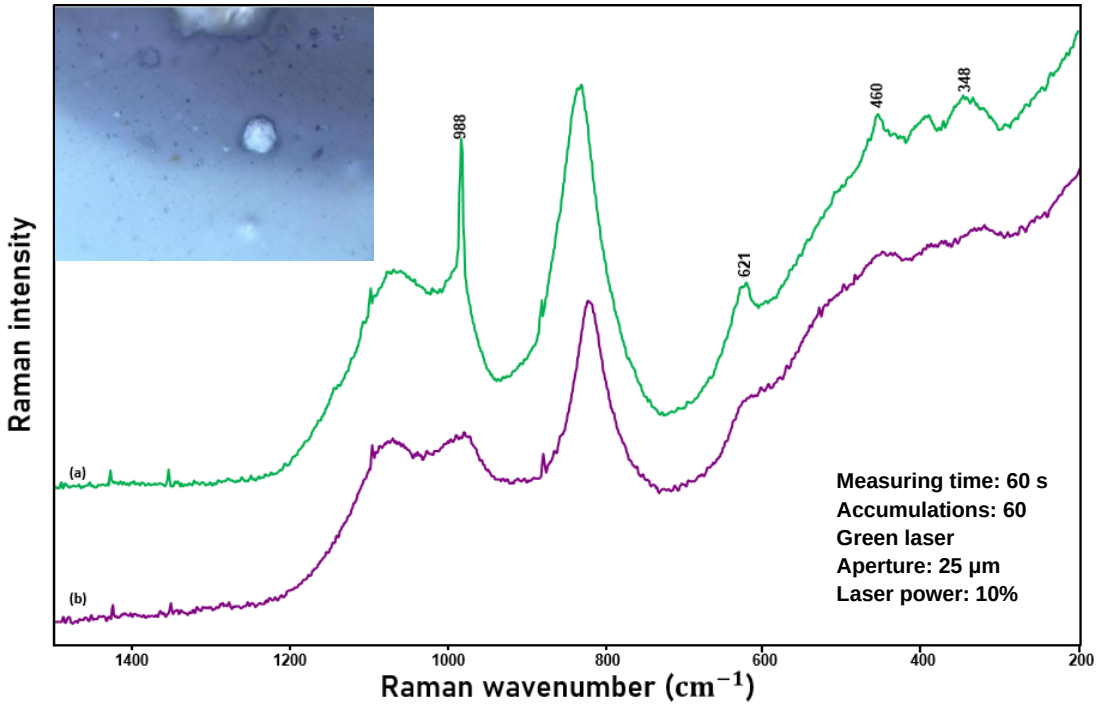

Figure 8: (a) spectrum of the lighter blue glaze recorded on sample CPEAS1. (b) The spectrum of the glaze, recorded on the dark blue area. Both spectra were recorded using the same parameters. These parameters are shown in the bottom right corner.

(7) White-Anatase

In sample CPE253, anatase (α-TiO_2) was identified together with ultramarine blue. This means that these pigments could have been blended together to obtain a lighter blue color.

The bands of interest regarding anatase are located at 143, 288, and 385 cm^{-1} (Figure 9).[35] The other bands are bands of ultramarine blue. The symmetrical stretch of titanium oxide can be observed at 143 cm^{-1} and is the most intense band visible in the spectrum. This band is used in literature as a measure for the identification of anatase.[36] The planar bending vibration of Fe-O is visible at 385 cm^{-1}. The band at 288 cm^{-1} is not of titanium oxide but of iron oxide, more specifically hematite (α-TiO_2). The slight red shift is due to the combination of Titanium oxide and iron oxide.[37] Anatase does contain a

slight amount of iron oxide and this is rather a contamination than a deliberately added substance. The reference spectrum (Appendix 2 Figure 6) was taken from the RRUFF database. As the anatase was from Pakistan, shifts in Raman bands are visible. This is due to differences in iron oxide content. There are two bands of anatase that are not visible in the recorded spectrum, namely bands at 517 and 638 cm^{-1}.

Titanium oxide has three different polymorphs namely anatase (α-TiO_2), rutile (β-TiO_2), and brookite (γ-Tio_2).[35, 38] Rutile is the more stable form and consists of 90% TiO2 and around 10% of iron oxides. These polymorphs can be converted into each other, especially anatase and rutile. Anatase and brookite are metastable, especially brookite is a rare form of TiO_2. The temperature at which anatase is converted to rutile is between 750-950 °C.[37] The transition temperature is dependent on different factors including the grain size and the amount of iron oxide present.

The presence of anatase has been positively concluded based on the intense band at 143 cm^{-1}. In addition to this, anatase is a component of kaolin, the base clay for the manufacturing of Chinese porcelain. This suggests the possibility that the detected anatase is coming from the body and that it was thus not necessarily added to the ultramarine blue. As anatase is a very strong Raman scatterer, this can overwhelm the spectrum rather easily, masking other Raman scatterers. However, if this was the case, this signature should have been noticed in other spectra as well.

The ratio of anatase-rutile is also used in research to determine the firing temperature of porcelain.[39] Anatase and rutile have been reported frequently in these types of samples. Mostly due to the body and less as a whitener to obtain lighter/brighter hues of a color.[36-37]

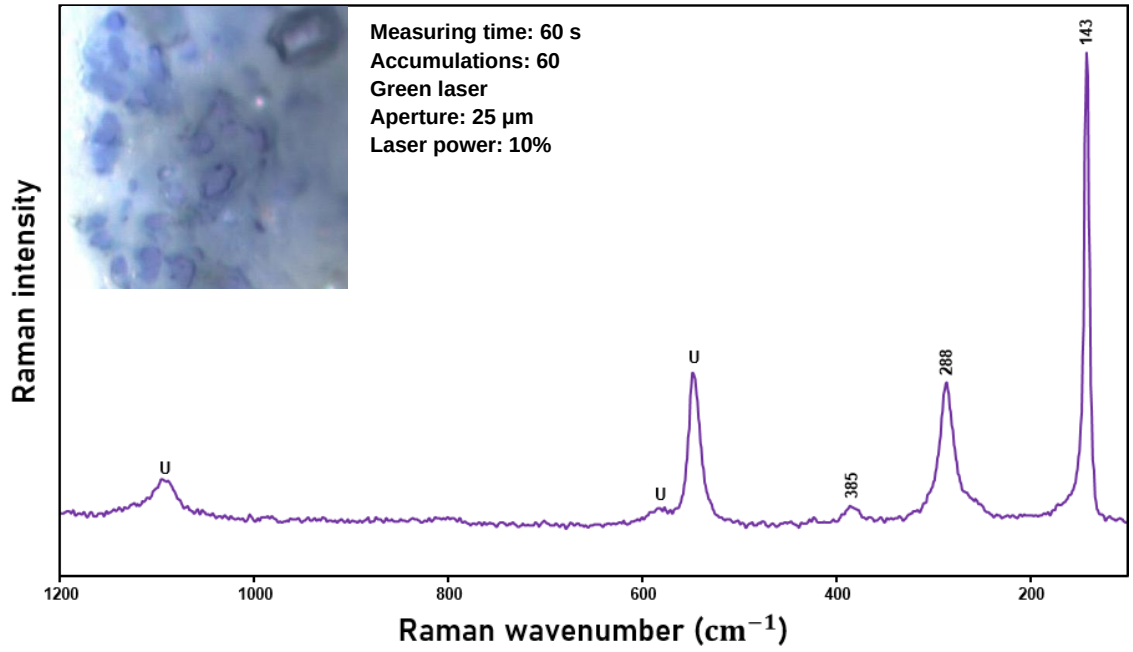

Figure 9: Spectrum of anatase recorded on sample CPE253. Image of the sample spot and the parameters are shown in the top left corner. U=Ultramarine blue

(8) White-Lead arsenate

The glaze of sample CPESU1 is light green. On this glaze, the signature of lead arsenate was found. Lead arsenate and arsenates in general were often used to whiten colors and were also commonly used as opacifiers.[3, 6-7, 40-42] Lead arsenates are strong Raman scatterers, so this is probably why in the recorded spectrum, only lead arsenate was detected and not a green pigment as would be expected. The spectrum and image of the sample spot are given in Figure 10.

It is not known which exact lead arsenate structure was identified. The recorded Raman spectrum corresponds to a spectrum recorded by Jolien Van Pevenage et al.[2] which did not specify the exact lead arsenate structure. Since it is really difficult to define one specific structure, They are addressed as lead arsenates in literature without specifying the exact structure.[3-4, 6-7, 28, 41]

The most pronounced band is located at 820 cm^{-1} and corresponds to the symmetric As-O stretching vibration of the AsO_4^--ion. The shoulder of this band, located at 774 cm^{-1} also corresponds to this symmetric stretching. In the region between 300 and 450 cm^{-1}, a couple of bands overlap. These bands correspond to the in-plane bending vibrations of the AsO_4^--ion.

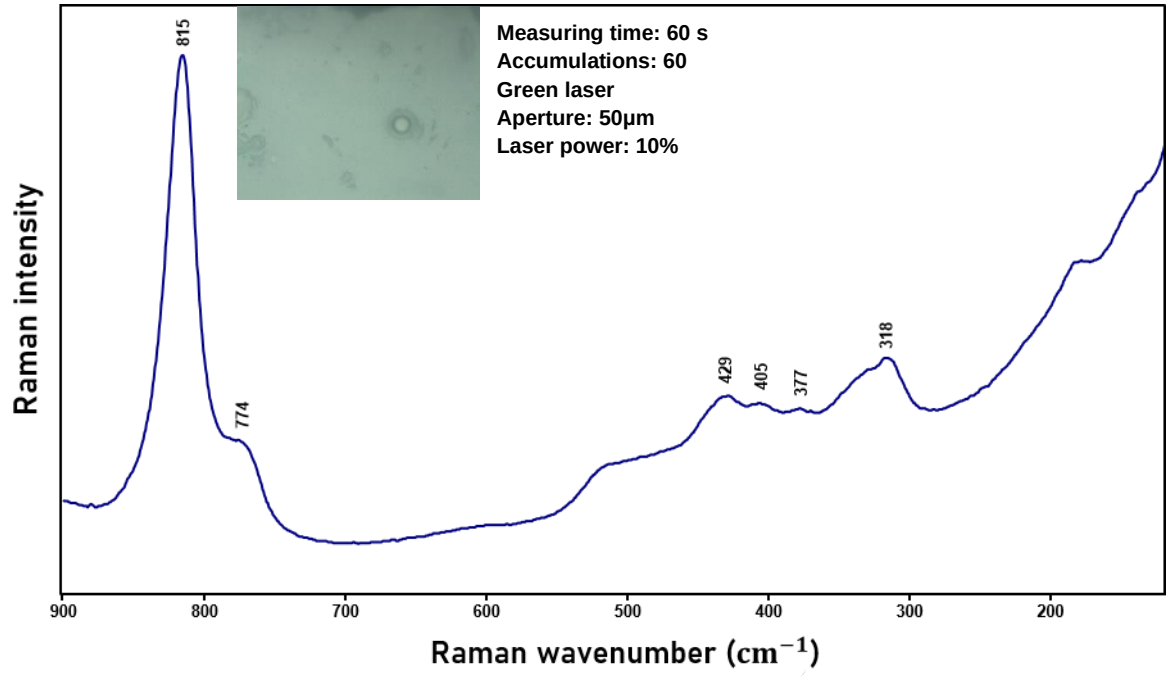

Figure 10: Raman spectrum of lead arsenate recorded on sample CPESU1. Image of sample spot and parameters are shown on the top of the spectrum.

b) Sample set 1

This second part consists of a preliminary study carried out on sample set 1. As these samples are porcelain shards, a number of difficulties were encountered. Firstly, focusing on the shards was more complicated, as they are not flat. Hence, a magnification of 20x or 50x was used instead of the 100x magnification. This means that a larger colored area was needed. Secondly, in contrast to sample set 2, which contains scalped off pieces, it was more difficult to measure underneath the glaze. Because the red laser can penetrate deeper into the sample than the green laser, it was therefore decided to use the red laser. On sample set 1, measurements were performed by the benchtop as well as the portable Raman Instrument.

i) Identification of the pigments – Senterra benchtop Raman instrument

As this was a preliminary study, the focus was on identifying the pigments which are strong Raman scatterers. Thus, mainly the reds and yellows were analyzed. Some green and blue areas were also investigated but no clear results were obtained from these.

(1) Red–Hematite

The red pigment on sample B.fr.1750.2 was positively identified as hematite. This is the same pigment that was found on the other sample set (2). The sample contained different hues of red, ranging from bright pink to dark red. Only the dark red areas were analyzed as these were more likely to yield usable spectra. Images of the analyzed spots and the recorded spectrum are given in Figure 11.

Hematite was detected on both sample sets. This underlines the popularity of hematite as a red pigment in this era. It was the most popular in China because of the different hematite ores that were present. Nonetheless, hematite was also reported as a red pigment in European porcelain.[4]

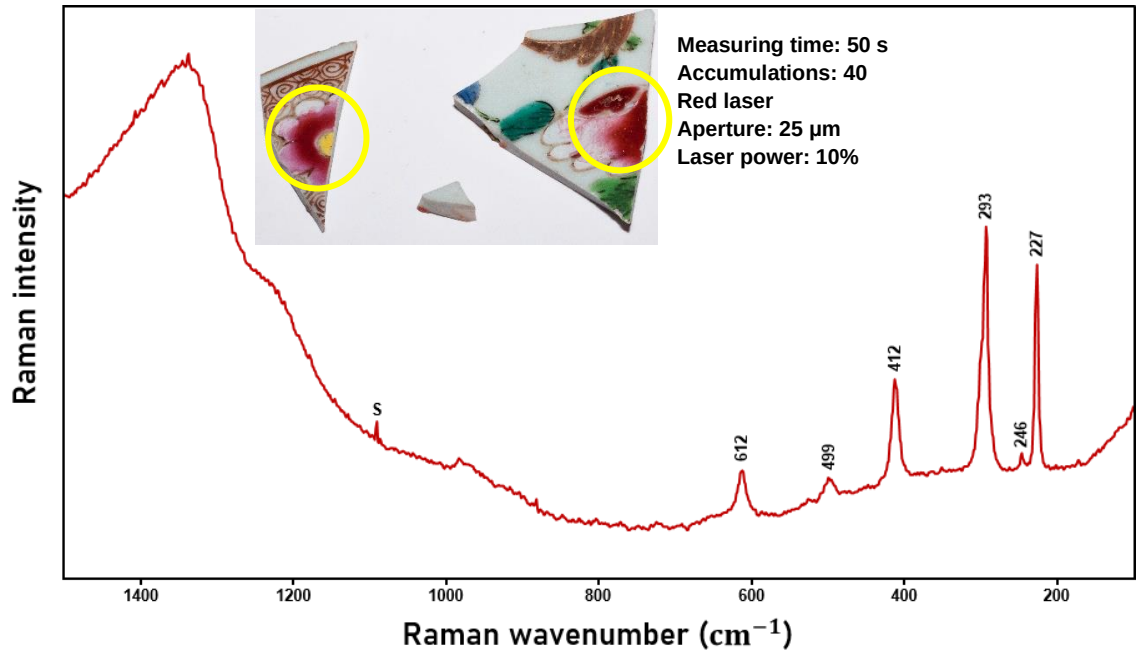

Figure 11: Raman spectrum of hematite, recorded on a dark red area of sample B.fr.1750.2. Sample spots are indicated with the yellow circle.

(2) Yellow–Lead tin yellow II

The yellow pigment on sample B.fr.1800.1 was identified as lead tin yellow II. This is the same yellow pigment that was found on samples from sample set 2. The spectrum and image of the analyzed spot are given in Figure 12. As can be seen in this spectrum, fewer bands are visible. The most intense band of the lead oxide vibrations is observable (139 cm^{-1}), although a slight upshift of this band (2 cm^{-1}) is noticeable. On the other hand, a slight downshift of the band at 323 cm^{-1} (2 cm^{-1}) can also be noticed. Again, some spikes are visible in the spectrum.

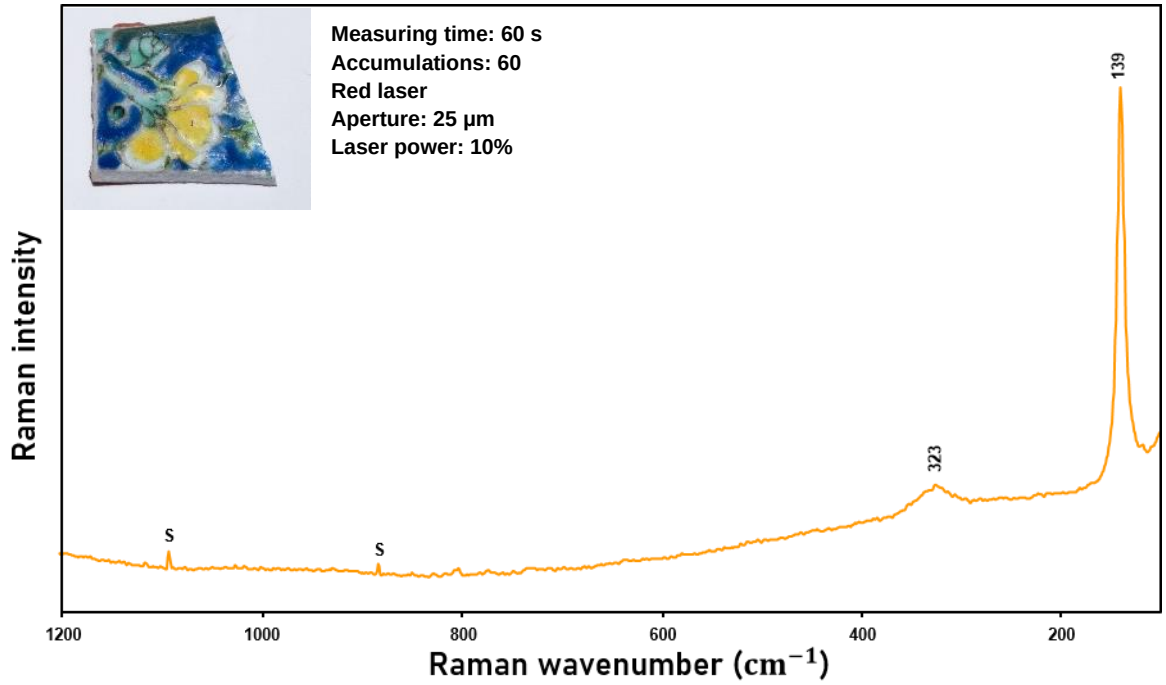

Figure 12: Raman spectrum of lead tin yellow II, recorded on a yellow area of sample B.fr.1800.1. The analyzed spot and experimental parameters are shown in the upper left corner.

ii) Identification of the pigments – portable Raman instrument

This part of the research aims to prove the utility of the portable instrument for the in situ analysis of porcelain artifacts. When using the portable instrument several advantages and disadvantages need to be considered.

Advantages

The first advantage is that the measurements can be performed *in situ*. As porcelain is fragile and museums or collection holders are understandably reluctant and cautious to move their collection to perform measurements on them. Using a portable Raman instrument avoids this risky transport of collections.

The second advantage of the portable instrument is the measurement time and coupled with it, the integration range. The detector has one grating that covers the full range of 100-2500 cm^{-1}. This range is perfect for the measurements of porcelain and its pigments. Because the detector covers the whole range, the measurement time is reduced by half. For example, for the benchtop instrument, if the range is measured between 40-2730 cm^{-1} (green laser), the detector measures the range of 40-1580 cm^{-1} first and then the detector changes position to measure the second range of 1540-2730 cm^{-1}. The

measurement time for the following parameters: 60 seconds and 60 accumulations is thus 120 minutes (2 times 60 minutes) for the Senterra instrument. For the portable instrument, the whole range is measured at once, meaning that the measurement time would be 60 minutes. Of course for *in situ* measurements the aim is to perform quick measurements. The instrument would therefore mostly be used for measurements up to about 20 minutes.

Another advantage of the instrument is that it possesses a near-IR laser (1064 nm). Because of the longer wavelength, the laser can penetrate deeper into the material. This way, it should be easier to measure underneath the glaze. Due to the longer wavelength, the detector is an InGaAs array detector. These detectors are more sensitive above 1000 nm.

The last advantage concerns the fluorescence background. Fluorescence occurs via absorption of the excitation wavelength as discussed in Part 1 section 3.e.iii Because fewer molecules absorb in this region, less fluorescence will be present in the spectra. This is one of the biggest advantages in terms of spectral quality.

Disadvantages

The first disadvantage is the resolution. As there are fewer lines/mm detector, the spectral resolution is set at 9.5 cm^{-1}. This means that the spectral quality is less than for the Senterra benchtop instrument (3-5 cm^{-1}).

A second disadvantage is the spot size. The spot size for the portable instrument is around 20 times bigger than for the Senterra instrument (50x magnification – spot size = ±4 µm). This means that the areas where the pigments have been applied should be larger than for the benchtop instrument. Also, because there is no built-in camera, it is more difficult to focus the laser. For focusing, continuous measurements were performed. When these continuous measurements were running, the laser was moved up and down until an acceptable S/N-ratio was achieved.

Thirdly, the laser is less energetic (as discussed in Part 1 section 3.c.ii). This means that the intensity of the Raman signals is less than for the more energetic green laser. This will translate into a lower intensity of the Raman bands. The laser power of the portable instrument is also much higher. Longer measuring times or higher laser powers should therefore be applied more carefully as there is a higher chance of damaging the sample. The detector is also less sensitive and gives a lower S/N-ratio.

Lastly, the integration range is starting from 100 cm^{-1}. This can be a problem for pigments that exhibit their most intense band(s) below this wavelength. The instrument has also a cut-off in this region so that the Raman spectrum is only useable in the range between ±110-2500 cm^{-1}. However, for most pigments this should not be an issue

(1) Yellow–Lead tin yellow II

On sample B.fr.1800.1 the yellow pigment was identified as lead tin yellow II (Figure 13). The same spot was analyzed with both the portable instrument as well as the benchtop one. This way, it was easier to compare the two obtained spectra. The total measurement time of this spectrum was 22.5 minutes. This is a little bit longer than what would be done in the field but this was required to obtain an acceptable spectral quality. The laser power was set at 10% to prevent degradation of the sample.

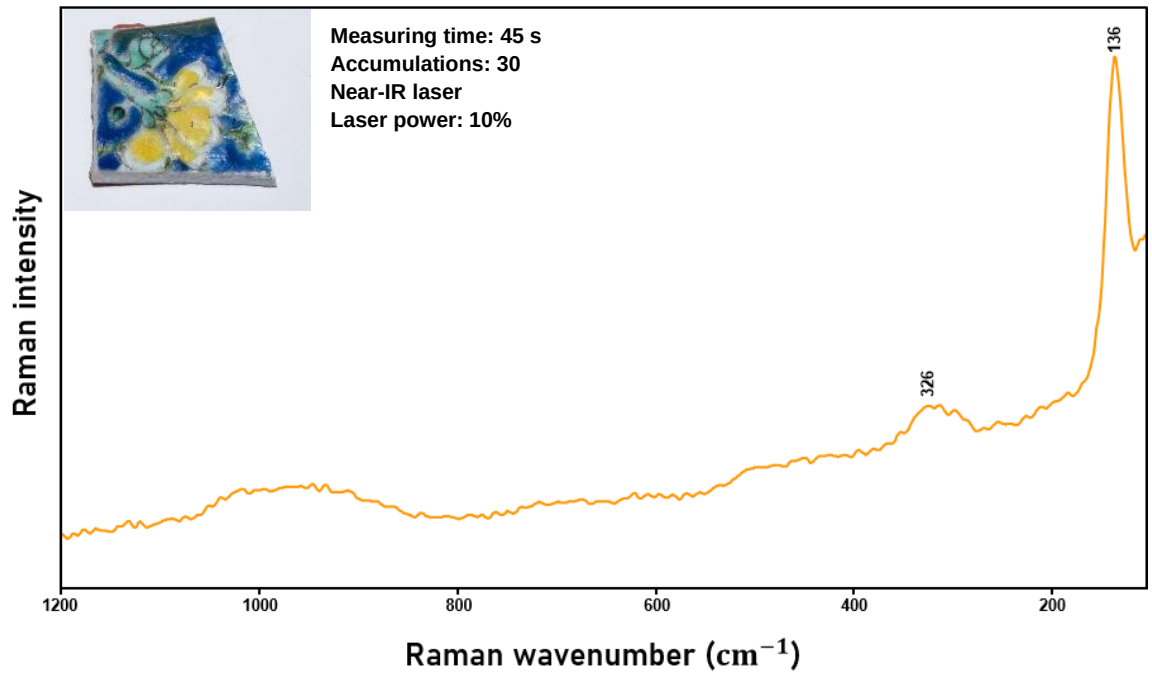

Figure 13: Raman spectrum of lead tin yellow II, recorded on a yellow area of sample B.fr.1800.1. The image of the sample spot and the experimental parameters are shown in the top left corner.

(2) Green–Lead tin yellow II

The pigment lead tin yellow II (Figure 14) was positively identified on a bright green area of sample B.fr.1800.1. Lead tin yellow II may have been blended with a blue pigment to obtain a green color. Nonetheless, no distinguishable bands of a blue pigment were observed in the Raman spectrum. The LA-ICP-MS data of R. Giannini et al.[43] showed elevated amounts of SnO_2 in these brighter green areas. This means that lead tin yellow II was most probably added to obtain a brighter green color.

This area was also analyzed using the benchtop instrument but no Raman signature of lead tin yellow II was detected. This underlines the advantage of the near-IR laser. Due to the fact that this could penetrate deeper underneath the glaze, the signal of this pigment could be measured. The concentration of SnO_2 detected by LA-ICP-MS was rather low (1.53 wt%), meaning that probably, just a little bit of lead tin yellow II was added. Even though the amounts added were probably small, the portable instrument could still pick up this signal due to the near-IR laser. Still, the intensity of the laser had to be increased to 20% to pick up this signal. With the benchtop instrument, a higher intensity of laser was also used, but still, no signal was recorded.

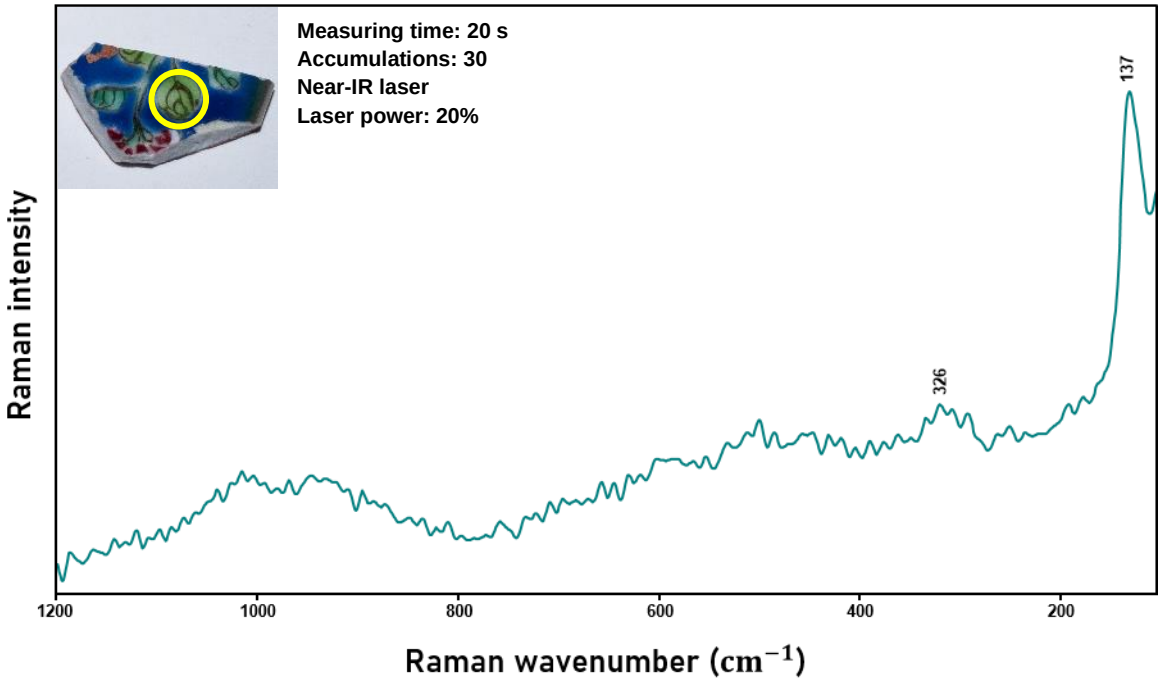

Figure 14: Raman spectrum of lead tin yellow II, recorded on a bright green area of sample B.fr.1800.1. The analyzed spot and experimental parameters are shown in the upper left corner.

3) Conclusion

Different pigments were positively identified using Raman spectroscopy. In the first part of the conclusions (section 3.a), the obtained results are displayed and discussed. Also, the data obtained by previous research on these samples and the new Raman insight of the current research will be compared. (section 3.b). This is followed by a comparison of the spectral quality obtained with and between the Raman spectrometers (section 3.c). The final conclusion reflects on the research question (see Part 1 section 2.c) formulated in the first part of this thesis (section 3.d).

a) Overview of the pigments

In total, seven pigments were identified: one red pigment, two blue pigments, one yellow pigment, and three white pigments. All these pigments and their characteristic Raman bands are summarized in Table 7.

Table 7: Overview of the different pigment and their characteristic Raman bands. vw=very weak, w=weak, m=medium, s=strong, vs=very strong, br=broad band, sh=shoulder

Pigment	Chemical formula	Raman wavenumbers (cm^{-1})
Hematite	α-Fe_2O_3	227(s), 246(w), 293(vs), 412(m), 449(vw), 613(w), 1319(s-br)
Phthalocyanine blue	$C_{32}H_{16}CuN_8$	174(w), 234(w), 259(w), 288(vw), 484(m), 595(w), 681(s), 748(vs), 781(w), 832(w), 848(w), 953(m), 1008(vw), 1109(w), 1144(m), 1185(vw), 1217(vw), 1340(m), 1451(w), 1531(s)
Ultramarine blue	$Na_{8-10}Al_6Si_6O_{24}S_{2-4}$	260(m), 549(vs), 585(m), 804(w), 1096(s), 1360(vw-br), 1644(m), 1904(vw-br), 2194(w-br)
Lead tin yellow II	$PbSn_{1-x}Si_xO_3$ (x=0.25)	68(w), 137(vs), 262(vw), 325(w-br), 451(vw-br)
Anatase	α-TiO_2	153(vs), 288(s), 385(vw)
Barium sulfate	$BaSO_4$	460(w), 621(w), 988(s)
Lead arsenate		318(w-br), 377 (vw-br), 405(vw-br), 429(w-br), 774(m-sh), 815(vs)

Figure 15 depicts a general overview concerning the different periods, porcelain styles, pigments, and samples. All the samples came from two different periods, namely the Qianlong (1736-1796) and the Jiaqing (1796-1820) periods. Some samples could not be appointed to one specific period and were thus assigned to both. The two different sample sets contained three different styles of porcelain. Sample set 1 consisted of *famille rose* porcelain. Sample set 2 had two different subsets. Subset 1 had *cloisonné*-style porcelain, while subset 2 consisted of a mixture of *famille rose* and *famille jaune* styles porcelain. Lastly, the different analyzed pigments were assigned to their respective time period and porcelain style. To be thorough, the sample names were also added.

Hematite was found in samples of the three different porcelain styles and was found in porcelains from both periods. This indicates the popularity and importance of hematite in 18th and 19th-century Chinese porcelain. Large pockets of hematite were being mined in the Guangdong and Shandong provinces since the Kangxi period (1654-1720).[44] This made hematite a very available and cheap pigment for porcelain manufacturers. An important advantage for porcelain manufacturers was also the different hues of red that could be obtained with hematite, ranging from pink to dark red and even purple.

Lead tin yellow II was found on *famille rose* and *famille jaune* styles porcelain. On one of the *famille jaune* porcelain samples, the glaze too contained lead tin yellow II. This was undoubtedly used to decorate little artifacts, but this data furtherly suggests that lead tin yellow II was also used as the main

yellow colorant for glazes in *famille jaune* porcelain. The LA-ICP-MS and Raman data also revealed that lead tin yellow II was added to green glazes to obtain a bright green glaze. This will be discussed in more detail in the next section (b.ii).

Phthalocyanine blue was found on two different samples. As already stated before, it is most likely a contamination. Both samples were from the same sample set (2) but were different styles of porcelain.

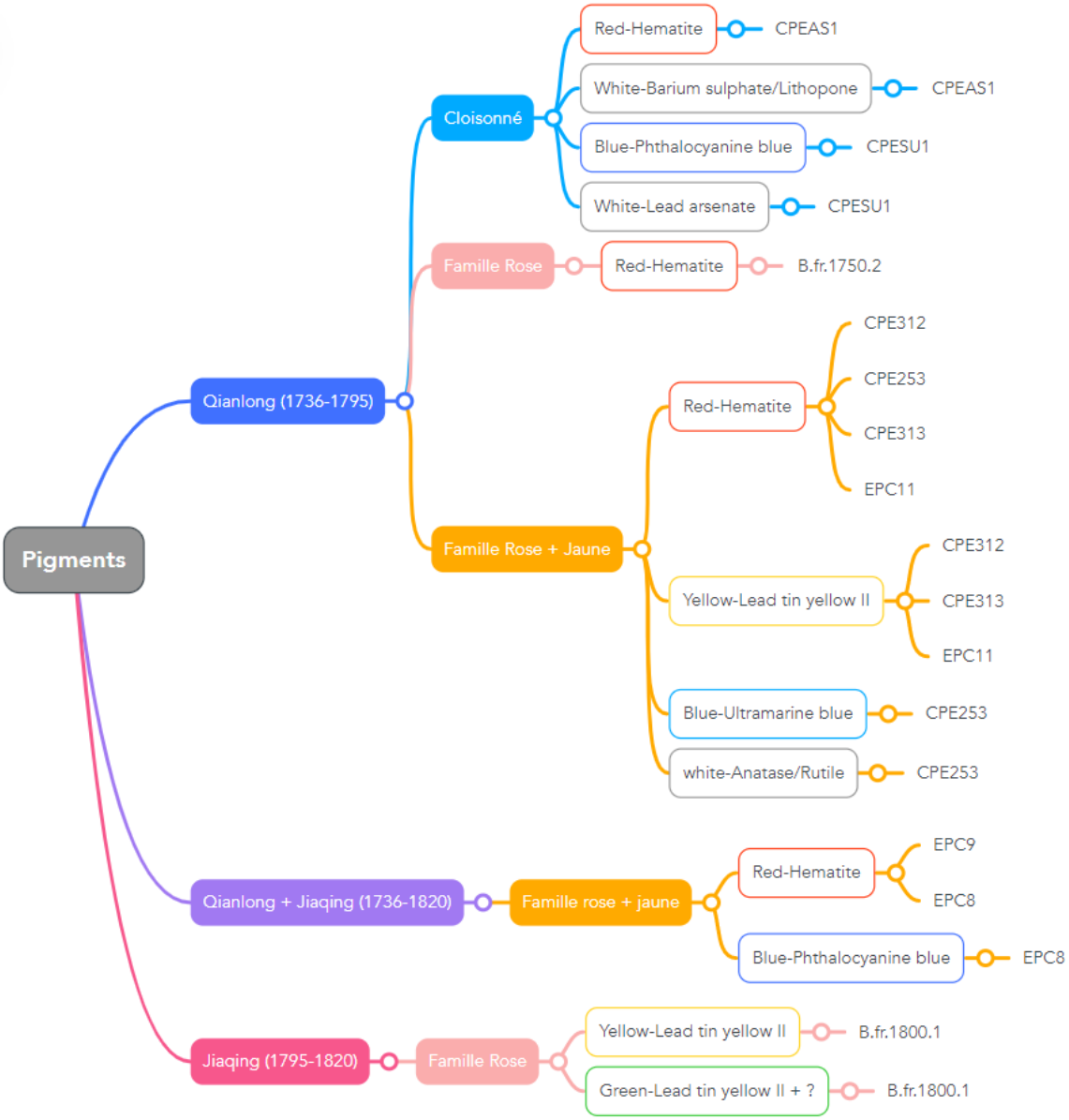

Figure 15: Summary of the different pigments found, connected to their respective style and time period.

One sample contained **ultramarine blue** as a pigment. This sample also contained the pigment **anatase**. It is an acceptable explanation that anatase was added to obtain a lighter shade of blue (see Part 2 section 2.b.ii.(7)). On the other hand, the anatase signature could also come from the body as this was manufactured using kaolin clay, which always contains a certain amount of TiO_2. Therefore, the ratio of anatase (α-TiO_2) and rutile (β-TiO_2) is commonly used in literature to determine the firing temperature of a porcelain.[36, 45] Consequently, anatase could have been present without the intention to lighten a color due to its high abundance. To confirm or refute, further research would be necessary.

Ultramarine blue on the other hand was a very expensive pigment making it very prestigious. The use of ultramarine indicates that this porcelain was a higher-end porcelain not destined for the common household. As stated before, ultramarine blue is gained out of the gemstone *lapis lazuli.* This gemstone was at that time only mined in Afghanistan.[20] This contributed to the high value of ultramarine blue. The Qianlong and Jiaqing periods were a transition period for the use of a new type of blue pigment, namely cobalt blue. Cobalt blue is a synthetic pigment that was introduced in the early 19th century.[46] Because this was cheaper, it was more commonly used instead of the more expensive ultramarine. Blue and white porcelain became popular at the beginning of the 19th century because it was cheaper and due to the bright blue color that was obtained.[15, 46]

The other blue areas of the sample could not be identified. The SEM-EDX data showed elevated amounts of cobalt. As cobalt blue was only available at the beginning of the Jiaqing period, smalt was likely used as a blue pigment. Smalt is obtained by pulverizing cobalt glass and is thus CoO embedded in a glassy matrix.[47] Because cobalt minerals are weak Raman scatterers, these could not be identified using Raman spectroscopy.

A **Barium sulfate/Lithopone** signature was found on a lighter blue glaze of a cloisonné-style porcelain, belonging to the Qianlong period. As discussed previously, the barium sulfate signature was found with a great degree of certainty, whereas the lithopone signature was rather questionable. It was not clear whether this signature was from lithopone or the glaze/matrix. Further research will have to point this out.

On the light green areas of another cloisonné-style porcelain, **lead arsenate** was found as an opacifier/whitener. This implies that these two whiteners seem to have both been used in the same period and in the same style of porcelain. Probably, this points toward them being from a different manufacturer. Or, this could mean that lead arsenate was mostly used as an opacifier more than a whitener. On all the whiteners discussed in this section, lead arsenates have been reported in literature the most in similar types of artifacts.[3-4, 6-7, 28, 41] Lead arsenates have both been used as opacifiers and to make colors lighter.

b) Comparison of Raman, LA-ICP-MS, and ESEM-EDX data

The identified pigments (Table 7) were compared to the data provided by Dr. Dennis Braekmans[1] in the case of sample set 2 and to the data of R. Giannini, Ph.D.[43] in the case of sample set 1. Dr. Dennis Braeckman provided SEM-EDX data. R. Giannini performed LA-ICP-MS and XRF on the sample set.

i) Comparison of the Raman and SEM-EDX data

SEM-EDX was utilized to analyze the different colors/colored glazes on sample set 2. Only the results of the cloisonné-style porcelains were already published. An overview of the results of the samples investigated by SEM-EDX are given in Table 8. The other data together with additional LA-ICP-MS data will be published together with the Raman data of this research, completing the comparison for the other samples.

Table 8: Overview of the ESEM-EDX data provided by Dr. Dennis Braekmans.[1]

Sample	Color	Metal oxide	wt%
CPEAS1	red	Fe_2O_3	5.33
	blue	CoO	2.14
	light blue	ZnO	0.27
CPESU1	light green	As_2O_3	8.84
		PbO	48.87
	turquoise green	CuO	2.61

SEM-EDX showed elevated amounts of Fe_2O_3 on the red surface of sample CPEAS1. In these red areas, the weight percentage of Fe_2O_3 was seven times higher than the average percentage of Fe_2O_3 measured on the white enamels of the samples (0.79±0.24 wt%). It can thus be concluded that the red areas of sample CPEAS1 were painted using hematite as a pigment. Of the other samples, no SEM-EDX data was yet available.

The Raman data showed the presence of PB15 on samples EPC8 and CPESU1. The (turquoise) green area of CPESU1 was investigated by SEM-EDX and showed that Cu(O) was present. This was present in elevated amounts compared to the average amount of Cu(O) on the white enamels (0.37±0.74 wt%). Nonetheless, this does not necessarily mean that this signature is of PB15, as a lot of green pigments are copper-based. This elevated amount can thus also be from a green pigment. The green pigment(s) could not be identified using Raman spectroscopy. So it might be that a slight signal of PB15 was observed, but it is more likely that the copper signal is from the green pigment present in the glaze. Further research could indicate if elevated amounts of Cu were from PB15, a green pigment, or both.

The dark blue area of sample CPEAS1 showed a significant amount of CoO. This points towards smalt as the unidentified blue pigment(s). As stated before, cobalt oxides are weak Raman scatterers, making them difficult to measure in the samples. It can therefore only be concluded that it is very likely that this area was painted using smalt. However, Raman spectroscopy was not able to confirm this statement.

For the white pigments investigated by Raman spectroscopy, a comparison could only be made for lithopone/barium sulfate and lead arsenate. The SEM-EDX data of sample CPEAS1 showed the presence of Zinc oxide in the blue areas. ZnO was not found in the red, pink, and green areas. Nonetheless, if a look is taken at the white enamels, the average ZnO present (0.28±0.79 wt%) is comparable. Consequently, it is not clear whether zinc is present from lithopone or that zinc is part of the enamel. To be more sure about this, further research should be conducted.

The SEM-EDX data of sample CPESU1 showed elevated amounts of PbO and As_2O_3. The average wt% PbO in the enamel for the samples was 41.10 wt%. Lead oxide is always present in the glaze, but the measurements do show an elevated amount. This means that the SEM-EDX results confirm that a lead arsenate is present in the light green glaze.

ii) Comparison of the Raman and LA-ICP-MS data

As discussed in part 1 of this thesis, Dr. R. Giannini performed LA-ICP-MS and XRF on sample set 1. The XRF data was focused on the provenance of these samples and are not relevant to this thesis. They will thus not be included here. LA-ICP-MS was performed on the body, glaze, and pigments. A summary of the results that are of interest to this research are given in Table 9. The elemental oxides that are shown are all present in elevated amounts in comparison to the glaze and body.

Table 9: A summary of the LA-ICP-MS data of sample set 1.

Sample	Color	Metal oxide	wt%
B.fr.1800.1	Yellow	PbO	69.98
		SnO_2	2.75
	Dark green	SnO_2	0.18
		CuO	2.71
	Bright green	SnO_2	1.07
		CuO	1.05
	Red	Fe_2O_3	3.37
B.fr.1750.2	Yellow	PbO	62.38
		SnO_2	4.42
	Dark green	SnO_2	0.02
		CuO	2.76
	Bright green	PbO	67.08
		SnO_2	1.53
		CuO	1.15
	Blue	CoO	0.64
	Red	Fe_2O_3	4.32

The yellow areas of sample B.fr.1800.1 showed elevated amounts of tin- and lead oxide. This points towards lead tin yellow II. Here, the silica content (measured by LA-ICP-MS) was difficult to compare, as the body contains silica and so does the pigment. The silica contents did not show any large variations and no elevated amounts of silica were detected on the yellow area of B.fr.1800.1. By extension, there was no elevated amount of silica on any sample that had yellow painted areas. B.fr.1750.2 also showed these elevated amounts of tin- and lead oxide. Although that, the tin content higher was and the lead content lower was than for sample B.fr.1800.1. The yellow area on sample B.fr.1750.2 was not analyzed by Raman spectroscopy so no potential differences could be observed between the Raman spectra. Purely based on a visual perspective, the yellow colors look alike. It might be interesting for further research to analyze the yellow areas on this sample to establish if the differences in LA-ICP-MS data also translate into differences in the Raman spectra.

The ICP-MS data of the dark and bright/light green areas show interesting differences. The tin content was higher in the light green areas compared to the darker green areas. Also, the copper contents were lower in these light green areas. So first off, the elevated amounts of copper point towards a

copper-based pigment as the green pigment(s). The SEM-EDX data revealed the same for sample set 2. The fact that the tin contents increase in the bright green glaze relative to the dark green glaze is due to the fact that lead tin yellow II was added to brighten the green color. Thus, lead tin yellow was added to obtain a lighter green color and was not blended with a blue pigment to obtain a green color.

The red areas on both samples had increased amounts of iron oxide. This confirms the presence of hematite. Also, again here, on the blue samples, CoO was present in increased amounts. Depending on the period of the sample this could most probably be smalt or cobalt oxide.

c) Spectral quality

Two different Raman spectrometers were used for the analyses of the samples. Sample set 1 was analyzed by the benchtop and the portable instrument. Sample set 2 was only examined by the benchtop instrument. The following section compares the quality of the spectra obtained by the two Raman instruments. This comparison is visually represented in Table 10. The spectral quality was subdivided into the signal-to-noise ratio, the presence of spikes, and the number of bands visible (of the pigment).

*Table 10: Comparison between the spectral qualities obtained by both Raman spectrometers on both sample sets. *For the green laser, the two-magnon scattering of hematite is also visible. **For spectrum (a) of Figure 6, a very weak band is present which has been discussed in section 2.a.ii.(5) yellow-lead tin yellow II. Only the bands of the pigment were taken into account, so no fluorescence bands or bands coming from the glaze were taken into account.*

Pigment	Sample set 1						Sample set 2		
	Benchtop instrument			Portable instrument			Benchtop instrument		
	#Visible bands	S/N-ratio	Spikes	#Visible bands	S/N-ratio	Spikes	#Visible bands	S/N-ratio	Spikes
Hematite	6	High	Present	X	X	X	6-7*	Medium	Present
Ultramarine	X	X	X	X	X	X	9	High	None
Lead tin yellow II	2	Medium	Present	2	Poor-Medium	None	5-6**	High	None
PB15:1	X	X	X	X	X	X	20	Medium-High	None
Barium sulfate/Lithopone	X	X	X	X	X	X	4	Medium	Present
Anatase	X	X	X	X	X	X	3	Medium	None

Benchtop vs portable Raman instrument

For a start, a look was taken at the signal-to-noise ratio between both instruments. The S/N-ratio is dependent on the ability of the bonds to Raman scatter but it also depends on some instrumental factors, such as type of detector, the cooling (amount of dark signal), the spectral resolution, the measurement times, and the number of measurements. For the S/N-ratio the following equation was used:

$$\frac{S}{N} = \frac{2H}{h} \qquad (1)$$

In this formula, the H stands for the height of the most intense band and h for the height of the baseline. This is also depicted in Appendix 3 Figure 2. The spectrum of hematite recorded on sample B.fr.1750.2 was used as an example to explain this.

⇔H=10,0071-8200

⇔h=8200-8138

⇔S/N=$\frac{2.(10,071-8200)}{(8200-8138)} = 60.35$

>60 S/N-ratio was considered as high, 40-60 considered as medium, and <40 was considered as a poor S/N-ratio.

For the benchtop instrument, a signal-to-noise ratio of medium to high could be achieved. For the portable instrument, only a poor (34) to medium (43) S/N-ratio was obtained. This is an expected result. The spectral resolution for the benchtop instrument is 3-5 cm^{-1} while for the portable the spectral resolution is set at 9.5 cm^{-1}. Another distinctive factor is that the portable instrument is designed for quick measurements while the benchtop instrument is designed to perform longer experiments. Longer measuring times and a higher number of accumulations will benefit the S/N-ratio positively. Of course, the benchtop instrument can also be used for quicker measurements, depending on the samples. In general, the total measurement times for the benchtop instrument were between 60-120 minutes. For the Portable Raman instrument, this was only 10-25 minutes.

There is also a difference in the number of visible bands between both Raman spectrometers. For the benchtop instrument, more bands were visible than for the portable instrument. With the portable instrument, only the most intense bands of the pigment were visible.

The portable instrument could only identify one pigment, namely lead tin yellow II. With the benchtop instrument, hematite could also be identified on sample set 1. The portable instrument can also be equipped with a 785 nm red laser. This might be necessary to identify more pigments on the sample such as hematite which could not be identified using the 1064 nm laser.

Overall, the benchtop instrument yielded better results. Nevertheless, the portable instrument has been proven useful for the *in situ* analysis of porcelain.

d) Research question and general conclusion

Raman spectroscopy is suited for the analysis of these art objects. The best results in terms of spectral quality and the amount of identified pigments were obtained using embedded samples and a benchtop Raman instrument. Nonetheless, the spectral quality obtained via the portable Raman instrument was sufficient to identify pigments on the porcelains shards.

In this research, the first aim was to optimize the Raman settings for the analysis of porcelain samples. To obtain high-quality spectra, a measuring time of 40-60 seconds and 50-60 accumulations yielded the best results using the benchtop instrument. In contrast to the samples, the references mostly needed shorter measuring times. With the same measuring times as the samples, the detector was overloaded. Every spot was analyzed using the two different lasers. Sometimes a switch in laser yielded better results. This was seen for ultramarine blue where an enhancement occurred with the green laser. Sometimes one laser or the other could not pick up any signal at all. For example, the white pigments were only measurable using the green laser.

Another aim was to identify as many pigments as possible. In part (a) of the conclusion, these have extensively been discussed. For some pigments, extra research has to be conducted to have more material for better conclusions. The spectrum of barium sulfate/lithopone will have to be examined further. If it turns out to be lithopone, this implies that the dating of this porcelain would be wrong. The first reports of the use of lithopone date back to the end of the 19th century. In this case, this would then correspond to the Dongzhi (1862-1874) or Guangxu (1875–1908) period. Another interesting result was the presence of PB15 in two different samples. Although it is unlikely that this pigment was applied during the firing process, suggesting that these would be wrongly dated. Extra research could point out the possible origin of PB15 in these samples.

4) Appendices

a) Appendix 1

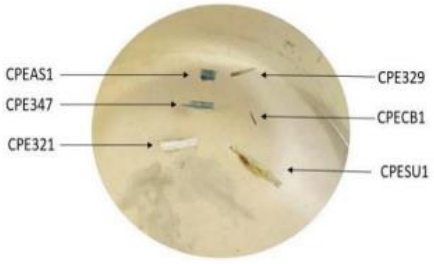

CPEAS1
Qianlong (1736-1795)

CPE347
Qianlong (1736-1795)

CPE321.b

CPE329
Qianlong (1736-1795)

CPECB1
Qianlong (1736-1795)

CPESU1
Qianlong (1736-1795)

Appendix 1 Figure 1: Subset 1 of sample set 2. All the artifacts are cloisonné style porcelain. Artifact CPE321.b was misattributed and is most likely 20th century porcelain based on the body composition and will not be included in this thesis.

Appendix 1 Figure 2: Subset 2 of sample set 2 consisting of a mixture of famille rose and famille jaune styles porcelain.

b) Appendix 2

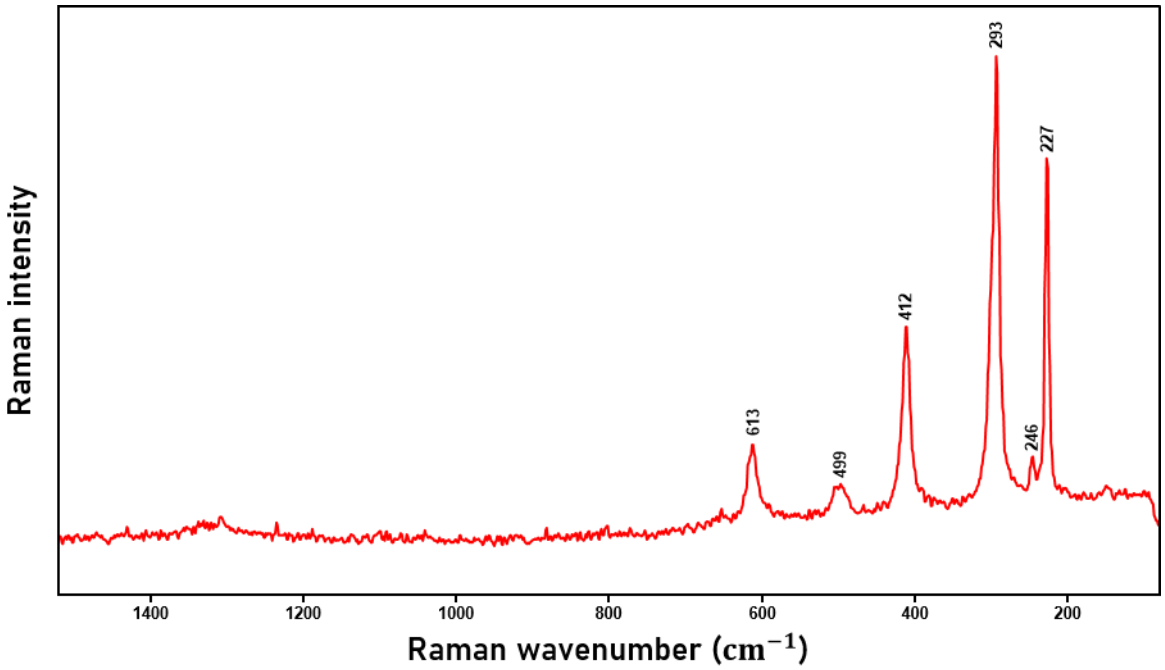

Appendix 2 Figure 1: Reference spectra of hematite. The spectrum was recorded with the red laser. Experimental parameters: 10 s, 25 acc, aperture=50 µm, 1% laser power.

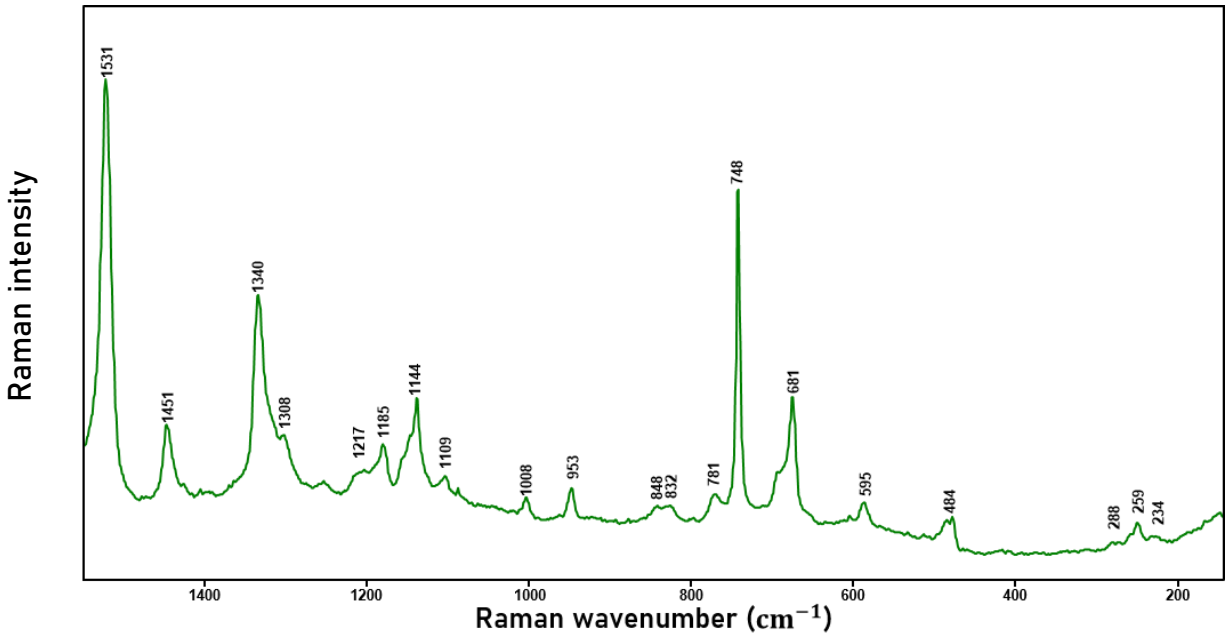

Appendix 2 Figure 2: Reference spectrum of phthalocyanine blue-β polymorph. The spectrum was recorded with the red laser. Experimental parameters: 60 s, 60 acc, aperture=50 µm, 10% laser power.

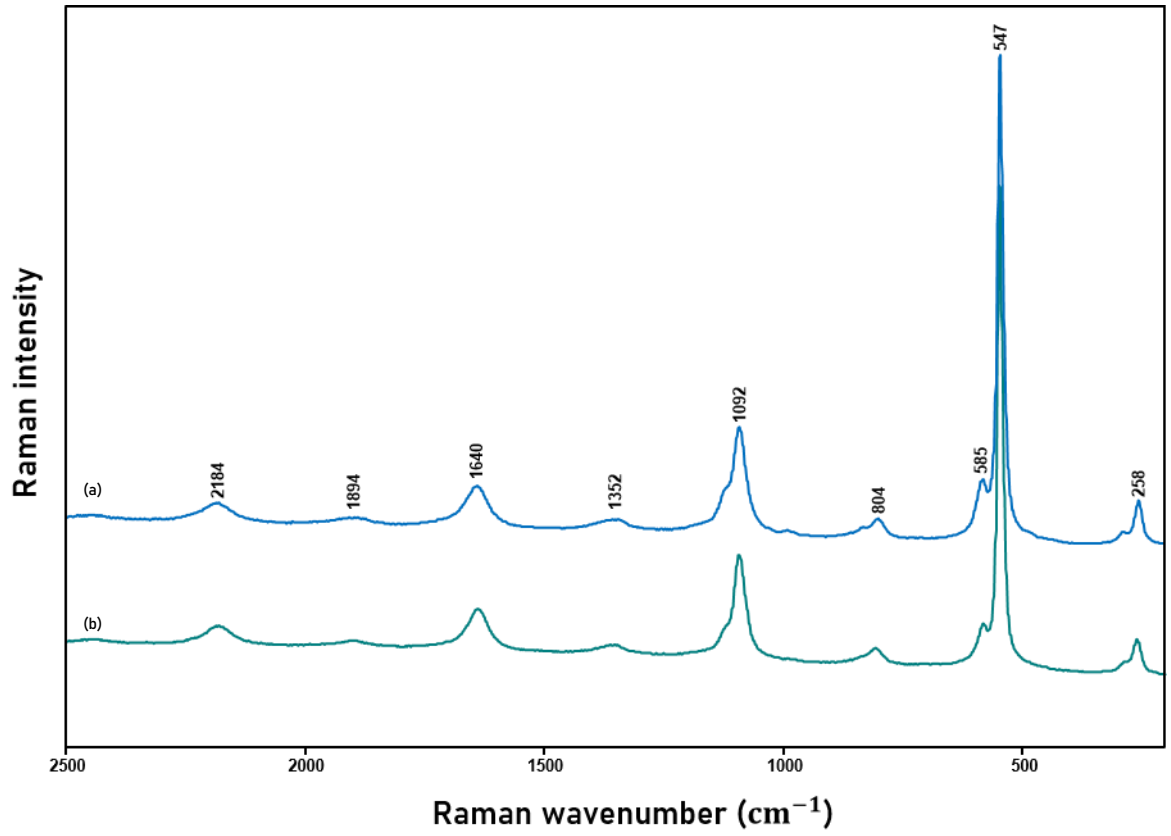

Appendix 2 Figure 3: Reference spectra of synthetic and natural ultramarine blue. The spectra were recorded with the green laser. (a) the spectrum of natural ultramarine blue. Experimental parameters: 10 s, 10 acc, aperture=50 µm, green laser, 10% laser power. (b) the spectrum of synthetic ultramarine blue. experimental parameters: 10 s, 10 acc, aperture=50 µm, 10% laser power.

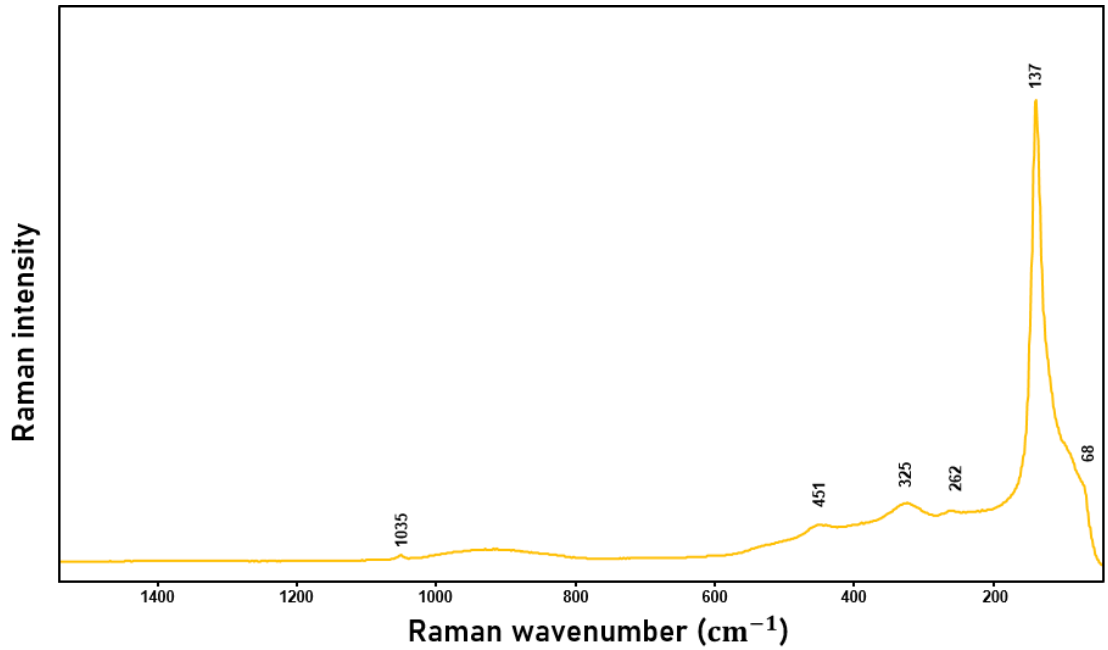

Appendix 2 Figure 4: Reference spectrum of lead tin yellow II. The spectrum was recorded with the green laser. Experimental parameters: 15 s, 6 acc, aperture=25 µm, 25% laser power.

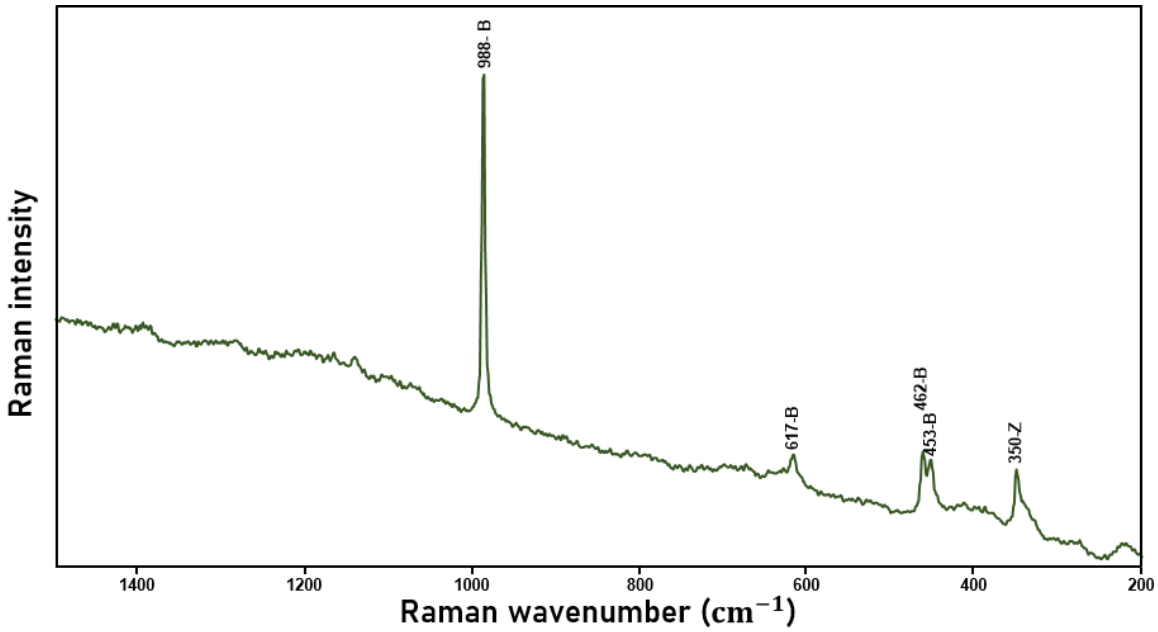

Appendix 2 Figure 5: Reference spectrum of lithopone. The spectrum was recorded with the green laser. Experimental parameters: 20 s, 5 acc, aperture=25 µm, 10% laser power. B= band of Barium sulfate, Z= band of Zinc sulfide

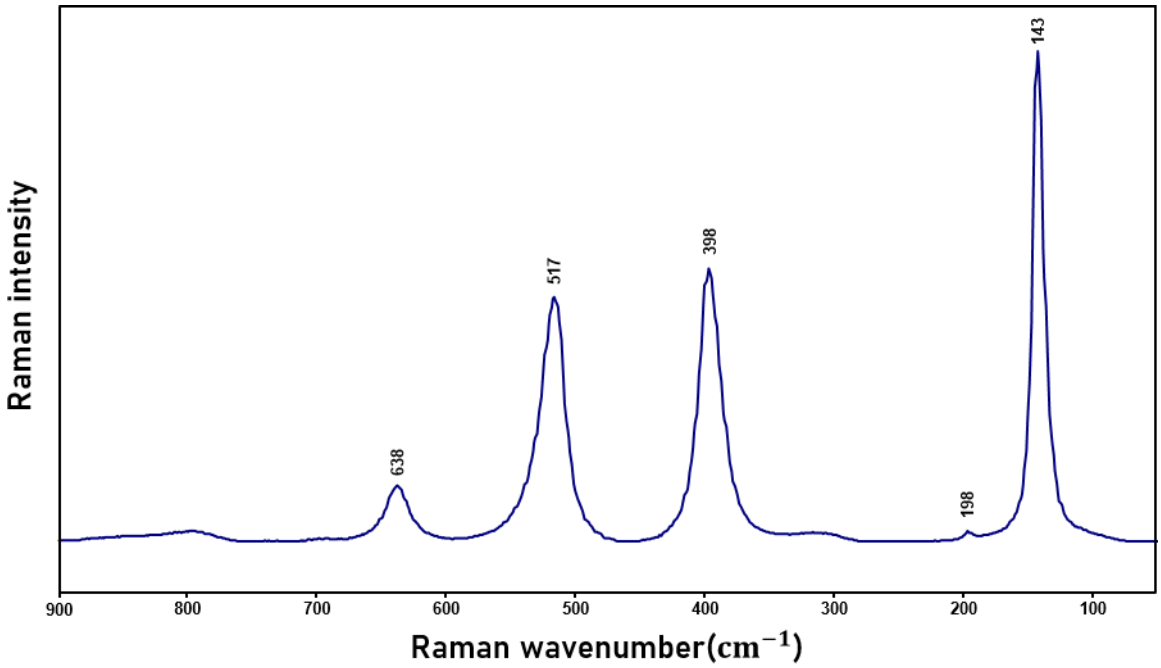

Appendix 2 Figure 6: Reference spectrum of anatase. Spectrum was taken from the RRUFF database.[48] The anatase was from Taftan, near Dalbandi, Baluchistan Province, Pakistan, and was recorded with a 532 nm green laser.

c) Appendix 3

Appendix 3 Table 1: Laser power of the green and red laser, measured at the level of the samples. All the values are given in mW.

green laser	1%	10%	25%	50%	100%
5x	0.14	0.90	2.53	6.00	10.60
20x	0.15	1.60	3.10	7.00	13.55
50x	0.13	1.52	2.88	6.66	12.35
100x	0.03	0.41	0.78	1.80	3.40
red laser	1%	10%	25%	50%	100%
5x	0.49	4.45	11.8	22.10	43.50
20x	0.40	3.70	9.50	18.35	36.30
50x	0.34	3.70	8.15	15.45	30.70
100x	0.13	1.18	3.06	5.83	11.60

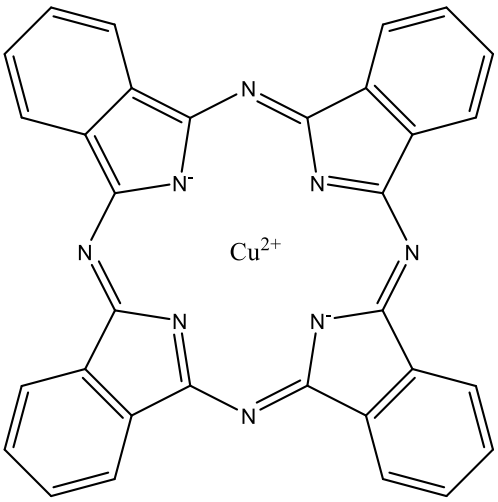

Appendix 3 Figure 1: Chemical structure of phthalocyanine blue.

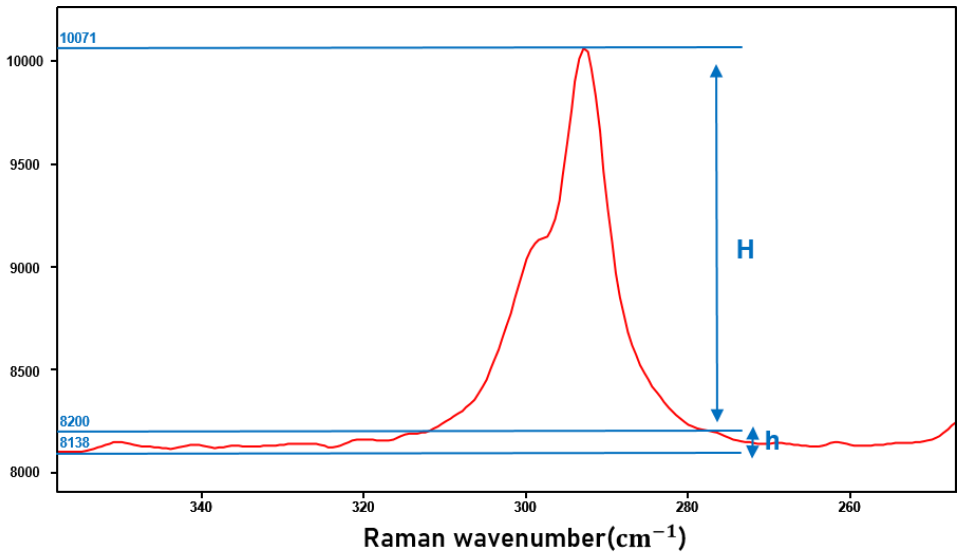

Appendix 3 Figure 2: Example of the calculations of the signal-to-noise ratio. H=height of the band, h=height of the baseline.

5) References

1. Norris, D.; Braekmans, D.; Shortland, A., Emulation and Technological Adaptation in Late 18th Century Cloisonné-Style Chinese Painted Enamels. *Archaeometry* **2022,** *64*.
2. Van Pevenage, J.; Lauwers, D.; Herremans, D.; Verhaeven, E.; Vekemans, B.; De Clercq, W.; Vincze, L.; Moens, L.; Vandenabeele, P., A combined spectroscopic study on Chinese porcelain containing ruan-cai colours. *Analytical methods* **2013,** *6*, 387-394.
3. Colomban, P.; Kırmızı, B.; Gougeon, C.; Gironda, M.; Cardinal, C., Pigments and glassy matrix of the 17th–18th century enamelled French watches: A non-invasive on-site Raman and pXRF study. *Journal of Cultural Heritage* **2020,** *44*, 1-14.
4. Colomban, P.; Maggetti, M.; d'Albis, A., Non-invasive Raman identification of crystalline and glassy phases in a 1781 Sèvres Royal Factory soft paste porcelain plate. *Journal of the European Ceramic Society* **2018,** *38* (15), 5228-5233.
5. Colomban, P.; Ngo, A.-T.; Fournery, N. Non-Invasive Raman Analysis of 18th Century Chinese Export/Armorial Overglazed Porcelain: Identification of the Different Enameling Techniques *Heritage* [Online], 2022, p. 233-259.
6. Colomban, P.; Zhang, Y.; Zhao, B., Non-invasive Raman analyses of Chinese huafalang and related porcelain wares. Searching for evidence for innovative pigment technologies. *Ceramics International* **2017,** *43* (15), 12079-12088.
7. Colomban, P.; Kırmızı, B.; Zhao, B.; Clais, J.-B.; Yang, Y.; Droguet, V., Investigation of the Pigments and Glassy Matrix of Painted Enamelled Qing Dynasty Chinese Porcelains by Noninvasive On-Site Raman Microspectrometry. *Heritage* **2020,** *3* (3).
8. Colomban, P.; Ngo, A.-T.; Fournery, N., Non-Invasive Raman Analysis of 18th Century Chinese Export/Armorial Overglazed Porcelain: Identification of the Different Enameling Techniques. *Heritage* **2022,** *5* (1), 233-259.
9. Jain, S.; Shah, J.; Negi, N.; Sharma, C.; Kotnala, R. K., Significance of interface barrier at electrode of hematite hydroelectric cell for generating ecopower by water splitting. *International Journal of Energy Research* **2019,** *43*.
10. Hajiyev, P.; Cong, C.; Qiu, C.; Yu, T., Contrast and Raman spectroscopy study of single- and few-layered charge density wave material: 2H-$TaSe_2$. *Scientific reports* **2013,** *3*, 2593.
11. Marshall, C.; Dufresne, W.; Rufledt, C., Polarized Raman spectra of hematite and assignment of external modes. *Journal of Raman Spectroscopy* **2020,** *51*.
12. Kırmızı, B.; Colomban, P.; Quette, B., On-site analysis of ChineseCloisonnéenamels from fifteenth to nineteenth centuries. *Journal of Raman Spectroscopy* **2009**, n/a-n/a.
13. Wang, L.; Zhu, J.; Yan, Y.; Xie, Y.; Wang, C., Micro-structural characterization of red decorations of red and green color porcelain (Honglvcai) in China. *Journal of Raman Spectroscopy* **2009,** *40*, 998-1003.
14. Colomban, P.; Gironda, M.; Vangu, D.; Kırmızı, B.; Zhao, B.; Cochet, V., The Technology Transfer from Europe to China in the 17th–18th Centuries: Non-Invasive On-Site XRF and Raman Analyses of Chinese Qing Dynasty Enameled Masterpieces Made Using European Ingredients/Recipes. *Materials* **2021,** *14* (23), 7434.
15. Colomban, P.; Ngo, A.-T.; Edwards, H. G. M.; Prinsloo, L. C.; Esterhuizen, L. V., Raman identification of the different glazing technologies of Blue-and-White Ming porcelains. *Ceramics International* **2022,** *48* (2), 1673-1681.
16. Erk, P.; Hengelsberg, H., Phthalocyanine Dyes and Pigments. *The Porphyrin Handbook: Phthalocyanines: Spectroscopic and Electrochemical Characterization* **2003,** *16*, 117-170.
17. Defeyt, C.; Van Pevenage, J.; Moens, L.; Strivay, D.; Vandenabeele, P., Micro-Raman spectroscopy and chemometrical analysis for the distinction of copper phthalocyanine polymorphs in paint layers. *Spectrochimica acta. Part A, Molecular and biomolecular spectroscopy* **2013,** *115C*, 636-640.
18. Defeyt, C.; Van Pevenage, J.; Vandenabeele, P.; Learner, T.; Strivay, D., Distinction by Micro-Raman Spectroscopy and Chemometrical Analysis of Copper Phthalocyanine Blue Polymorphs in Oil-

Based and Acrylic Paint Samples. In *Issues in Contemporary Oil Paint*, van den Berg, K. J.; Burnstock, A.; de Keijzer, M.; Krueger, J.; Learner, T.; Tagle, d. A.; Heydenreich, G., Eds. Springer International Publishing: Cham, 2014; pp 105-116.
19. Agnieszka, P.; Rybinski, P.; Grażyna, J.; Agnieszka, K.-J., The thermal properties and the flammability of pigmented elastomeric materials. Part I. Phthalocyanine pigments. *Journal of Thermal Analysis and Calorimetry* **2014,** *117*, 789-798.
20. Radini, A.; Tromp, M.; Beach, A.; Tong, E.; Speller, C.; McCormick, M.; Dudgeon, J. V.; Collins, M. J.; Rühli, F.; Kröger, R.; Warinner, C., Medieval women’s early involvement in manuscript production suggested by lapis lazuli identification in dental calculus. *Science Advances* **2019,** *5* (1), eaau7126.
21. Vandenabeele, P.; De Paepe, P.; Moens, L., Study of the 19th century porcelain cards with direct Raman analysis. *Journal of Raman Spectroscopy* **2008,** *39* (8), 1099-1103.
22. Ballirano, P.; Maras, A., Mineralogical characterization of the blue pigment of Michelangelo's fresco - "The Last Judgment". *AMERICAN MINERALOGIST* **2006,** *91*, 997-1005.
23. Osticioli, I.; Mendes, N. F. C.; Nevin, A.; Gil, F. P. S. C.; Becucci, M.; Castellucci, E., Analysis of natural and artificial ultramarine blue pigments using laser induced breakdown and pulsed Raman spectroscopy, statistical analysis and light microscopy. *Spectrochimica Acta Part A: Molecular and Biomolecular Spectroscopy* **2009,** *73* (3), 525-531.
24. Long, D., The Raman Effect: A Unified Treatment of the Theory of Raman Scattering by Molecules. 2002; pp 49-84.
25. Košařová, V.; Hradil, D.; Hradilová, J.; Čermáková, Z.; Němec, I.; Schreiner, M., The efficiency of micro-Raman spectroscopy in the analysis of complicated mixtures in modern paints: Munch's and Kupka's paintings under study. *Spectrochimica Acta Part A: Molecular and Biomolecular Spectroscopy* **2016,** *156*, 36-46.
26. Franquelo, M. L.; Duran, A.; Herrera, L. K.; Jimenez de Haro, M. C.; Perez-Rodriguez, J. L., Comparison between micro-Raman and micro-FTIR spectroscopy techniques for the characterization of pigments from Southern Spain Cultural Heritage. *Journal of Molecular Structure* **2009,** *924-926*, 404-412.
27. Miao, J.; Yang, B.; Mu, D., Identification and differentiation of opaque Chinese overglaze yellow enamels by Raman spectroscopy and supporting techniques. *Archaeometry* **2009,** *52*, 146-155.
28. Colomban, P.; Gironda, M.; Simsek Franci, G.; d'Abrigeon, P., Distinguishing Genuine Imperial Qing Dynasty Porcelain from Ancient Replicas by On-Site Non-Invasive XRF and Raman Spectroscopy. *Materials (Basel, Switzerland)* **2022,** *15* (16).
29. Ciaramitaro, V.; Armetta, F.; Mollica Nardo, V.; Ponterio, R. C.; Saladino, M. L., Portable Spectroscopic Techniques for the Non-invasive Identification of two historical yellow pigments: Applications and Practical Challenges. *Journal of Physics: Conference Series* **2022,** *2204* (1), 012056.
30. Šefců, R.; Chlumská, Š.; Otmarová Hostašová, A., An investigation of the lead tin yellows type I and II and their use in Bohemian panel paintings from the Gothic period. *Heritage Science* **2015,** *3*.
31. Cazzanelli, E.; Grande, D.; Rizzuto, C.; Nucera, A.; Barberi, R.; Castriota, M., Micro-Raman Analysis of the Pigments on a Crucifix in Calabria. *Applied Sciences* **2022,** *12*, 6715.
32. Bellei, S.; Nevin, A.; Cesaratto, A.; Capogrosso, V.; Vezin, H.; Tokarski, C.; Valentini, G.; Comelli, D., Multianalytical Study of Historical Luminescent Lithopone for the Detection of Impurities and Trace Metal Ions. *Analytical Chemistry* **2015,** *87* (12), 6049-6056.
33. Srilakshmi, C.; Widjaja, E.; Anderson, B. G.; Garland, M., Fourier transform Raman spectral measurements of powdered quaternary mixtures of organic compounds: Exceptional pure component spectral reconstruction using band-target entropy minimization (BTEM). *Talanta* **2007,** *72* (2), 847-853.
34. Franguelli, F.; Barta-Holló, B.; Petrusevski, V.; Sajó, I.; Klébert, S.; Farkas, A.; Bódis, E.; Szilágyi, I.; Pawar, R.; Kótai, L., Thermal decomposition and spectral characterization of di[carbonatotetraamminecobalt(III)] sulfate trihydrate and the nature of its thermal decomposition products. *Journal of Thermal Analysis and Calorimetry* **2020,** *145*.

35. Buzgar, N.; Bodi, G.; Buzatu, A.; Apopei, A., The Raman study of the white pigment used in Cucuteni pottery. *Analele științifice ale Universității "Al. I. Cuza" din Iași. Seria Geologie.* **2013,** *59*, 41-50.
36. Tezza, V.; Scarpato, M.; Felipe, L.; Silva, L.; Bernardin, A., Effect of firing temperature on the photocatalytic activity of anatase ceramic glazes. *Powder Technology* **2015,** *276*.
37. Zhu, S.-C.; Xie, S.-H.; Liu, Z.-P., Nature of Rutile Nuclei in Anatase-to-Rutile Phase Transition. *Journal of the American Chemical Society* **2015,** *137* (35), 11532-11539.
38. Balasubramaniam, R.; Kumar, A. V. R.; Dillmann, P., Characterization of Rust on Ancient Indian Iron. *Current Science* **2003,** *85*.
39. Carter, E.; Wood, M.; de Waal, D.; Edwards, H., Porcelain shards from Portuguese wrecks: Raman spectroscopic analysis of marine archaeological ceramics. *Heritage Science* **2017,** *5*.
40. COLOMBAN, P., Colouring Agents for Glass, Glaze and Enamel: Tracing Innovation and Exchange Routes *The Royal Society of Chemistry 2019* **2019**.
41. Colomban, P.; Arberet, L.; Kirmizi, B., On-site Raman analysis of 17th and 18th century Limoges enamels: Implications on the European cobalt sources and the technological relationship between Limoges and Chinese enamels. *Ceramics International* **2017,** *43* (13), 10158-10165.
42. Colomban, P.; Lu, T.-A.; Milande, V., Non-invasive on-site Raman study of blue-decorated early soft-paste porcelain: The use of arsenic-rich (European) cobalt ores – Comparison with huafalang Chinese porcelains. *Ceramics International* **2018,** *44* (8), 9018-9026.
43. Giannini, R. Optimisation of the LA-ICP-MS technique to provenance and authenticate Chinese porcelain. Cranfield University, 2014-2015.
44. Guangrong, L., The Chinese Iron Ore Deposits and Ore Production. In *Iron Ores and Iron Oxide Materials*, Volodymyr, S., Ed. IntechOpen: Rijeka, 2018; p Ch. 1.
45. Galizia, P.; Maizza, G.; Galassi, C., Heating rate dependence of anatase to rutile transformation. *Processing and Application of Ceramics* **2016,** *10*, 235–241.
46. Jiang, X.; Ma, Y.; Chen, Y.; Li, Y.; Ma, Q.; Zhang, Z.; Wang, C.; Yang, Y., Raman analysis of cobalt blue pigment in blue and white porcelain: A reassessment. *Spectrochimica Acta Part A: Molecular and Biomolecular Spectroscopy* **2018,** *190*, 61-67.
47. Merriam-Webster Smalt. https://www.merriam-webster.com/dictionary/smalt.
48. RRUFF Anatase R060277. https://rruff.info/Anatase/R060277.